The influence of the cardiac cycle phase on the volumetry of pulmonary nodules

Erique Manuel Correia Guedes Pinto

Tese para obtenção do Grau de Doutor em
Medicina
(3º ciclo de estudos)

Orientador: Prof. Doutor Klaus Loureiro Irion
Co-orientador: Prof. Doutor Luís Taborda-Barata

Juri

Prof. Doutor Miguel Castelo Branco Craveiro de Sousa
Prof. Doutor Alexandre Xavier Falção
Prof. Doutor Nuno Miguel Albuquerque Castro Almeida Cardim
Prof. Doutor François Ascagne Pontana

27 de Junho de 2024

Declaração de Integridade

Eu, Erique Manuel Correia Guedes Pinto, que abaixo assino, estudante com o número de inscrição D2337, do 3º ciclo de estudos em Medicina da Faculdade de Ciências da Saúde da Universidade da Beira Interior, declaro ter desenvolvido o presente trabalho e elaborado o presente texto em total consonância com o **Código de Integridades da Universidade da Beira Interior**.

Mais concretamente afirmo não ter incorrido em qualquer das variedades de Fraude Académica, o que aqui declaro conhecer, que em particular atendi à exigida referenciação de frases, extratos, imagens e outras formas de trabalho intelectual, e assumindo assim na íntegra as responsabilidades da autoria.

Universidade da Beira Interior, Covilhã 26/07/2024

Dedication

To my parents, that gave me life.

To my father, whose footsteps in the sand I try to follow.

To my wife, whose light fills me whole.

Acknowledgements

My heartfelt thanks to my PhD supervisors, Professor Klaus Irion and Professor Luís Taborda-Barata, for their support, mentorship, vigil and wisdom.

To Professor Klaus, my gratitude for his teaching and friendship. Thank you for the insights in chest imaging and thought-provoking challenges.

To Professor Luís Taborda-Barata, my gratitude for the steady hands and rigorous scientific thinking that was crucial in driving this work to completion.

To Professor Edson Marchiori, my gratitude for generously reviewing the work and sharing your wisdom.

To Colin Monaghan, who made it all possible in the first place.

Resumo

Existe uma sobreposição significativa na população em risco e nos fatores de risco do cancro do pulmão e na doença arterial.

O rastreio do cancro do pulmão já provou conseguir reduzir a mortalidade relacionada com o cancro, e existe um esforço em curso, a nível mundial, para implementar programas de rastreio do cancro do pulmão. Estes programas irão inevitavelmente aumentar o número de pedidos de estudos de TC torácicos de baixa-dose. Da mesma forma, é igualmente expectável o aumento do número de pedidos de estudos de AngioTC das artérias coronárias nesta população, à medida que aumenta a disponibilidade de equipamentos modernos de TC, visto que as doenças cardiovasculares continuam a representar uma das principais causas de morbilidade e mortalidade no mundo industrializado.

Esta tendência cria uma oportunidade para o rastreio duplo de cancro do pulmão e da doença coronária, previamente sugerida, mas ainda não adequadamente investigada. A possibilidade de realizar rastreio do cancro do pulmão utilizando estudos de AngioTC coronária poderá evitar a duplicação desnecessária de recursos, melhorar a relação custo-eficácia dos programas de rastreio e evitar os efeitos secundários da exposição desnecessária de radiação.

A presente dissertação irá explorar o uso de ferramentas de volumetria de nódulos pulmonares em estudos de AngioTC coronária.

Na abordagem desta questão, foi revista a literatura científica referente a achados incidentais em estudos de AngioTC coronária e identificaram-se achados incidentais pulmonares como sendo, de facto, os achados incidentais mais frequentes, apesar da falta de consenso referente à forma como os mesmos são relatados e investigados. A prevalência de achados incidentais pulmonares, que correspondem na sua maioria a pequenos nódulos pulmonares, suporta a relevância da presente investigação e do rastreio duplo.

A volumetria de nódulos pulmonares tem um papel central na investigação de nódulos pulmonares indeterminados. O tempo de duplicação de volume é atualmente considerado o melhor indicador de malignidade destes nódulos pulmonares indeterminados e crucial para o diagnóstico precoce de cancro do pulmão. No entanto, é

conhecida a influência que múltiplos factores exercem no resultado das ferramentas de volumetria, alguns dos quais relevantes para descrever as diferenças entre protocolos de TC torácica de baixa dose usado no rastreio do cancro do pulmão, e o protocolo de AngioTC coronária, usado na avaliação de doença coronária. Este facto é relevante uma vez que as ferramentas de volumetria dedicada à análise de nódulos pulmonares não estão validadas no contexto da AngioTC coronária.

Foi feita uma revisão sistemática da literatura referente aos factores que influenciam as ferramentas de volumetria, a qual contribuiu para consolidar a evidência científica disponível, salientar a elevada heterogeneidade entre os numerosos estudos e explicar a dificuldade da sua aplicação na prática clínica.

A investigação do efeito da fase do ciclo cardíaco na volumetria de nódulos pulmonares toma duas abordagens complementares. No primeiro estudo original, foi desenvolvido um modelo de regressão linear múltipla para identificar fatores hemodinâmicos cardiopulmonares que influenciam a volumetria de nódulos pulmonares de forma estatisticamente significativa. Estes fatores incluem a fase do ciclo cardíaco, a distância vascular entre o tronco da artéria pulmonar e o nódulo, a localização do nódulo nos eixos ântero-posterior e crânio-caudal, no sentido em que se relacionam com a pressão hidrostática e a área de secção vascular. Contrariamente aos resultados apresentados pelo único estudo prévio investigando esta temática, por Boll et al., a fase do ciclo cardíaco não foi estatisticamente significativa no presente estudo, enquanto os restantes fatores o foram.

No segundo estudo original, foi realizada análise de Bland-Altman relativa, a qual mostrou que fases opostas do ciclo cardíaco (e.g., sístole e diástole) apresentam aumento da variabilidade da medição volumétrica. Este aumento da variabilidade da medição pode ser clinicamente significativa e potencialmente resultar em falsos-positivos na avaliação do crescimento de nódulos.

Com bases nestes dois estudos originais, foi apresentado um modelo que explica a influência dos fatores hemodinâmicos cardiopulmonares, como a fase do ciclo cardíaco, baseado no contexto fisiológico de 'tempo de trânsito'. A presente dissertação argumenta que eventos cardiopulmonares com a descompensação aguda de insuficiência cardíaca, a qual poderá ocorrer ou resolver no intervalo de tempo entre duas avaliações de seguimento no contexto de um programa de rastreio do cancro do pulmão, poderá induzir a um resultado falso-positivo, e deverá ser tido em consideração. De forma a minimizar a variabilidade de medição, quando realizada

volumetria de nódulos pulmonares em estudos de TC sincronizado por ECG, a mesma deverá ser realizada em diástole.

A revisão sistemática realizada identificou falhas significativas no atual conhecimento neste campo, motivando futura investigação.

Palavras-chave

Cancro do pulmão; nódulo pulmonar, volumetria; hemodinâmica cardiopulmonar.

Summary

There is a significant overlap in the risk factors and population at risk of lung cancer and coronary artery disease (CAD).

Lung cancer screening (LCS) has proven to reduce cancer-related mortality, and there is an ongoing, worldwide effort to implement LCS programmes. This will undoubtedly increase requests for low-dose CT (LDCT) scans. Likewise, as new CT scanner technology becomes more ubiquitous, demand for coronary CT angiography (CCTA) is also expected to rise in this population, as cardiovascular diseases remain one of the main causes of morbidity and mortality in the industrialised world.

This trend creates an opportunity for dual-screening of lung cancer and CAD, which has been suggested before but not yet investigated. The ability to screen for lung cancer using CCTA scans, could avoid unnecessary duplication of resources, improve the cost-effectiveness of screening programmes and avoid side effects of radiation exposure.

In this thesis dissertation, I will explore the use of pulmonary nodule volumetry tools in CCTA scans.

To approach this question, we reviewed the scientific literature on incidental findings (IF) in CCTA scans and found that pulmonary IFs are the most common despite the lack of consensus regarding their reporting and management. The prevalence of pulmonary IFs, mostly small pulmonary nodules, supports the premise of dual-role screening and our research's clinical relevance.

Volumetry plays a crucial role in managing indeterminate pulmonary nodules. Volume doubling time (VDT) is currently considered the best predictor of malignancy for indeterminate nodules and is critical to their management and the early diagnosis of lung cancer. However, volumetry is affected by numerous known influencing factors, some of which will be relevant when comparing different scanning protocols such as LDCT and CCTA. Importantly, the volumetry tools dedicated to pulmonary nodules are not validated in CCTA scans.

This research has systematically reviewed the current body of evidence regarding the influencing factors of volumetry and consolidated the current knowledge, highlighting its high heterogeneity and poor clinical applicability.

I approached the question from two complementary perspectives. In the first original study, a multiple linear regression model was used to identify the statistically significant cardiopulmonary hemodynamic factors affecting pulmonary nodule volumetry, including the cardiac cycle phase, the vascular distance between the main pulmonary artery (MPA) and the nodule, and the anteroposterior and craniocaudal location of the nodule as it relates to hydrostatic pressure and vascular cross-sectional area, respectively. Contrary to the results from Boll et al., the cardiac phase was not significant in this study, while the other factors were.

In the second original study, a relative Bland-Altman analysis between the same and opposing cardiac phases found that measurement variability between opposing cardiac phases was increased in a matter that could be clinically significant, potentially resulting in false-positive growth estimation.

Based on the results from these two original studies, a model is presented explaining the influence of cardiopulmonary hemodynamic factors of volumetry based on the physiological notion of 'transit time'. This dissertation argues that cardiopulmonary events like heart failure, which could occur or resolve between two follow-up examinations in LCS, can potentially lead to false positive screening results and must be considered. To minimise measurement variability, measurements in diastole should be consistently favoured when using volumetry in ECG-gated scans.

Significant gaps in current knowledge are exposed and are suggested for future research.

Keywords

Lung cancer; pulmonar nodule; volumetry; cardiopulmonary haemodynamic

Index

List of Figures

List of Tables

List of Acronyms

ACCP	American College of Chest Physicians
ACR	American College of Radiology
AJCC	American Joint Commision on cancer
CAD	Coronary artery disease
CCTA	Coronary CT angiography
CT	Computed tomography
CXR	Chest X-ray
DANTE	Detection and Screening of Early Lung cancer with Novel Technology
DLCST	Danish Lung Cancer Screening Trial
ELCAP	Early Cancer Action Project
HR	Hazard ratio
ICER	Incremental cost-effectiveness ratio
I-ELCAP	International Early Cancer Action Project
IF	Incidental finding
LCS	Lung cancer screening
LDCT	Low-dose CT
LHLP	Liverpool Healthy Lung Programme
LLP	Liverpool Lung Project
LOA	Limits of agreement
Lung-RADS	Lung Imaging Reporting and Data System
LUSI	German Lung Cancer Screening Intervention Study
MILD	Multicentric Italian Lung Detection trial
MPA	Main Pulmonary Artery
NCCN	National Comprehensive Cancer Network
NICE	National Institute for Health and Care Excellence
NELSON	Dutch-Belgian Lung Cancer Screening Trial
NLST	Nation Lung Screening Trial
NNS	Number needed to screen to prevent a single death
NSCLC	Non small cell lung cancer
QALY	Quality adjusted life years
RCT	Randomised control trial
UK	United Kingdom
UKLS	UK Lung cancer Screening
USA	United States of America

1. Introduction

1.1. Lung cancer screening – the road to implementation

Lung cancer has been, and remains, the second most diagnosed malignancy and the leading cause of death from any cancer worldwide. The 5-year survival rate of lung cancer is 16%, despite the significant reduction of smoking in recent years and advances in the various treatment modalities (1,2). In 2020, the International Agency for Research on Cancer reported 2.2 million new diagnoses (11.4% of all cancer diagnoses) and 1.8 million deaths (18% of all cancer mortality) globally (3).

The poor prognosis of lung cancer is partly due to the lack of early symptoms and an effective screening strategy, delaying diagnosis despite clearly known risk factors and a well-defined population at risk (1). Early-stage lung cancer has relatively good outcomes; however, 70% of patients are diagnosed with locally advanced or metastatic disease (2,3). Survival rates in non-small cell lung cancer (NSCLC) are strongly related to the stage at diagnosis, with 5-year survival rates dropping from 90% for stage IA1 to 0% for stage IVB, according to the American Joint Commission on Cancer (AJCC) (3,5).

The first attempts to define a strategy for early diagnosis of lung cancer started in the 60s with chest X-ray (CXR) and sputum cytology as potential screening tests but proved unable to improve mortality rates.

In the 1990s, the Early Lung Cancer Action Project (ELCAP) in the United States of America (USA), which was later expanded internationally (I-ELCAP), screened patients at risk with both CXR and low-dose CT (LDCT), proving the superiority of LDCT for early diagnosis of lung cancer, reducing the radiation dose exposure (from 7 to 1.6mSv when compared to standard dose CT scans) while preserving sensitivity and specificity for the detection of pulmonary nodules (1). Since then, multiple other studies confirmed the usefulness of LDCT in early diagnosis, but it was not until the National Lung Screening Trial (NLST), published in 2011, that lung cancer screening (i.e., three annual rounds of LDCT) was proven to reduce lung cancer-related mortality by 20% and overall mortality by 6.7%. The number needed to screen to prevent a single death (NNS) was 320 screening participants, which compares favourably to other screening programmes like breast (NNS = 570) (6) and colon (NNS = 455) (7). This study helped

to establish the recommendation for annual lung cancer screening in the USA using LDCT (1,8).

Meanwhile, in Europe, the Detection and Screening of Early Lung Cancer with Novel Technology (DANTE) and the Danish Lung Cancer Screening Trial (DLCST) started simultaneously with the NLST. Still, they could not confirm the expected decrease in mortality from lung cancer screening (9,10). The Dutch-Belgian Lung Cancer Screening (NELSON) trial was published in 2018 and demonstrated that LDCT screening in high-risk participants reduced lung cancer mortality by 26% in men and 61% in women at ten years of follow-up (11). In this trial, 69% of lung cancer diagnoses were at stage I, with surgical treatment thrice more common in the screened arm than in the control arm of the study or general population (67.7% vs 24.5%) (11).

The results from the NELSON trial have since been confirmed by the Multicentric Italian Lung Detection (MILD) trial, published in 2019, showing a reduction in mortality from lung cancer of 39% (hazard ratio [HR] of 0.61) and a reduction in overall mortality of 20% (HR 0.8) (12). The German Lung Cancer Screening Intervention Study (LUSI) confirmed a decrease in lung cancer mortality of 26%, which was also more significant in women (HR 0.31) than in men (HR 0.94), suggesting possible sex-specific differences in tumour subtypes (13).

Given these results, multiple medical societies and health organisations have begun to endorse and implement lung cancer screening pilot programmes for high-risk participants.

In the United Kingdom (UK), the UK Lung Cancer Screening (UKLS) randomised controlled trial (RCT) ran from 2010 to 2015. It showed the benefit of LDCT screening by diagnosing 85% of lung cancers at an early stage (stage I and II), 90% of which benefited from potentially curative therapy (14). In 2013, the Liverpool Healthy Lung Programme (LHLP) started and was expected to last three years (15). However, given the very positive preliminary results, it is still recruiting patients with a smoking history or chronic obstructive pulmonary disease (COPD) diagnosis, aged 58 to 75. The five-year risk of lung cancer is estimated using the 'MyLungRisk' calculator, based on the Liverpool Lung Project (LLP) risk model (16). Participants with a ≥5% risk for lung cancer are then screened with LDCT. As of the last preliminary results of the LHLP in 2019, 64% of the lung cancer cases were diagnosed at stage I and reduced lung cancer mortality by 22%, in line with other worldwide trials (15).

Despite these RCTs, pilot screening programmes, and other high-level evidence supporting a screening strategy, formal LCS programmes still need to be implemented nationally in the public healthcare sector worldwide (13,17-20). The long and difficult road taken to prove the benefit of LCS since the 90s emphasises the challenges in implementing a cost-effective LCS strategy and the potential benefit that dual-screening opportunities may have, reducing unnecessary duplication of scans and improving the selection of participants at risk.

1.2. Pros and Cons of lung cancer screening

Persistent open questions regarding the implementation of LCS include the balance between benefits and harms to the patient, the cost-efficiency of the health system, requirements of screening reports, use of risk-stratification tools, integration of tobacco cessation, service implementation, participation rates, etc.

Potential harms of LCS on a high-risk but potentially healthy screening population include radiation exposure, which is known to increase the risk of cancer (2). The increase in lifetime risk of lung cancer in healthy men and women between 50- and 75-year-olds from yearly LDCT scans is estimated to be 0.23 and 0.85%, respectively (21).

False-positive screening results presenting as mostly benign, small, non-calcified pulmonary nodules are present in 22-51% of participants. They may cause morbidity by leading to unnecessary interventions (e.g., follow-up LDCT, referral to a pulmonologist, biopsy, or surgery) (22). Benign pulmonary nodules are highly prevalent in the screening population and represent false positive results, which impact the LCS programmes' cost-effectiveness (23). The definition of a positive screening result in the NLST was any non-calcified pulmonary nodules greater than 4mm. Twenty-seven per cent of scans in the first two rounds of the programme presented a positive result and justified further investigation, although 96% of these were false positives (8). The NELSON trial introduced an additional requirement to positive screening results of >25% volume change, which reduced the positive result rate to 2.7% (from 96% in the NLST) and the false-positive rate to 50% (8, 24-25). Missed lung cancer diagnoses (false negatives) with LDCT range from 0 to 20%, outperforming screening mammography and sigmoidoscopy (20 and 48%, respectively) (26).

Psychological stress and anxiety have been associated with screening for lung cancer, although there is no proven impact on health-related quality of life (27).

Incidental findings (IFs) in LCS are unexpected, unrelated to lung cancer, detected in 19 to 94% of screening LDCT scans, and can potentially impact the patient's health. IFs present as pulmonary, cardiovascular, and gastrointestinal findings in 69, 67 and 25% of scans. These require prompt recognition and often management (17,28). IFs provide an opportunity to diagnose and treat other pathologies, including cardiovascular pathology, non-cancer pulmonary pathology and incidental neoplasms of the thyroid, breast, kidney, liver, oesophagus, pancreas, and mediastinum (2,29). However, IFs cause patient stress and anxiety, raise the cost of LCS, and lack standards regarding reporting and management (which likely explains their wide range of reported prevalence).

The reports on LCS cost-effectiveness are heterogeneous and range from very favourably to unfavourable, related to variability in screening protocols, local cost of LDCT and uncertainty regarding the reduction in mortality (30-34). In the USA, the cost estimate for the NSLT was $81,000 per quality-adjusted life years (QALY) gained per person, with an incremental cost-effectiveness ratio (ICER) of $52,000 per life year (34). These estimates are below the $100,000/QALY recommended in the USA and compare favourably to other well-established screening programmes for breast, colon, and cervical cancer (35). Likewise, the cost-effectiveness of LCS has been investigated in the UK (ICER between £8,000 and £10,000/QALY), also within the recommended threshold by the National Institute for Health and Care Excellence (NICE) (14,36).

In short, adopting LCS programmes on a national and international scale ultimately depends on the balance between its advantages (ability to reduce mortality) and disadvantages (financial cost and the morbidity of unnecessary interventions). There is evidence that, when done properly, LCS can be cost-effective and reduce mortality.

1.3. The measuring problem

Perhaps the major challenge to LCS cost-effectiveness is the need to distinguish cases of early-stage cancer in a population with a high prevalence of benign, small, and non-calcified pulmonary nodules as IFs (false-positive screening results). To this end, the NELSON trial was a landmark trial that changed our understanding of the natural history of lung cancer. Before the NELSON trial, any pulmonary nodule was considered potentially malignant until proven stable for two years. However, the results from the NELSON trial linked the risk of malignancy to the nodule's size. Small nodules (≤100mm^3 in volume or ≤5mm in diameter) were shown to have a low risk of lung cancer (0.4%). The risk of cancer from these small pulmonary nodules is similar to the risk in the absence of any pulmonary nodule, meaning that small pulmonary nodules do not need to be followed over time. Large nodules (>300mm^3 or >10mm) see this risk rise to

16.9% and thus require further management (e.g., PET-CT, biopsy, active surveillance). The risk of malignancy for medium-sized nodules depends on their growth rate, which can be estimated by calculating the nodule's volume doubling time (VDT). The VDT is the time needed for a nodule to double in volume at the current growth rate, calculated using two volume measurements at two different time points. It is considered the best biomarker for estimating the risk of cancer in the group of intermediate-sized nodules (11).

According to the NELSON trial, for nodules between 5 and 10mm in size, the risk of malignancy increases from 0.8% for nodules with a VDT ≥600 days to 9.9% for nodules with a VDT <400 days (22).

Determining the accuracy of volume measurements is possible in phantom or *ex vivo* studies, where the artificial nodules have a specific known volume. Still, the actual volume of an *in vivo* nodule is unknowable. Surgical excision is the gold standard for measuring a nodule's volume. However, cutting the nodule from its dynamic *in vivo* environment causes it to dry and shrink, underestimating the true *in vivo* volume (39). Although artificial nodules are relatively easy to make and study, *in vivo* pulmonary nodules are more complex (i.e., irregular, heterogeneous) and, therefore, more susceptible to partial volume artefacts. Breathing, circulation, parenchymal elastic recoil, and other potential *in vivo* factors may also change its shape and help explain the higher measurement variability of *in vivo* nodules.

Because there is no ground truth regarding the *in vivo* volume of pulmonary nodules, *in vivo* studies often use a test-retest study design (i.e., coffee-break study), where a patient with a pulmonary nodule is scanned twice over a short period (usually a few minutes) with the expectation that real growth has not occurred (i.e., zero-change datasets). This study design investigates the measurement variability of pulmonary nodules' volumetry tools, which is more relevant to growth estimation than measurement accuracy (39). The first coffee-break studies investigated the interscan variability of volumetry tools, which is accepted to be about 25% (22). This interscan variability of volume measurement determines the shortest interval between follow-up CT scans needed to confidently differentiate growth from measurement error (i.e., a stable pulmonary nodule from a suspicious, slow-growing one). This is the rationale for the optimal waiting period of three months between follow-up scans in both clinical follow-up and screening recommendations.

This can be better understood by considering different interscan variability values, as seen in Figure 1.

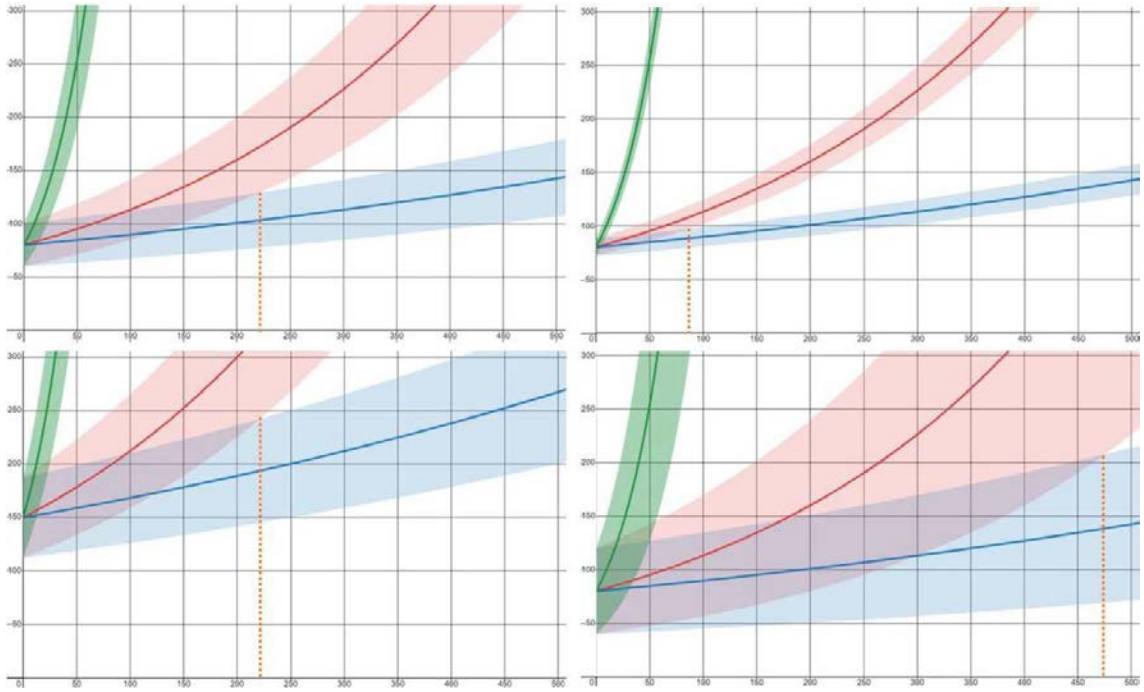

Figure 1. The importance of interscan measurement variability in growth assessment. All graphs present expected volume measurements of 3 pulmonary nodules with different growth rates [i.e., VDT = 30 days, as in inflammatory changes (green); VDT = 250 days, as in malignancy (red); and VDT = 600 days, as in benign pathology (blue)]. The shaded areas represent possible volume measurements over time given the different measurement variability values [top left and bottom left —25%; top right—10%; and bottom right—50%]. Volume measurements in overlapping shaded areas cannot be confidently attributed to one growth rate or another. The starting volume of a nodule [top left—80 mm3; bottom left—150 mm3] does not change the optimal waiting time between follow-up scans for confident discrimination between suspicious and benign pathology (dashed orange line). Still, the measurement variability can be significantly shortened.

To understand the problem, let's consider a stable pulmonary nodule of 113mm^3 (i.e., the volume of a perfect sphere with a 6mm diameter), measured repeatedly with a volumetry tool with a 15% inherent measurement variability (error). In this scenario, the measurements will range from 96mm^3 (5.7mm) to 130mm^3 (6.3mm) in 95% of cases (113mm^3 ± 15%). In the unfortunate event that the lowest measurement is followed by the largest one three months later, this apparent growth of 0.6mm in diameter (i.e., often less than the size of a voxel) is interpreted as a 35% growth in volume and a VDT of 206.38 days, thus suggesting a suspicious lesion (i.e., false positive). This scenario would be unlikely, as each measurement is normally distributed around the mean value of 113mm^3. Still, it does illustrate how a small diameter error translates to a significant volume error and can significantly impact growth estimation.

Volumetry has consistently outperformed other measurement methods, including several 2-D and 3-D methods and the RECIST 1.1. Its ability to estimate the growth rate

of indeterminate pulmonary nodules is why several international scientific societies recommend volumetry for the follow-up of pulmonary indeterminate nodules (22,37-38).

1.4. Volumetry tools

Volumetry tools dedicated to the analysis of pulmonary nodules are automatic (i.e., without human intervention) or semi-automatic (i.e., requiring an initial action from the user) software packages that segment a pulmonary nodule from its surrounding pulmonary structures (e.g., parenchyma, vessels, pleura, etc.). The volume result is the sum of the volume of all voxels that it identifies as being a part of the nodule.

These tools have been available for clinical use for the last two decades. They have gained relevance with their inclusion in the guidelines and recommendations for pulmonary nodule follow-up and pilot LCS programmes' implementation.

Volumetry tools segment pulmonary nodules from surrounding structures using different strategies. Conventional segmentation algorithms use techniques such as region growing, starting from a voxel known to belong to the nodule, and then looking at the surrounding voxels for their attenuation value or other features (e.g., using the contrast between solid tissue and aerated lung parenchyma) to decide on whether to include those latter voxels in the segmentation result. Recently, other strategies, like deep learning algorithms, are being increasingly investigated and making their way into commercially available clinical tools. Deep learning tools are revolutionising the field of volumetry, but new concerns regarding their 'black box' nature and lack of explainability are being debated.

Volumetry is known to be susceptible to several influencing factors, which may be related to the scanner hardware (e.g., radiation dose, slice thickness, kernel, etc.), software (e.g., software package and version), nodule (e.g., size, shape, margins, etc.), patient (e.g., breathing artefacts, pulmonary parenchyma disease), or observer (e.g., manual correction, experience, training). Many studies regarding the impact of these influencing factors have been published, often showing statistical proof of a change in volume measurement or adequacy of the segmentation. However, the clinical relevance of these findings is much less clear and remains an open question.

Studies investigating the radiation dose exposure, the slice thickness, kernel, reconstruction algorithms and software have informed the standard around LDCT protocols used in LCS.

1.5. Follow-up of pulmonary nodules

Despite open questions regarding volumetry tools, international guidelines and recommendations have incorporated the notions of volumetry, VDT and optimal waiting time for intermediate-risk nodules requiring follow-up.

The selection of patients for surveillance is based on the risk assessment, which may be clinical, according to the patient's risk factors and nodule features or use a validated risk model.

The 2013 Evidence-based clinical practice guidelines from the American College of Chest Physicians (ACCP)(40) recommends CT surveillance of pulmonary nodules with low and very low risk of malignancy and in patients at high risk for complications of surgical resection or biopsy and suggests the use of volumetry for growth estimation.

According to the 2015 BTS guidelines (41), CT surveillance is recommended for solid nodules between 5 and 8mm or low-risk solid nodules >8mm, according to the Brock or Herder risk model. These nodules are considered stable and can be discharged if their size does not change significantly (VDT >600 days) over two years using 2-D measuring methods or over one year using volumetry. Conversely, persistent solid nodules with a VDT <400 days show suspicious growth and require further work-up.

The 2017 Fleischner Society's guidelines do not require volumetry, but it allows for the use of volume instead of diameter (42). As such, recommendations are given for small (<6mm or <100mm^3), intermediate (between 6 and 8mm, or 100 and 250mm^3), and large solid pulmonary nodules (≥8mm or ≥250mm^3).

The American College of Radiology (ACR) updated its lung cancer screening proposal, the Lung Imaging Reporting and Data System (Lung-RADS), in November 2022 (43). In Lung-RADS, nodules may be measured using diameter or volume, but unlike the Fleischner guidelines, the volumes are calculated from the diameter-equivalent sphere. This means that volume thresholds are more precise (6mm = 113mm^3, 8mm = 268mm^3, 15mm = 1767mm^3).

The National Comprehensive Cancer Network (NCCN) has published guidelines for use in LCS (1.2022), including criteria for patient selection, evaluation, and follow-up, mostly harmonised with Lung-RADS (44).

1.6. The case for dual-screening

As mentioned, there is a significant overlap between the population at risk of lung cancer and coronary artery disease (CAD), given the common risk factors of age and smoking history. Both diseases are prevalent and leading causes of morbidity and mortality, with high costs to healthcare systems. The number of requests for LDCT and coronary CT angiography (CCTA) is expected to increase sharply in the former case due to the implementation of LCS and in the latter due to the rising availability of CCTA. The ageing demographics of the industrialised world will increase the population that may benefit from either evaluation or, more precisely, from both. LDCT scans are very sensitive to calcified coronary plaques, while CCTA scans also include a significant portion of the lung parenchyma, potentially revealing previously unknown pulmonary nodules. Therefore, patients being followed for one of these diseases may be referred to further evaluation because of IFs related to the other, with some patients being followed for both reasons simultaneously.

This potential duplication of resources creates the opportunity for dual screening between lung cancer and CAD. Perhaps more importantly than avoiding duplication of scans, the ability to use volumetry in CCTA increases the pool of useful previous scans for growth estimation, potentially allowing growth estimation by VDT calculation on the first scan (either CCTA or LDCT) instead of deferring this decision to a subsequent follow-up scan.

However, volumetry is only recommended for indeterminate-risk nodules and non-enhanced CT scans, with surveillance performed using LDCT. Contrary to LDCT, CCTA uses high radiation dose exposure, i.v. contrast enhancement and medication to induce vasodilation. Multiple protocol parameters, including contrast enhancement, are known to alter the volume measurement of currently used volumetry tools and may limit the usefulness of comparing volume measurements between LDCT and CCTA protocols for growth estimation. Despite these difficulties, the ability to use volumetry measurements obtained from both LDCT and CCTA scans could expedite further work-up and diagnosis. Investigating the role of dual-screening and the performance of volumetry tools using CCTA scans may also reveal insights into haemodynamic influences in volumetry. These haemodynamic influences are relevant for participants of LCS as this population shares risk factors that put them at high risk for cardiovascular events, potentially impacting the growth estimation of nodules under follow-up.

This dissertation explores the potential for dual screening and is based on four publications. Work on the edges of the research investigated the prevalence of IFs of CCTA, as reported in the literature, and in particular, the prevalence of incidental

pulmonary nodules that may benefit from clinical management and surveillance (46). This work helped establish the potential need for dual screening, identified the lack of standardisation for reporting IFs and proposed a clinical checklist with clear recommendations regarding their reporting and management. Still at the edges of the research, another publication summarised in a systematic review the large body of evidence regarding influencing factors of volumetry tools dedicated to pulmonary nodules (47). This systematic review summarised 137 original studies investigating the impact of all known influencing factors in the outcomes of volumetry tools, critically assessed the current scientific literature regarding the clinical relevance of the available body of evidence, exposed the gaps in current knowledge, and provided a model for understanding the mechanism of the impact of these influencing factors on volumetry tools. It sets the current state-of-the-art and illustrates the differences between our approach and the single previous study (45) investigating our research space.

At the core of the research, two publications addressed from two complementary perspectives, the impact of cardiopulmonary haemodynamic factors, like the cardiac cycle phase, on volumetry tools. The first study investigates the effects of these factors using a multiple linear regression model (48). The second study investigates the measurement variability in different phases of the cardiac cycle using a Bland-Altman analysis (49). This dual approach to the problem is reflected in the proposed model explaining the effects of these cardiopulmonary haemodynamic factors based on the physiological notion of 'transit time'.

2. Aims and outline of the thesis

2.1.The Problem:

The relevant scientific societies recommend volumetry for the follow-up and screening of indeterminate pulmonary nodules. However, these tools present variability in their measurement, which is significantly under-investigated and may change therapeutic decisions in specific cases, putting patients at potential risk.

The known overlap of patients at risk of lung cancer and CAD (e.g., age, smoking history) supports dual screening of both diseases by either LDCT or CCTA.

Cardiopulmonary hemodynamic interactions are complex and may impact volumetry tools via the propagation of blood pressure through the pulmonary vessels, hydrostatic pressure differences, and propagation of the shock wave induced by the moving heart. These interactions may be assessed using the cardiac cycle phase and other factors related to pulmonary blood pressure (e.g., the difference in the calibre of the main pulmonary artery [MPA] between systole and diastole, vascular distance from the heart to the nodule), hydrostatic pressure (e.g., location of the pulmonary nodule along the anteroposterior axis) and vascular cross-sectional (e.g., location along the craniocaudal axis). The influence of these factors on the outcome of volumetry tools dedicated to pulmonary nodules of intermediate size needs to be appropriately studied and understood. Faced with this problem, the research question is posed as follows: do cardio-pulmonary haemodynamic interactions influence the volumetry of pulmonary nodules?

2.2. Hypothesis:

We suggest that cardiopulmonary haemodynamic interactions can change the accuracy and variability of volumetry tools dedicated to pulmonary nodules between 5 and 8mm in size and impact their usefulness in growth estimation.

2.3. Primary objective:

1. To investigate how the cardiac cycle phase and other factors related to cardiopulmonary haemodynamic interactions affect volumetry tools dedicated to pulmonary nodules between 5 and 8mm in size.

2.4. Secondary objectives:

1. To investigate the potential role of dual screening using CCTA scans.

2. To consolidate the available evidence regarding factors influencing the outcome of volumetry tools dedicated to pulmonary nodules.

3. Materials and Methods

3.1. Study 1: The impact of cardio-pulmonary factors in pulmonary nodule volumetry

This study aimed to investigate how factors known to be related to cardiopulmonary circulation, namely the cardiac cycle phase during image acquisition, the distance between the MPA and the pulmonary nodule, the change in diameter of the MPA between systole and diastole, location of the pulmonary nodule (concerning hydrostatic pressure and vascular cross-sectional area), and presence of cardiomegaly, affect the results of volumetry tools currently in clinical use so that we can better understand their potential applications and limitations.

The Institutional Research Committee Review Board approved this retrospective study (cross-sectional, observational, analytical) and waived the requirement for written informed consent because of the exclusive use of existing data.

3.1.1. Study sample

The study sample included all consecutive CCTA examinations performed at a tertiary cardiothoracic centre from 2016 to 2019. All scans were performed with the same equipment (Somatom Definition Flash; Siemens).

The imaging protocol used for the CCTA examinations is shown in Table 1.

Table 1. Imaging protocol for coronary CT angiography (CCTA)

CCTA Imaging protocol parameters	
Range	From the carina to the apex of the heart
Respiratory phase	Inspiration, breath-hold
Contrast enhancement	75 – 95ml of Niopam 370 (iopamidol), at 5 – 7ml/s
Image reconstruction	2mm thickness, 0.75mm overlap
Kernels	B20f smooth/mediastinum, B60f sharp/lung
Acquisition parameters	Peak kilovoltage (kVp) between 100 and 120kV; current modulation (CareDose 4D) with 320mAs as reference
Average acquisition time	1-2s

The inclusion criteria comprise scans showing at least one solid non-calcified pulmonary nodule with a long-axis diameter between 5 and 8 mm. Exclusion criteria

include the absence of an adequate systolic or diastolic phase archived in the hospital's picture archiving and communication system (PACS), defined as 30–40% for systole and 70–80% for diastole; or if the pulmonary nodule was not shown in the field of view (FOV) of both systole and diastole.

3.1.2. Readers and measurements

Two cardiothoracic radiologists with ten (reader 1) and five (reader 2) years of experience identified and measured solid non-calcified pulmonary nodules according to the protocol described in Figure 2 and using the Carestream Vue PACS v 11.4.01.1011 (Carestream Health, Inc, Rochester, NY; tool 1) and Syngo via VB20 (Siemens Healthineers AG, Erlangen, Germany; tool 2) commercially available volumetric software packages based on region-growing algorithms.

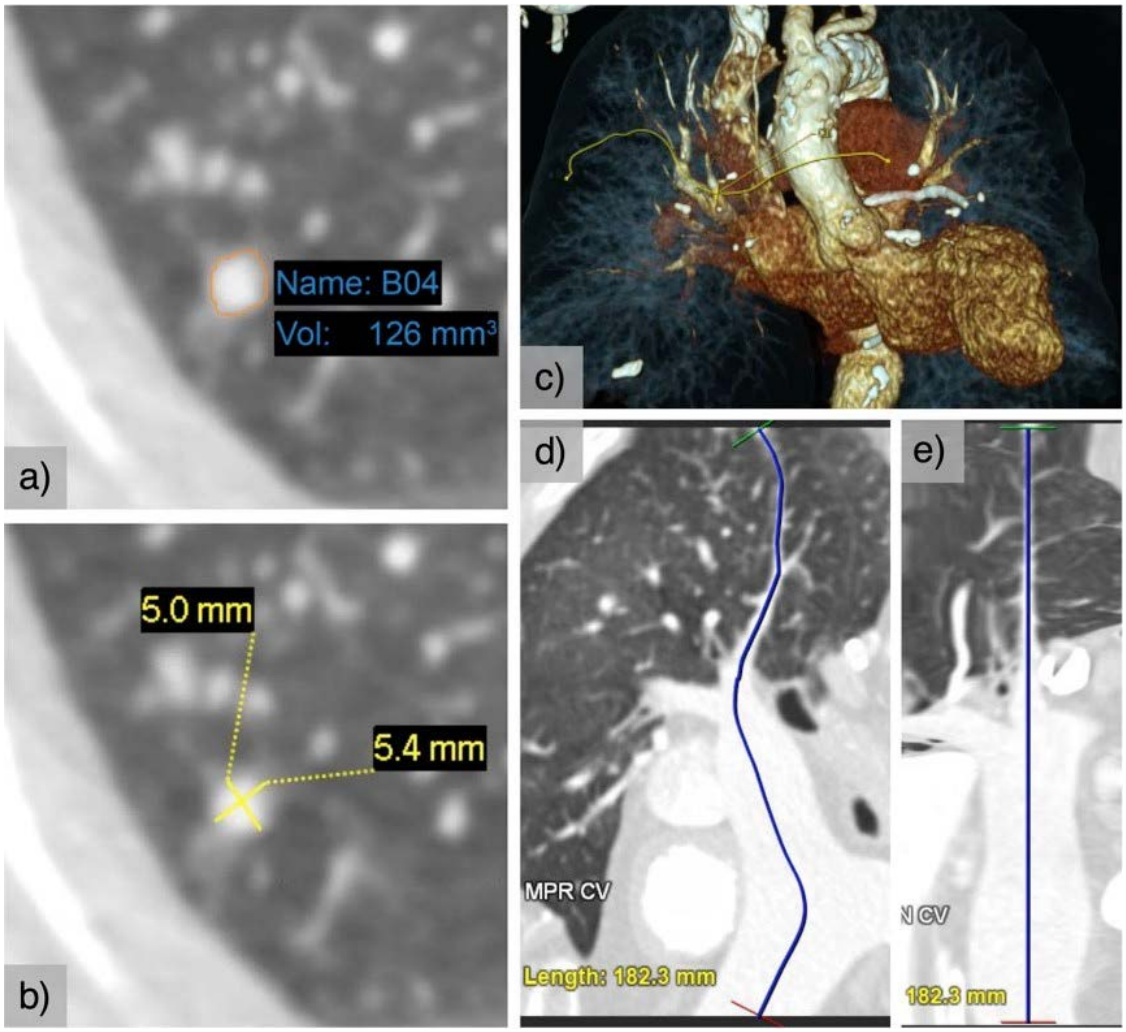

Figure 2 – Measurements performed on the pulmonary nodules using the volumetry tools, electronic callipers and multiplanar reconstructions. **a)** Volume measurement using the volumetry tool; **b)** manual long- and short-diameter measurement using electronic calipers; **c-e)** tracking the vascular distance between the proximal MPA (at the level of the pulmonary valve) and the nodule.

Both these tools performed semiautomatic segmentation by placing one seed point in the centre of the nodule. The readers did not correct the resulting segmentation.

If the two readers disagreed on whether an appearance was a true nodule, a consensus decision was made between the two readers and another cardiothoracic radiologist with more than 25 years of experience.

For each nodule identified, the following information was recorded: reader; software package used; patient age and sex; failed segmentation of the nodule, defined as three consecutive failed attempts; nodule segmentation appropriateness, defined as complete pulmonary nodule inclusion with the exclusion of adjacent structures; semiautomatic volume measurement; long- and short-axis diameters in the axial plane, measured manually and semiautomatically, and rounded to one decimal place; distance from the MPA, at the level of the pulmonary valve, to the nodule (vascular distance) measured using curved plane reconstruction; location of the pulmonary nodule in the axial (anterior; middle; posterior) and coronal plane (superior; middle; inferior); the diameter of the MPA in systole and diastole, measured at the level of the pulmonary valve and in the axial plane; and the presence of cardiomegaly.

3.1.3. Statistical analysis

Data were analysed using SPSS software (ver. 26.0; IBM Corporation, Armonk, NY, USA).

The interquartile range (IQR) method detected outliers in volume measurements. Outliers and cases where segmentation failed were excluded from further analysis.

The average of long- and short-axis manually measured diameters (average diameter) was calculated for all included cases according to the recommendations of the Fleischner Society [42]. In addition, a continuous variable representing the difference in the MPA diameter between systole and diastole measured in the axial plane and at the level of the pulmonary valve was calculated for all nodules.

A multiple linear regression model using a stepwise automatic selection of significant variables was used to predict volume measures based on the reader, software package, cardiac cycle phase, appropriateness of segmentation, average diameter, vascular distance, the difference of the MPA diameter between systole and diastole, location of the pulmonary nodule in both axial and coronal planes, presence of cardiomegaly, age, and sex.

The intraclass correlation coefficient (ICC) with an absolute agreement-type two-way mixed model was used to assess inter-observer and inter-software agreement.

3.2. Study 2: Variability of pulmonary nodule volumetry on coronary CT angiograms

The Institutional Research Committee Review Board approved this retrospective cross-sectional study (observational, analytical) and waived the requirement for written informed consent due to the use of existing clinical data.

3.2.1. Study sample

The study sample includes consecutive patients who underwent a CCTA scan in our institution between January 1, 2016, and December 31, 2019. This study sample is identical to the study sample used in the previous study (section 3.1.).

All patients had one or more CCTA scans performed on the same equipment (Somatom Definition Flash; Siemens). Images were acquired during inspiration and contrast injection (75–95 mL of Niopam 370, at 5–7 mL/s), with anatomical coverage from the carina through the cardiac apex. Acquisition parameters include peak kilovoltage (kVp) between 100–120 kV; current modulation (CareDose 4D) with 320 mAs as the reference; average acquisition time of 1–2 seconds; collimation of 128×0.6mm; and pitch of 3.4. Reconstruction parameters include 2mm and 0.75mm overlapping slices through the prescribed range, with a B20f algorithm and field of view (FOV) of 22 cm.

The study's inclusion criteria comprise scans with one or more incidental solid, noncalcified pulmonary nodules within the FOV in systole and diastole, measuring between 5 and 8mm in long-axis diameter. Exclusion criteria comprise the absence of systolic (30–40%) or diastolic phase (70–80% of the cardiac cycle) in the archive; or when one of the cardiac phases did not present the pulmonary nodule in its FOV.

3.2.2. Observers and measurements

Two cardiothoracic radiologists with ten (observer 1) and five years of experience (observer 2) identified nodules fitting the eligibility criteria within the study sample. In addition, a consensus decision between both observers and a third chest radiologist (with >25 years of experience) resolved disagreements regarding whether an appearance met the inclusion criteria.

Each observer measured each nodule using two different pulmonary nodule volumetry software packages in systole and diastole. The software packages used were Carestream Vue PACS v 11.4.01.1011 (Carestream Health, Inc, Rochester, NY) and Syngo via VB20 (Siemens Healthineers AG, Erlangen, Germany), as tool1 and tool2, respectively.

Both tools performed semiautomatic segmentation by placing one seed point in the middle of the nodule. The observers did not correct the resulting segmentation. Still, they recorded the adequacy of the segmentation as "inadequate" if three consecutive segmentation attempts had failed or when the segmentation did not adequately represent the nodule. Also recorded were the observer's initials; software package used; cardiac phase; long-axis diameter of the nodule; location of the nodule in axial and coronal planes; and nodule volume calculated using the volumetry tool.

3.2.3. Statistical analysis

The data were analysed using SPSS software (ver. 26.0; IBM Corporation).

A descriptive statistical analysis of the included nodules was performed.

All cases with inadequate nodule segmentation were excluded from further analysis.

The association of volume measurements was tested using Kendall tau correlation coefficients (τ) between different cardiac phases, software packages and observers.

The Bland-Altman analysis is a well-known statistical tool for method comparison and has been used previously to study the variability of pulmonary nodule volumetry (50). Bland-Altman analysis and plots tested the volume measurement agreement. In addition, further inter-observer analyses of the systolic and diastolic data subsets were performed.

The estimation of the limits of agreement (LOA) in the Bland-Altman analysis used the nonparametric quartile analysis after the exclusion of normality of the differences of measurements. Possible reasons for this non-normal distribution include the presence of a natural limit (i.e., volume must be a positive number) and the restriction of the nodules' diameter between 5 and 8mm (i.e., sorted by diameter).

3.3. Study 3: Incidental chest findings on coronary CT angiography: a pictorial essay and management proposal

Numerous incidental pulmonary findings were detected during the review of the cases for this research. Lack of uniformity in how we report and express management recommendations to the IFs observed during the study justified the need for a separate publication proposing a more uniform approach to IFs in CCTA scans, guiding their reporting and management.

The Institutional Research Committee Review Board approved the research study and waived the requirement for written informed consent due to using existing clinical data.

3.3.1. Study sample

The study is a retrospective cross-sectional study.

The study sample is a subset of the study sample of the main study, with scans performed between 2018 and 2019 using the same CT scanner equipment and CCTA protocol.

3.3.2. Readers and measurements

A single thoracic radiologist reviewed the images and identified scans with features of IFs, defined as CCTA findings that can potentially affect the patient's health and are unrelated to the primary purpose of identifying lung cancer.

3.3.3. Statistical analysis

A simple descriptive statistical analysis was performed, including the incidence of each identified incidental finding.

3.4. Study 4: Influencing factors in pulmonary nodule volumetry tools: Systematic review and attempted meta-analysis

The protocol and search strategy were registered with PROSPERO with the registration number CRD42022370233. The PRISMA flow diagram is presented in Figure 3.

The authors defined the primary and secondary research questions as "What factors influence the outcome of volumetry tools dedicated to pulmonary nodules?" and "What is the clinical significance of their effect?" respectively.

The authors searched the following databases on the 21st of September 2022: MEDLINE, SCOPUS, Journals@Ovid, Embase, and Ovid Emcare, using the query: (((Volume OR Volumetry OR Volumetric) AND (lung OR pulmonary) AND (nodule OR nodules)).

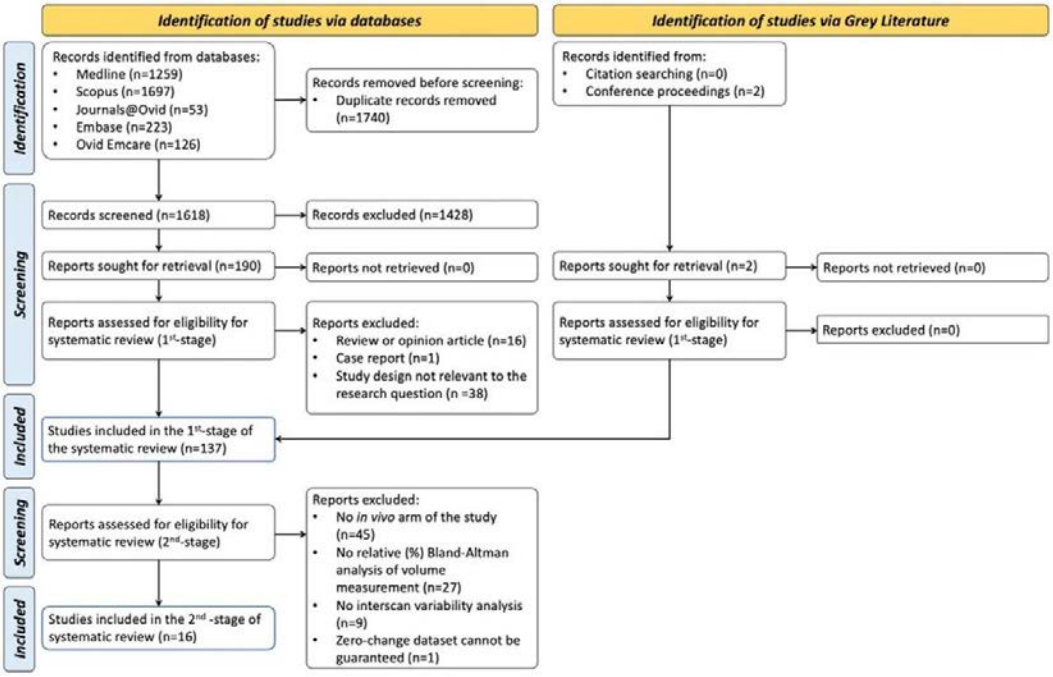

Figure 3. Prisma flow diagram describing the results of the search and selection process.

3.4.1. Eligibility criteria

The inclusion criteria were defined as follows:

• Original research studies using dedicated volumetry tools in solid or part-solid pulmonary nodules.

• Study design explicitly testing the potential impact of influencing factors on these tools' outcome (i.e., volume, segmentation quality).

The exclusion criteria were defined as follows:

• Case reports, reviews or opinion articles.

• Study design exclusively investigating ground-glass opacities (GGOs), using a dedicated (i.e., less generalisable) segmentation algorithm.

The authors excluded duplicate records using the Rayyan online tool (Perdue University).

3.4.2. Assessment of methodological quality

The quality of the included studies was assessed independently by two authors (chest radiologists with over five years of experience in LCS) based on the revised Quality Assessment of Diagnostic Accuracy Studies (QUADAS-2), and all disagreement was

resolved through discussion with a third chest radiologist. The risk of bias was rated as high, low, or unclear.

3.4.3. Data extraction

Both authors agreed on the final list of reports and retrieved the respective full articles.

Non-English articles (i.e., Chinese, German) were translated using an online service (www.translated.com).

The authors then screened the complete reference lists of all included articles for additional pertinent entries. Grey literature reports were used to identify potential candidate studies.

The variables collected included population, nodule features, statistical methodology, influencing factor(s), outcome variable, observed effect(s), interactions between different influencing factors, and the statistical significance of relevant tests.

3.4.4. Statistical analysis and Data presentation

To assess the evidence for clinical significance, we selected all in vivo studies reporting interscan variability using relative Bland-Altman analysis. The variables collected at this stage included: influencing factor(s), systematic bias, LOA, and sub-group analysis. The LOA was deduced from the standard deviation and systematic bias if needed. When appropriate, the authors synthesised LOA and systematic bias from groups of studies using the inverse-variance method with a random-effects model (SPSS v26 [IBM, Armonk, NY, USA]).

The heterogeneity between the primary studies was assessed using the heterogeneity variance (τ^2) and Forest plots. If comparing more than ten studies, the Deeks' funnel plot was planned to evaluate study asymmetry and potential publication bias.

Missing values were excluded after an unsuccessful attempt to contact the corresponding author of the primary study.

4. Results

4.1. Study 1: The impact of cardio-pulmonary factors in pulmonary nodule volumetry

Of 5973 CCTA scans performed, 4478 were excluded because either a systolic or diastolic phase was missing from PACS. In addition, 1357 scans were excluded for not presenting qualifying solid pulmonary nodule(s) in both systolic and diastolic FOV, and 31 scans were excluded after a consensus decision because they did not represent true nodules. Of the remaining 107 CCTA scans, 195 solid, non-calcified nodules were identified with a long-axis diameter between 5 and 8 mm.

The mean age of the patients was 67.8 years, and the male-to-female ratio was 1.38 (Table 2).

Table 2. Patient demographics and indications for CCTA

Patient characteristics	**(n = 107)**
Age (years): M ± SD	67.8 ± 11.7
Sex: Male / Female (Male % / Female %)	62 /45 (57.9% / 42.1%)
Male to Female ratio	1.38
Indication for the CCTA examination: n (%)	
Acute or chronic chest pain	47 (43.9%)
Hypertension	16 (14.9%)
Diabetes Mellitus	13 (12.1%)
Abnormal or equivocal stress test	9 (8.4%)
Dyspnea	8 (7.4%)
Pre-operative	5 (4.7%)
Abnormal ECG	3 (2.8%)
Congestive heart failure	3 (2.8%)
Palpitations	3 (2.8%)

M – mean; **SD** – standard deviation

Each reader measured each pulmonary nodule in systole and diastole using each software tool. A total of 1560 measurements (8 measurements per nodule) were performed.

Nodule segmentation failed in 11 measurements (1.41%) using the Carestream Vue PACS software package and in 15 measurements (1.92%) using the Syngo via the software package. However, the segmentation was considered appropriate more often using the

Syngo via software package (n = 685; 87.8%) than the Carestream Vue PACS software package (n = 623; 79.9%).

A total of 204 measurements were identified as outliers using the IQR method and removed from further analysis.

The outliers' mean volume and standard deviation were 586.8 ± 1500.8 mm^3, with a minimum of 159 mm^3 and a maximum of 13,300 mm^3.

Nodules were more frequently identified in the upper third (49.2%) in the axial plane, and between the middle (39.5%) and posterior (40.5%) thirds of the FOV, in the coronal plane.

A descriptive statistical analysis is provided in Table 3.

Table 3. Descriptive statistical analysis of quantitative variables

n = 1322	**M±SD**	**Min**	**Q1**	**Q2**	**Q3**	**Max**
Volume (mm^3)	43.527±30.065	2.0	22.0	34.1	58.1	152.0
Automatic long-axis diameter (mm)	6.375±1.697	3.9	5.2	6	7.2	13.0
Automatic short-axis diameter (mm)	5.386±1.104	2.9	4.7	5.3	6	7.7
Manual long-axis diameter (mm)	6.101±1.001	4.3	5.2	6.5	7.1	8.5
Manual short-axis diameter (mm)	4.255±0.789	2.9	3.9	4.2	4.7	6.5
Average diameter (mm)	5.178±0.773	3.5	4.4	5.5	5.9	7.5
Vascular distance (cm)	18.405±3.178	10.6	16.0	18.4	20.7	26.4
Difference of the MPA diameter between systole and diastole (mm)	2.295±1.522	0.1	1.0	2.0	3.3	6.3

MPA – main pulmonary artery

The results of the regression model are presented in Table 4. The model explains 55.3% of the variation in volume measurement ($R^2 = 0.553$) and yields significant results ($F_{8,1313} = 202.785$, $p < 0.001$) without significant autocorrelation (DW = 1.871) or multicollinearity (VIF < 2).

Table 4. Parameter estimates for the prediction of nodule volume

Variable	**B**	**CI_{95}**	***t***	**p**	**Effect size**
(Constant)	-37.40	[-48.82,-25.98]	-6.426	***<0.001	0.030
Appropriate segmentation	-32.69	[-37.17,-28.20]	-14.291	***<0.001	0.135
Average diameter	24.10	[22.66,25.54]	32.824	***<0.001	0.451
Vascular distance	-0.98	[-1.42,-0.54]	-4.368	***<0.001	0.014
Difference of the MPA diameter between systole and diastole	2.26	[1.52,2.99]	6.019	***<0.001	0.027

Lower third (coronal)	13.38	[9.84,16.93]	7.410	***<0.001	0.040
Posterior third (axial)	7.87	[5.46,10.29]	6.407	***<0.001	0.030
Sex (male as reference)	-3.45	[-5.79,-1.11]	-2.895	**0.004	0.006
Cardiomegaly	7.05	[2.59,11.51]	3.103	**0.002	0.007
Excluded variables					
Cardiac cycle phase				0.348	
Reader				0.590	
Volumetry tool (software package)				0.341	
Middle third (axial)				0.978	
Middle third (coronal)				0.505	
Age				0.165	

MPA – main pulmonary artery, **B** – parameter coefficient, **CI_{95}** – 95% confidence interval, ***t*** – t-test
*** $p < 0.001$; ** $p < 0.01$; **Effect size** – partial eta square (ζ^2)

The results show that the volume measurement increases with the average diameter (B = 24.10; CI_{95} [22.66, 25.54], $p < 0.001$), with the increasing difference of the MPA diameter between systole and diastole (B = 2.26; CI_{95} [1.52, 2.99], $p < 0.001$); when it is in the lower third (B = 13.03; CI_{95} [9.00, 17.06], $p < 0.001$) compared to the upper (reference) in the coronal plane; and when it is in the posterior third (B = 8.94; CI_{95} [5.64, 12.24], $p < 0.001$) compared to the anterior (reference) in the axial plane.

Volume measurement decreases when segmentation is considered appropriate (B = – 32.69; CI_{95} [– 48.82, – 25.98], $p < 0.001$), and with increasing vascular distance (B = – 0.98: CI_{95} [– 1.42, – 0.54], $p < 0.001$).

The effect size is larger for the average diameter ($\zeta^2 = 0.451$, large), followed by the appropriateness of segmentation ($\zeta^2 = 0.135$, intermediate to large), the location of the pulmonary nodule in the lower third ($\zeta^2 = 0.040$, small to intermediate) or the posterior third ($\zeta^2 = 0.030$, small) of the FOV, the difference of the MPA diameter between systole and diastole ($\zeta^2 = 0.027$, small) and for the distance between the MPA and the pulmonary nodule ($\zeta^2 = 0.014$, small).

The results also show a tendency for the nodule to be slightly larger in the presence of cardiomegaly (B = 7.05; CI_{95} [2.59, 11.51], $p = 0.002$) and somewhat smaller in women (B = – 3.45; CI_{95} [– 5.79, – 1.11], $p = 0.004$), but with a negligible effect size.

The cardiac cycle phase is not statistically significant in our regression model ($p = 0.348$), and there was no statistically significant difference in volume measurements based on the cardiac phase using multivariate tests ($F_{7,1518} = 0.428$, $p = 0.885$, Wilks' lambda (Λ) = 0.998, partial $\eta^2 = 0.002$).

Intraclass correlation analysis (Table 5) shows very high reliability between the two readers (ICC = 0.870; CI_{95} [0.850, 0.887]) with no statistically significant difference

between them ($F_{1,764}$ = 0.561, p = 0.561). There is no reasonable reliability between the two software packages (ICC = 0.059; CI_{95} [– 0.083, 0.183], p = 0.002), and there is a statistically significant difference between the measurement made with the two software tools ($F_{1,760}$ = 9.473, p = 0.002).

Table 5. ICC between readers and software tools for volume measurement

	ICC	**CI_{95}**	**F**	**p**
Between readers				
Global sample	0.870	[0.950,0.887]	0.561	0.454
Systole	0.865	[0.834,0.889]	0.692	0.409
Diastole	0.965	[0.958,0.972]	0.373	0.542
Between software packages				
Global sample	0.059	[-0.083,0.193]	9.473	**0.002
Systole	0.027	[-0.186,0.203]	6.302	*0.012
Diastole	0.545	[0.441,0. 630]	12.559	***<0.001

ICC – Intra class coefficient, **CI95** – 95% confidence internal
*** p < 0.001; ** p < 0.001; * p < 0.1

4.2. Study 2: Variability of pulmonary nodule volumetry on coronary CT angiograms

Of 5973 candidate CCTA scans performed between 2016 and 2019, 4478 were excluded for not having both a systolic and diastolic phase in the archive. Of the remaining 1495 scans, 1357 were excluded for not having qualifying solid pulmonary nodules in both systolic and diastolic phases, and 31 scans were excluded after a consensus decision (as not representing true nodules).

From the 107 scans included, 195 nodules were identified with a manual long-axis measurement between 5 and 8 mm. Nodules were more frequently identified in the upper thirds of the FOV in the coronal plane (49.2%) and between the middle (39.5%) and posterior (40.5%) thirds in the axial plane.

For each nodule, each set of volume measurements was repeated by each observer for systole and diastole, using each software package, resulting in a total of 1560 volume measurements. Figure 4 provides an example of measurement. The quality of the nodule segmentation was considered inadequate in more cases using one software package (tool 1; n = 157; 20.1%) than the other (tool 2; n = 95; 12.2%)

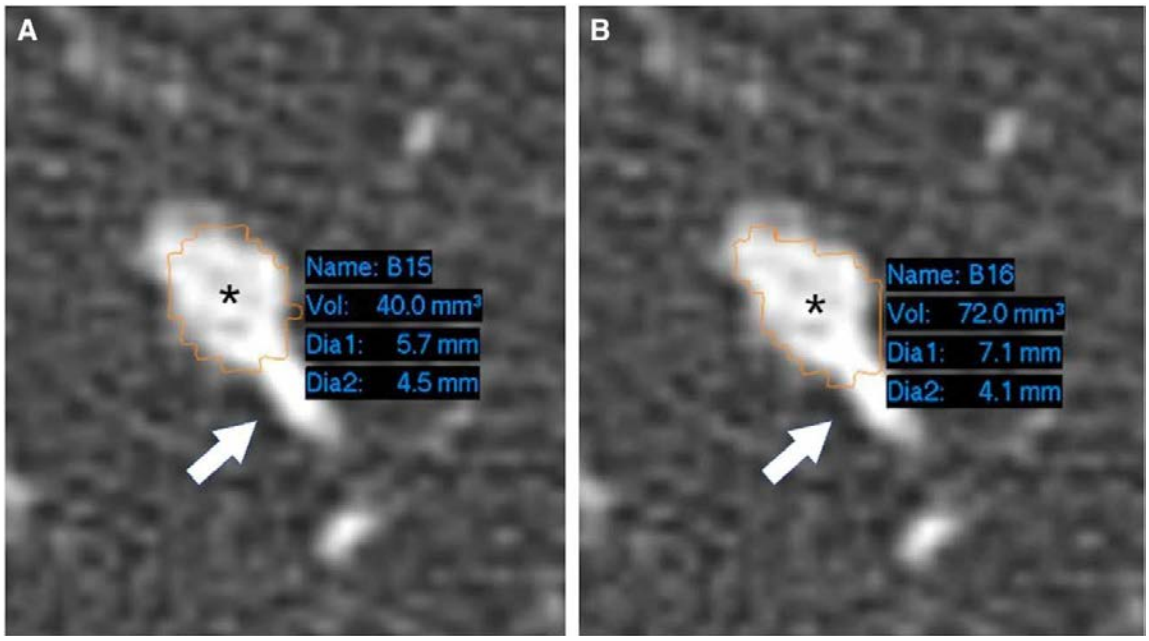

Figure 4. Example of measurements using one volumetry tool in systole and diastole. An example of a nodule included in the study was measured in systole (A) and diastole (B). The seed points (*) were placed in the nodule centre, and the yellow lines show the semiautomatic segmentation result, which both observers did not correct and considered adequate. Notice the small vessel (arrows) approaching the nodule, which was excluded from the segmentation in both instances. The volume measured in diastole was 80% greater than in systole.

The mean volume was close to 50mm^3 with a median of 35mm^3, ranging from 10.4 to 400 mm^3 (Table 6).

Table 6. Descriptive statistical analysis of volume measurements in the sample population and at different phases of the cardiac cycle, using different software packages and by different observers

Volume	n	Mean (mm^3)	SD (mm^3)	Q_1 (mm^3)	Median (mm^3)	Q_3 (mm^3)
Sample population	1237	63.282	68.039	24.5	38	69
Between systole and diastole						
Systole	645	51.99	46.11	23.375	36	62
Diastole	645	50.836	44.947	23.3	35.5	60.4
Difference		-1.154	13.13	-3.6	-0.5	1.7
Between different observers						
Software tool 1	616	47.108	38.438	23.3	34.5	59.8
Software tool 2	616	48.807	42.257	22	35	59
Difference		1.699	15.942	-3.25	-2	6.7
Between different observers						
Observer 1	642	53.62	46.993	24	36.6	62.9
Observer 2	642	52.91	47.172	23.4	36.2	62

Difference		-0.701	8.723	0	0	0
Between different observers (systolic dataset)						
Observer 1	318	44.668	29.936	23.4	34.9	59
Observer 2	318	43.751	29.583	23	34.05	58
Difference		-0.917	9.911	0	0	0
Between different observers (diastolic dataset)						
Observer 1	322	43.862	29.316	23	34.6	57.2
Observer 2	322	43.019	28.611	23	34	55
Difference		-0.842	6.806	0	0	0

Q_1 – first quartile, **Q_3** – third quartile, **SD** – standard deviation

The volume measurements of the solid pulmonary nodule show a very strong association between systole and diastole, with a Kendall tau correlation coefficient (τ) of 0.812 (CI_{95} = [0.785; 0.838], df = 645, P < .0001); between software packages with a τ = 0.744 (CI_{95} = [0.714; 0.771], df = 616, P < .0001); and between different observers, with a τ = 0.942 (CI_{95} = [0.916; 0.957], df = 682, P < .0001) globally; τ = 0.928 (CI_{95} = [0.874; 0.955], df = 338, P < .0001) for the systolic dataset; and τ = 0.956 (CI_{95} = [0.931; 0.971], df = 344, P < .0001) for the diastolic dataset.

The Bland-Altman plots show an increase in the differences' variability as the measurement's magnitude increases, particularly for different cardiac phases and software packages. The estimated LOA of the per cent Bland-Altman plots are [−47.0%; 52.3%] between phases of the cardiac cycle and [−50.1%; 68.2%] between software packages (Figure 5 and Table 7), with no significant bias.

The estimated LOA of the per cent Bland-Altman plots between different observers are [−14.5%; 27.8%] globally, [−13.6%; 31.4%] for the systolic dataset and [−13.9%; 19.7%] for the diastolic dataset.

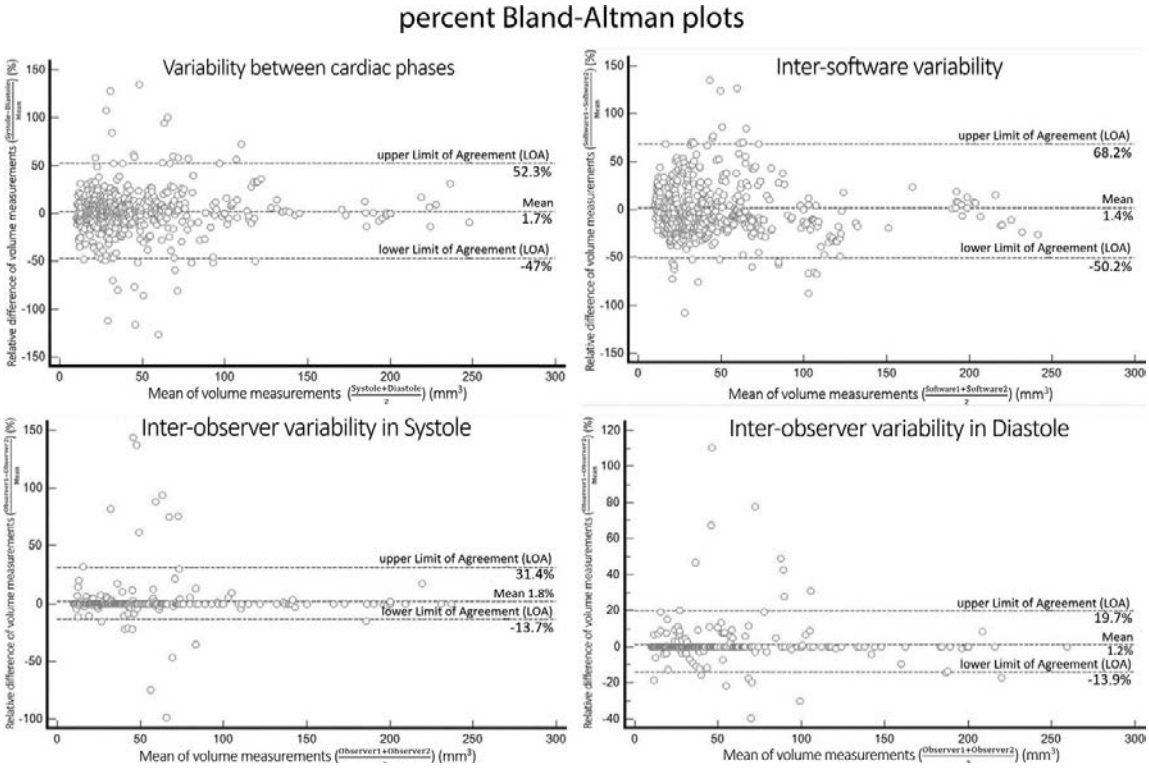

Figure 5. Relative Bland-Altman plots with estimated limits of agreement of volume measurements in different phases of the cardiac cycle, different software packages and different observers. The top left corner shows the comparison between volume measurements in systole and diastole, followed by the comparison between different software packages (top right corner), between different observers in systole (bottom right corner) and in diastole (bottom left corner).

Table 7. Results of the Bland-Altman analysis

	Bland-Altman (mm³)			**Per cent Bland-Altman (%)**		
	Bias	**Lower LOA**	**Upper LOA**	**Bias**	**Lower LOA**	**Upper LOA**
Between systole and diastole	1.15	-24.91	36.76	1.73	-47.02	52.29
Between software packages	1.7	-39	34.08	1.35	-50.16	68.21
Between observers	0.7	-6.2	17.39	1.49	-14.45	27.77
Between observers (systolic dataset)	0.88	-4.7	24.47	1.75	-13.63	31.36
Between observers (diastolic dataset)	0.53	-8.58	15.85	1.23	-13.92	19.66

LOA – estimated limits of agreement

4.3. Study 3: Incidental chest findings on coronary CT angiography: a pictorial essay and management proposal

The results from this study confirm that pulmonary IFs are common in CCTA scans. We used the collected iconography to illustrate the wide range of pathologies incidentally identified in CCTA.

We present a pictorial essay and systematic checklist of IF in CCTA scans to illustrate the most common IFs organised by organ.

In the publication, the author reviews the current literature on IFs on CCTA scans, focusing on their prevalence, appropriate communication and triggering of clinical pathway systems.

The proposed checklist of IFs on CCTA scans per organ or system is presented in Table 8.

Table 8. Checklist of incidental findings on CCTA per organ/system

Lung

Solid pulmonary nodule

< 5 mm or < 80 mm3 with no suspicious features (e.g., granulomas, IPLNs)

→ Reporting is optional, and no follow-up is required

> 5 mm, previously unknown or with suspicious features

→ Report and alert the respiratory team

5-8 mm → Baseline LDCT and provide an LDCT follow-up schedule

5-6 mm: LDCT within one year

6-8 mm: LDCT within three months

> 8 mm or > 300 mm3 → Assess the risk of cancer (Brock model)

< 10% risk of cancer: baseline LCDT and follow-up LDCT within one year

≥ 10% risk of cancer: referral to lung cancer MDT

Subsolid pulmonary nodule

≥ 5 mm → Report to and alert the respiratory team

→ Baseline LDCT and provide a follow-up schedule within three months

Stable after ≥ 3 months: assess the risk of cancer (Brock model)

< 10% risk of cancer: follow-up LDCT within one year

≥ 10% risk of cancer: referral to lung cancer MDT

Growing or altered morphology → Referral to lung cancer MDT

Pulmonary emboli → Report and urgent referral to the respiratory team

ILAs → Report to and alert the respiratory team

In the presence of respiratory symptoms, physiological abnormalities, gas transfer abnormalities and extensive CT changes → Referral to the respiratory team/ILD MDT meeting

In the presence of risk factors for progression → Follow-up may be appropriate even after exclusion of ILD (the optimal interval for follow-up CT scanning is unknown)

Infection/Consolidation

→ Report and referral to the respiratory team if not already under their care

→ CT reassessment after therapy

Emphysema → Report and grade severity

Bronchiectasis, atelectasis → Report

Pleura

Pneumothorax (rare) → Report and urgent referral to the medical emergency team

Pleural plaques → Report

in lung cancer patients: differentiate pleural plaques from pleural metastases

in asbestos exposure: assess signs suspicious for mesothelioma

Pleural effusion → Report

in cardiac patients it may be related to heart failure: trigger an alert

Mediastinum

Pneumomediastinum (rare) → Report and urgent referral to the medical emergency team

Mediastinal nodule or mass → Report

if presenting suspicious features → Referral to the cardiothoracic surgical team

if benign-looking → Suggest annual CT follow-up or MRI characterisation

Aorta and pulmonary vessels → Report abnormalities in the context of the patient's cardiovascular disease

Lymphadenopathy → Report

if suspicious features or absence of an explaining disease to justify lymphadenopathy → Consider providing a follow-up schedule or suggest further characterisation with PET-CT or biopsy

Oesophageal hiatus hernia → Report

In the presence of heartburn (confounding symptom) → Referral to gastrointestinal evaluation

Chest wall

Bone

'Do not touch' lesions → Report but no follow-up required

Degenerative bony changes → Report (may cause atypical chest pain)

Suspicious bone lesions → Report and trigger an alert

Skin, subcutaneous and muscle lesions → Report new or previously undiagnosed lesions

Breast → Report new or previously undiagnosed lesions and alert breast team

Upper abdomen

Liver

Simple hepatic cysts → Reporting is optional, and no follow-up is required

Other focal parenchymal lesions → Report if previously undiagnosed and suggest further evaluation with triple-phase CT or MRI

Biliary system

Abnormal appearance of the gallbladder wall, biliary obstruction or pneumobilia → Report and suggest further evaluation

Gallstones → Reporting is optional, and no follow-up is required

Adrenal glands, pancreas, stomach, and spleen

Any cystic or solid lesions, or splenomegaly → Report and suggest further evaluation if previously undiagnosed

Kidneys

Simple or minimally complex renal cysts (Bosniak I and II) → Reporting is optional, and no follow-up is required

Complex renal cysts → Report and suggest further evaluation

Solid renal masses → Report and trigger an alert

Peritoneum

Nodules, infiltrative masses, haziness, ascites, peritoneal thickening or implants → Report, alert and suggest further evaluation

Lymphadenopathy → Report and suggest further evaluation

IPLNs - intrapulmonary lymph nodes; **LDCT** - low-dose CT; **MDT** - multidisciplinary team; **ILAs** - interstitial lung abnormalities; **ILD** - interstitial lung disease.

4.4. Study 4: Influencing factors in pulmonary nodule volumetry tools: Systematic review and attempted meta-analysis

The search returned 1259 (MEDLINE), 1697 (SCOPUS), 53 (Journals@Ovid), 223 (Embase), and 126 (Emcare) results from 1960 to 2022. The PRISMA flow diagram is presented in Figure 3.

The first stage of the systematic review included a cohort of 137 studies. A consolidated summary of results is presented in Table 9, and the full list of the summarised results is provided in Appendix 5.

Table 9. Summary of studies included in the systematic review

Factor	Statistical significance	Clinical relevance	Observations
Acquisition parameters			
Radiation dose exposure, tube current and tube potential	No consensus	Yes	Despite usually considered as non-significant, there are numerous contradictory study results, with some studies even showing inter-scan variability of volumetry measures in the realm of clinical relevance.
Signal-to-noise ratio (SNR)	No	No	Not an independent factor
Collimation	Yes	Untested	Generally considered as clinically irrelevant, but untested
High-resolution scan mode	Yes	Untested	Single study showing reduced volume overestimation of pulmonary nodules
Field of view (scan FOV)	No	No	
Pitch	No	No	Not significant unless using high pitch mode (pitch factor = 3) in small nodules (<5mm)
Contrast enhancement	Yes	Untested	Overestimates the volume of the pulmonary nodule
Reconstruction parameters			
Slice thickness	Yes	Yes	Thinner slice thickness improves accuracy, precision, and segmentation quality. Should be thin enough to allow any nodule to be visible in ≥3 consecutive slices.

Field of view (display FOV)	No	No	A thickness ≥2.5mm is inadequate to detect 1mm changes in nodule's diameter.
Reconstruction interval	No consensus	Untested	Overlap (interval < thickness) improves accuracy and precision of volumetry in smaller nodules and thicker slices. Likely not significant using 1mm slice thickness
Raw-data reconstruction algorithm	No	Yes (sub-solid nodules)	Iterative reconstruction (IR) algorithms outperform filtered back projection (FBP) for small part-solid nodules and at lower tube currents improving performance of volumetry tools. The noise reduction provided by IR is not uniform and less significant at the nodules' edges.
Kernel	Yes	Yes (sub-solid nodules)	Sharp kernel improves volumetry performance in thin 1mm slices. Smooth kernel outperforms sharp kernel in thicker ≥2.5mm slices.
Post-processing	No	No	Image compression and vessel suppression considered as not significantly influencing volumetry tools
CT scanner equipment			
Vendor	Yes	Untested	Only for small nodules not requiring follow-up
Technology	No consensus	Untested	Multi-detector CT, flat-panel, dual energy spectral CT
Software			
Software package, version, and segmentation algorithm	Yes	No	The same software package and version should be consistently used through the follow-up of any pulmonary nodule.
Nodule			
Size	Yes	Yes	Performance of volumetry tools is degraded in smaller nodules and considered unreliable for growth estimation of nodules <5mm
Density	Yes	Untested	Volumetry of non-solid nodules has worse accuracy and precision than for solid nodules.
Shape	Yes	Untested	Volumetry of nodules with irregular and spiculated shapes has lower accuracy and precision than volumetry of nodules with round, elongated, smooth or lobulated shapes.
Margin	Yes	Untested	Volumetry of nodules with poorly defined margins have higher variability.
Location	Yes	Untested	Attachment to surrounding structures (e.g., pleura, vessels, bronchial walls) degrades the performance of volumetry tools.
Patient			
Parenchymal changes	Yes	Untested	Only with increased attenuation of surrounding parenchyma (e.g., ILD)
Breathing	Yes	Yes	Breathing artifacts are related to volume overestimation and increased measurement variability.
Cardiopulmonary hemodynamics	Yes	Yes	Complex cardiopulmonary interactions affecting the amount of blood inside or around a nodule, leading to increased volume measurement variability.
Observer			
Manual correction	Yes	Untested	Selectively correcting obvious segmentation errors improves the performance of volumetry tools.
Experience	No	No	
Training	Yes	Untested	Training with the volumetry tool is important in unexperienced observers.

The second stage of the review identified a cohort of 16 studies, summarising their results in Table 10.

Table 10. Summary of studies reporting per cent Bland-Altman analysis of interscan variability

Ref	Population	(n)	Independent variable / Subgroup	bias	$_{lower}$LOA	$_{upper}$LOA
(50)	Patients with known pulmonary nodules					
		100	size: all	-0,90%	-16,40%	14,60%
		58	size: 30 - <80mm^3	-0.3%	-16.8%	16.2%
		42	size: 80 - 150mm^3	-1.7%	-15.5%	12.3%
(49)	Patients with pulmonary nodules detected on CCTA	195	Cardiac cycle phase (systole vs diastole)	2.65%	-47.0%	52.3%
(53)	Patients with part-solid nodules	66	Kernel			
			solid component segmentation	-3.2%	-45.0%	39.0%
			whole nodule segmentation	13,00%	-21.0%	46.0%
(51)	Patients under surveillance for <2mm solid nodules		Radiation dose exposure (LDCT vs. ULDCT)			
		170	all nodules	-2.0%	-18.0%	22.7%
		97	indeterminate nodules	-6.0%	-12.7%	21.9%
		68	BMI < 25	-2.5%	-17.5%	23.6%
		102	BMI > 25	-1.0%	-18.3%	20.8%
(54)	Patients with preoperative scans for subsolid nodules	66	Reconstruction algorithm: FBP vs. MBIR			
			solid component segmentation	6.3%	-51.9%	64.6%
			whole nodule segmentation	3.2%	-20.5%	27,00%
(55)	Patients with emphysema	88	Level of inspiration (end-inspiratory vs end-expiratory)	7,5%	-24,1%	39,1%
(56)	Patients were enrolled prospectively	105	Radiation dose (LDCT vs. ULDCT with FBP or SAFIRE)			
			FBP	0.2%	-20.0%	20.4%
			SAFIRE	0.3%	-9.7%	10.4%
(57)	Patients with subsolid nodules	94	intraobserver (R1)	-1,5%	-17,3%	16,5%
			intraobserver (R2)	0,4%	-14,8%	18,5%
(58)	Patients retrospectively enrolled	202	Radiation dose exposure (SDCT vs. ULDCT)			
			intraobserver (R1)	1.4%	-25.1%	26.2%
			intraobserver (R2)	1.9%	-25.1%	28.9%
			interobserver (R1 vs R2)	1.2%	-25,0%	27.4%
			interobserver (R2 vs R1)	2.1%	-23.9%	28.1%
(59)	Consecutive patients referred for known or suspected pulmonary metastases (3.3mm - 30mm)	89	Software			
			software A	0,0%	-17,0%	17,0%
			software B	0,0%	-13,1%	13,1%
			software C	0,0%	-20,8%	20,8%
			software D	0,0%	-13,4%	13,4%
			software E	0,0%	-20,5%	20,5%
			software F	0,0%	-19,6%	19,6%
(60)	Patients on follow-up for lung cancer or scanned because of suspicious pulmonary nodules		Radiation dose exposure (SDCT vs. ULDCT)			
		229	size: all			
			intraobserver (R1)	1.5%	-25.1%	28.1%
			intraobserver (R2)	2,0%	-26.4%	30.4%
			interobserver (R1 vs R2)	1.3%	-26.5%	29.1%
			interobserver (R2 vs R1)	2.2%	-25.2%	29.6%
		153	size: <10mm			
			intraobserver (R1)	2.3%	-28.5%	33.1%
			intraobserver (R2)	2.6%	-29.4%	34.6%
			interobserver (R1 vs R2)	1.9%	-28.3%	32.1%
			interobserver (R2 vs R1)	2.1%	-29,10%	33.3%
		76	size: ≥10mm			
			intraobserver (R1)	1.4%	-18.6%	21.4%
			intraobserver (R2)	0.4%	-18.6%	19.4%
			interobserver (R1 vs R2)	0.4%	-17,00%	17.8%

		interobserver (R2 vs R1)	0.6%	-18.4%	19.6%
(61) Patients with known nodules were prospectively enrolled	83	Radiation dose: SDCT vs. LDCT			
		SDCT	12.8%	-27.0%	40.0%
		LDCT	17.0%	-38.0%	60.0%
(62) Patients with contrast-enhanced chest CT	101	slice thickness: 1mm	-0.1%	-21.6%	20.3%
	101	slice thickness: 3mm	1.0%	-15.4%	15.2%
	101	slice thickness: 5mm	1.6%	-21.8%	27.6%
(63) Patients with pulmonary metastases	218	segmentation: all	1.3%	-21.2%	23.8%
	106	segmentation: complete	0.28%	-11.9%	12.4%
	112	segmentation: incomplete	1.61%	-26.8%	30.0%
(64) Patients with pulmonary metastases	96	Segmentation algorithm	0.0%	-26.9%	26.9%
(65) Patients with pulmonary metastases	151	size: all	0.7%	-20.4%	21.9%
	105	size: <10mm	0.55%	-19.3%	20.4%

Meta-analysis was attempted in two groups of studies, with results presented in Table 11 and Figures 6 and 7. Funnel plots were not performed since the minimum of 10 studies was unmet.

Table 11. Results of the attempted meta-analysis of two sets of similar studies.

	bias	**$_{lower}$ LOA**	**$_{upper}$ LOA**	**$_{lower}$ CI$_m$**	**$_{upper}$ CI$_m$**	**$_{lower}$ CI$_{rv}$**	**$_{upper}$ CI$_{rv}$**	τ^2
SDCT vs ULDCT (58,60)	1,67%	-26,22%	29,56%	-36,56%	39,89%	-36,55%	39,89%	-2,19E-05
Patients with pulmonary metastases (50,63,65)	0,36%	-19,77%	20,49%	-29,21%	29,93%	-29,88%	30,60%	7,14E-05

lower Cim - 95% Confidence interval of the lower LOA using a model-based estimator; **upper Cim -** 95CI of the upper LOA using a model-based estimator; **lower CIrv -** 95CI of the lower LOA using robust variance estimation (RVE); **upper CIrv -** 95CI of the upper LOA using RVE; τ^2 **-** estimator for between-study variation in bias in the LOA.

Figure 6. Forest plot of studies comparing SDCT (60) vs ULDCT (58) with combined results

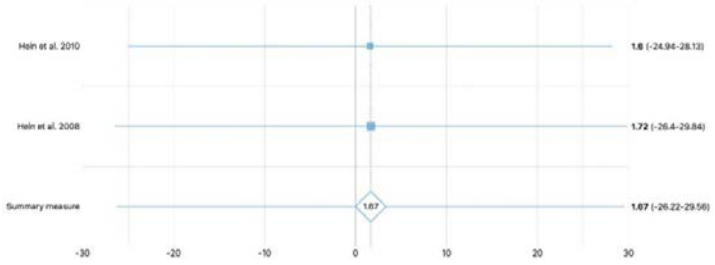

The red vertical dotted lines represent the *a priori* LOA of 25%.

Figure 7. Forest plot of studies with pulmonary metastases (50,63,65) with combined results

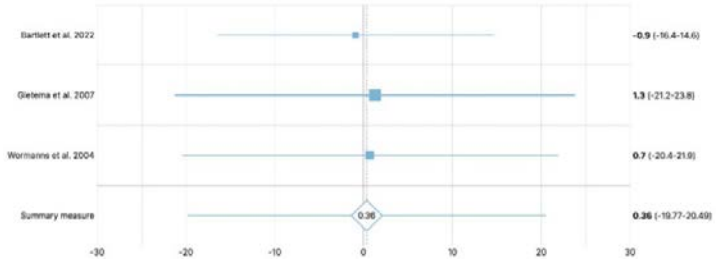

The red vertical dotted lines represent the *a priori* LOA of 25%.

5. Discussion

The four studies presented in this dissertation aim to describe the multiple facets of the research problem, which is the potential use of pulmonary nodule volumetry in CCTA scans. The pictorial essay and management proposal for incidental chest findings on CCTA (study 3; 46) establishes the opportunistic clinical usefulness (i.e., the 'why') of the research by showing that incidental chest findings, of which small indeterminate pulmonary nodules are among the most prevalent, can be detected in CCTA scans and may benefit from surveillance. The systematic review and meta-analysis establish the field's current state-of-the-art (i.e., the 'what'), namely influencing factors in pulmonary nodule volumetry tools (study 4; 47). Finally, the two original research studies (study 1 and study 2) describe the complex cardiopulmonary haemodynamic interactions (i.e., the 'how') that have the potential to change the outcome of volumetry tools and the clinical decisions that depend on them (48, 49).

The motivation for this research arises from acknowledging the overlap of risk factors of CAD and lung cancer (e.g., smoking history and age). Therefore, it is assumed that participants of LCS are more likely to have previous CCTA scans, which could reveal the earliest signs of lung cancer.

Pulmonary IFs are reported in 14-38% of CCTA scans, with indeterminate pulmonary nodules being the most frequent despite the reduced lung parenchymal coverage. Given the lack of guidelines for reporting and managing IFs, the true figure is likely higher. In our pictorial review, we proposed reporting and managing recommendations for IFs in CCTA scans, including pulmonary findings, which we believe can increase the pool of screening participants (study 3; 46). The recognition of pulmonary IFs in CCTA scans can generate further work-up, expedite diagnosis and allow better management of resources, which was a motivation for our research.

The obvious challenge to dual-screening using current CCTA protocols is the differences between CCTA and LDCT protocols. Volumetry tools are only validated for LDCT protocols. Although these tools have not been properly tested in CCTA protocols, differences in technical parameters (e.g., standard-dose, contrast-enhanced, multi-detector CCTA protocol, often using medication to lower the heart rate and dilate the coronary arteries) are known to influence the volumetry tools. We summarised all original research studies (n = 137) investigating how multiple influencing factors (n = 27) affect the outcome of volumetry tools dedicated to pulmonary nodule analysis, thus establishing the current state-of-the-art in this field (study 4; 47). Contrast enhancement has been shown to increase the volume measurement, the difference in radiation dose

between standard and low-dose protocols significantly increases variability, and the impact of medication (e.g., beta-blockers and vasodilators) has yet to be studied.

LDCT protocols developed for LCS and mirrored in consensus recommendations and guidelines recognise that CT acquisition parameters like slice thickness, kernel, and software package (and version) have been shown to influence volumetry tools. This is perhaps where the wide consensus stops. Despite the many studies published in this field in the last two decades and the restricted scope of our systematic review, we still found the body of evidence suffering from high heterogeneity given the large number of potential influencing factors, study population, study design, and methodology (study 4; 47). More importantly, only a few authors directly link the statistically significant results to the potential to change clinical decisions. Simply put, the design and methodology of most of these studies do not easily translate to clear recommendations supporting clinical practice.

This was surprising as it reveals significant gaps in our understanding when volumetry tools have already been fully included in international guidelines and recommendations for follow-up and screening pulmonary nodules.

To advance our understanding of the field, we proposed a new intuitive model explaining how all these factors may influence the volumetry tools' outcome via two fundamental concepts: the contrast between nodule and surrounding parenchyma and the surface-to-inner voxel ratio (study 4; 47).

This model allowed us to predict the mechanism by which cardiopulmonary haemodynamic changes could influence the outcome of volumetry tools. Assuming that changes in the intravascular blood pressure are felt inside the pulmonary nodule and in the surrounding capillary bed, we predict that an increasing blood pressure inside the nodule results in an increase of blood volume inside and around that same nodule. Consequently, the total number of inner voxels included in the segmentation result will increase, thus decreasing the surface-to-inner voxel ratio (i.e., increasing the volume measurement and decreasing its variability). Conversely, by expanding the capillary bed surrounding the nodule, the increased attenuation of the voxels of the surrounding parenchyma will reduce the contrast between the nodule and the surrounding parenchyma. This will increase the surface-to-inner voxel ratio (i.e., increasing the volume measurement while also increasing the measurement variability). The result will be the sum of both effects.

This model implies the nodule size as the most important factor influencing volumetry - a smaller nodule includes fewer voxels, which increases the ratio between surface and inner voxels. Surface voxels are more susceptible to partial volume artefacts,

thus explaining greater measurement variability and increased interactions with most other factors (study 4; 47).

For solid pulmonary nodules between 5 and 8mm, the smaller the nodule, the greater impact most factors will have on their volumetric assessment. Reducing the slice thickness and measuring nodules of increasing size decreases the surface-to-inner voxels' ratio, improving the performance of volumetry tools. Hwang et al. suggested that increasing the follow-up threshold to ≥9mm would ease most concerns regarding the performance of these tools (i.e., the effect of influencing factors would no longer be relevant) and result in a 60% reduction of follow-up scans at the cost of delaying the diagnosis of 1.9% of lung cancer patients (52). In short, these authors suggest treating indeterminate pulmonary nodules as low-risk and only follow-up nodules above 9mm, which we know from the NELSON trial to require further diagnostic workup (and not growth assessment using volumetry). This position highlights the questionable clinical significance of statistically significant results of many of the 137 published studies. The applicability of the evidence in clinical decisions is poor (study 4; 47).

Therefore, a clarification of clinical significance seems needed.

In the follow-up of indeterminate pulmonary nodules, the optimal waiting period between scans is based on the inherent *in vivo* interscan measurement variability of volumetry tools, accepted as ≤25% of total volume (39). Higher measurement variability implies a longer waiting period between follow-up scans to distinguish real growth from measurement error. This can be better understood by considering different interscan variability values, as Figure 1 shows (49). We can define clinical significance as interscan variability >25% of volume change since false-positive growth estimation would become more likely in this setting.

The influencing factors investigated regarding their clinical relevance include radiation dose exposure, slice thickness, raw-data reconstruction algorithms, kernels, size, cardiac cycle phase, software package, segmentation algorithm, and level of inspiration. Overall, the number of studies addressing the clinical relevance of their results, as defined here, corresponds to only 11% of the total number of studies included in our systematic review (study 4; 47).

The use of volumetry in CCTA scans had only been investigated once before, by Boll et al., which suggested that cardiovascular motion resulting from the interaction of the cardiac cycle phase, location, and mean size of the pulmonary nodule may influence its volumetric assessment (45).

Our two original studies (studies 1 and 2) differed from the earlier study by Boll et al. by using a larger study population, more modern scanner equipment (e.g., 128 vs 16 slices), and current and updated segmentation algorithms in clinical use (45,48,49). Unlike the results published by Boll et al. (which have not yet been replicated), our study (study 1) did not confirm any statistical significance to the choice of the cardiac cycle phase. We tested several factors related to cardio-pulmonary circulation in a multiple linear regression model, namely the location of the solid pulmonary nodule in the axial (i.e., related to hydrostatic pressure differences) and coronal plane (i.e., related to the vascular cross-sectional area), the difference of the MPA diameter between systole and diastole (i.e., related to pulmonary hypertension), and the vascular distance between the MPA and the nodule (study 1; 48).

We proposed a physiological model of cardiopulmonary hemodynamic interactions centred around the notion of 'transit time', which is the time required for the pressure wave originated by the cardiac systole to propagate through the pulmonary artery and capillary network until it reaches the pulmonary nodule being measured. This model includes complex interactions between vascular and hydrostatic pressures, vascular resistance, vascular distance, and the cross-sectional area of the vessels along the way. Because transit time depends on the nodule's location, the propagating pressure wave peak will be felt at different times in different nodules. This explains the counter-intuitive nature of our results that showed that the cardiac cycle phase was not statistically linked to a change in volumetry measurements, while other factors related to cardiopulmonary hemodynamic interactions were (studies 1 and 2; 48,49).

This physiological model has clear implications for growth estimation using volumetry and VDT. During the follow-up of pulmonary nodules, cardiovascular events such as congestive heart failure with pleural effusion could have an impact on volumetry measurements by changing the nodule's position and vascular distance (as the effusion displaces the aerated lung parenchyma) and intravascular pressure dynamics. Chronic thromboembolism and vasculitis are also associated with increased resistance and tortuosity of the distal vessels, which affects the propagation of the pressure wave and increases the vascular distance. Clinically, these hemodynamic changes can lead to pulmonary hypertension and, ultimately, right ventricular dysfunction, with an increase in the calibre of the MPA, which persists in diastole (i.e., reducing the difference in calibre between systole and diastole). Conversely, pulmonary valve insufficiency would increase this difference in calibre throughout the cardiac cycle. Such cardiovascular events can occur, progress, or even resolve between two follow-up scans, under or overestimating the volume measurements.

Over or underestimation of a nodule's volume implies a reduction of the accuracy of the measurement method. Growth estimation is still reliable in the presence of systematic bias, meaning that all volumes are consistently under or overestimated by the same amount on all follow-up scans (49). However, growth estimation is affected if the error is inconsistent (i.e., measurement variability). As mentioned earlier, the currently proposed schedule of follow-up scans assumes a variability of volumetry tools below 25% of volume change. A higher measurement variability implies a longer optimal waiting period between follow-up scans to confidently distinguish true growth from measurement error. In other words, with the currently proposed schedule of follow-up scans, using a volumetry tool with a variability above 25% of volume change could result in measurement error being interpreted as true growth (i.e., false positives), potentially leading to unnecessary work-up and interventions, and putting the patient at risk (49).

We investigated the variability of pulmonary nodule volumetry tools in CCTA scans using Bland-Altman analysis and *a priori* LOA within 25% of volume change (study 2; 49). We used the differences in cardiopulmonary haemodynamic interactions between systole and diastole as a proxy for the interactions occurring during cardiovascular events. We argue that real-life events, such as heart failure with pleural effusion and parenchymal oedema, are, in fact, more likely to change the outcome of volumetry tools because of increased attenuation of the surrounding parenchyma and perfusion-ventilation mismatch, among other factors (49).

Our results showed that volumetry tool variability was greater than 25% when comparing opposing cardiac cycle phases (i.e., systole vs diastole)(study 2; 49). These results fulfil the criteria we defined earlier for clinical relevance and could potentially lead to false positive results. Comparison of measurements acquired in the same phase did not surpass this *a priori* LOA, and comparison between diastolic measurements showed the least variability, likely due to less cardiac motion during diastole (study 2; 49).

At first, it may seem counter-intuitive that the cardiac cycle phase is not statistically significant in our first study, but the variability of volumetry measurement between opposing cardiac cycle phases is significant and clinically relevant. According to the physiological model we present, this incongruency is explained by the dephasing effect of the transit time. In our first study, the multiple linear regression model investigates the effect of the cardiac cycle phase on a population of solid pulmonary nodules, each with their individual transit time. Because of this dephasing effect, each nodule will be scanned at a different point along the propagating pressure wave, thus affecting the cardiopulmonary hemodynamic interactions in different measures. However, in our

second study, we investigate the variability of volumetry between opposing cardiac cycle phases (i.e., systole and diastole) in each nodule. The transit time is constant as both measurements relate to the same nodule. In other words, we are comparing the volume measurements at opposing points along the propagating pressure wave, independently of the transit time. When one of the measurements matches the wave's peak, the other will match its low amplitude zone and highlight the effect of the cardio-pulmonary hemodynamic interactions. Therefore, the results from the second study are also consistent with our proposed physiological model.

Based on this model, we extrapolate that comparison of volume measurements before and after significant cardiovascular events will not be reliable for growth estimation. Given the overlap of risk factors between lung cancer and cardiovascular disease, we expect this clinical scenario to be frequent and needs to be kept in mind.

Our research suggests that volumetry of pulmonary nodules is feasible using CCTA scans if the same cardiac cycle phase is used between follow-up CCTA scans, preferably in diastole, to minimise measurement variability.

Both original research studies share a limitation due to the low percentage of cases included from the large study population. This was due to the many CCTA scans with missing systolic or diastolic phases in PACS, related to the department's policy of sending only the most diagnostically relevant phases for archiving. Nevertheless, to our knowledge, this dataset represents the largest published series on pulmonary node volumetry in ECG-gated CT scans.

Our series is only the second to focus on pulmonary volumetry in ECG-gated CT scans and directly contradicts the previous results by Boll et al., using a larger study population, current scanners and updated volumetry tools in clinical use. The research's second study is also the first published study to measure the *in vivo* variability of pulmonary nodule volumetry on CCTA, which is the main requirement for growth estimation. However, our conclusions still need to be reproduced and validated independently.

Despite sharing the same dataset, the different approach taken by each study regarding its aims and statistical methodology provides two complementary views of the problem, which combine to form a novel, robust and elegant model explaining the complex cardiopulmonary haemodynamic interactions and their impact on pulmonary nodule volumetry. We realise that the model simplifies the *in vivo* processes and does not attempt to address the systemic bronchial arteries or the regulatory mechanisms of ventilation and perfusion. Other non-hemodynamic factors may also influence the measurement, like the distribution of the nodules along the airways, which may also be

confounded with the vascular distance. Another limitation of both studies is the lack of information on risk factors such as smoking. Given the substantial overlap between lung cancer and CAD risk factors, we assume their prevalence is high in the study population.

The research also produced an exhaustive systematic review, which is the largest published in the field. We argue that the failure of meta-analysis to produce significant new evidence is not a limitation but instead illustrates the problem with heterogeneity between the many different studies. This problem limits the clinical usefulness of the body of evidence. To address this limitation, we proposed a standard for future studies around the Bland–Altman analysis restricted to nodules between 5 and 10 mm where growth estimation is useful, focusing on clinical applicability and currently available technology.

A concern related to the systematic review and attempted meta-analysis is the long period of the included studies in a rapidly changing field, suggesting that this review may not reflect current performance. A comparison of recent (i.e., last five years) and older studies shows an improving performance trend likely related to software and scanner technology innovations. In a recent study by Bartlett et al., the reported interscan variability was not clinically relevant ($_{95}$CI [– 16.8%; 16%]) even for very small (30–80 mm^3) solid, non-metastatic and non-calcified pulmonary nodules (n = 58), suggesting that a shorter optimal waiting time may already be appropriate.

6. Conclusions

Regarding the primary objective of the research (i.e., to investigate how factors related to cardiopulmonary haemodynamic interactions affect volumetry tools dedicated to pulmonary nodules between 5 and 8mm in size), this dissertation presents a novel physiological model of cardiopulmonary haemodynamic effects through a complex set of interactions, based on the concept of transit time.

These factors include the cardiac cycle phase, the vascular pressure within the pulmonary circulation (linked to the variability of the MPA diameter between systole and diastole), and the location of the nodule (linked to the vascular distance between the MPA and the pulmonary nodule, the hydrostatic pressure, and the vessel cross-section area). These factors can impact the accuracy and variability of volumetry and meet our criterion for clinical significance.

Regarding the first secondary objective of the research (i.e., to investigate the potential role of dual screening using CCTA scans), we have documented the high prevalence of lung nodules as IFs of CCTA scans and argue that the overlap in risk factors of CAD and lung cancer creates opportunities for dual screening, potentially improving candidate selection for LCS, expedite lung cancer diagnosis, and improve the management of available resources.

Growth assessment implies comparing volume measurements of a given pulmonary nodule over time, which could possibly be between an LDCT and a CCTA scan. However, technical differences between LDCT and CCTA protocols can independently influence the outcome of volumetry tools. These differences include the radiation dose, contrast enhancement, and medication.

Regarding the last secondary objective of the research, this work consolidates the available evidence regarding factors influencing the outcome of volumetry tools dedicated to pulmonary nodules, showing the body of evidence to be very heterogeneous and with poor clinical applicability. We have presented a theoretical model that explains the influence on the outcomes of volumetry tools based on two core concepts: the contrast between the nodule and the surrounding lung parenchyma and the ratio of surface-to-inner voxels. We have also defined the criterion for clinical relevance of any statistically significant result as the ability of an influencing factor to increase the *in vivo* interscan variability of volumetry above the 25% threshold. Meeting this criterion implies that false-positive growth of pulmonary nodules is more likely.

Besides the potential for dual-screening of CAD and lung cancer, our results and proposed model suggest that volumetry may also be unreliable in the case of

cardiopulmonary events that may occur between follow-up scans, like the onset of acute heart failure or pleural effusion.

7. Future perspectives

Future research is still needed to compare the volume measurements in CCTA and LDCT scans directly. We expect that the variability of volumetry between non-ECG-gated CT and CCTA scans will be lower than when comparing opposing cardiac cycle phases because non-ECG-gated scans average the cardiopulmonary hemodynamic interactions along the cardiac cycle. Investigating the reliability of growth estimation using measurements in both types of scans would require a coffee-break study with the acquisition of two independent scans (i.e., a CCTA and an LDCT) or preferably by tailoring of the CCTA protocol to include an additional low-dose acquisition of the lung parenchyma, as proposed by Gaudio et al. (29).

Another avenue for future research is to compare the volumetry of pulmonary nodules before and after significant cardiovascular events. For example, such research could compare volumetry measurements on two independent chest CT scans obtained in a short enough period to assume no real growth. This kind of study could include patients admitted to intensive care units (ICU), which are often scanned daily, before and after acute cardiovascular events (e.g., acute onset of heart failure, etc.), or treatment optimisation (e.g., diuretic therapy, percutaneous drainage of pleural effusion, etc.). However, the significant differences in the clinical setting between the ICU patient population and the participants of LCS would need to be addressed and the results interpreted carefully.

Future research should also explore the cost and benefits of potential changes to current practices, like raising the threshold for follow-up or shortening the optimal waiting period in the follow-up schedule.

8. References

1. Sharma D, Newman TG, Aronow WS. Lung cancer screening: history, current perspectives, and future directions. Arch Med Sci. 2015 Oct 12;11(5):1033-43. doi: 10.5114/aoms.2015.54859.
2. Brownlee AR, Donington JS. Update on Lung Cancer Screening. Semin Respir Crit Care Med. 2020 Jun;41(3):447-452. doi: 10.1055/s-0039-3400480.
3. Sung H, Ferlay J, Siegel RL, Laversanne M, Soerjomataram I, Jemal A, et al. Global Cancer Statistics 2020: GLOBOCAN Estimates of Incidence and Mortality Worldwide for 36 Cancers in 185 Countries. CA Cancer J Clin. 2021 May;71(3):209-249. doi: 10.3322/caac.21660.
4. Bade BC, Brasher PB, Luna BW, Silvestri GA, Tanner NT. Reviewing Lung Cancer Screening: The Who, Where, When, Why, and How. Clin Chest Med. 2018 Mar;39(1):31-43. doi: 10.1016/j.ccm.2017.09.003.
5. Goldstraw P, Chansky K, Crowley J, Rami-Porta R, Asamura H, Eberhardt WEE, et al. The IASLC lung cancer staging project: Proposals for revision of the TNM stage groupings in the forthcoming (eighth) edition of the TNM Classification for lung cancer. J Thorac Oncol. 2016 Jan;11(1):39-51. doi: 10.1016/j.jtho.2015.09.009.
6. Keen JD, Keen JE. What is the point: will screening mammography save my life? BMC Med Inform Decis Mak. 2009. doi: 10.1186/1472-6947-9-18.
7. Bretthauer M, Løberg M, Wieszczy P, Kalager M, Emilsson L, Garborg K, et al. Effect of Colonoscopy Screening on Risks of Colorectal Cancer and Related Death. N Engl J Med. 2022 Oct 27;387(17):1547-1556. doi: 10.1056/NEJMoa2208375.
8. Aberle DR, Adams MA, Berg CD, Black WC, Clapp JD, Fagerstrom RM, et al. Reduced Lung-Cancer Mortality with Low-Dose Computed Tomographic Screening. N Engl J Med. 2011 Aug 4;365(5):395-409. doi: 10.1056/NEJMoa1102873.
9. Infante M, Cavuto S, Lutman F, Romano, Passera E, Chiarenza M, et al. Long-Term Follow-up Results of the DANTE Trial, a Randomized Study of Lung Cancer Screening with Spiral Computed Tomography. Am J Respir Crit Care Med. 2015 May 15;191(10):1166-75. doi: 10.1164/rccm.201408-1475OC.
10. Wille MMW, Dirksen A, Ashraf H, Saghir Z, Bach KS, Brodersen J, et al. Results of the randomized danish lung cancer screening trial with focus on high-risk profiling. Am J Respir Crit Care Med. 2016 Mar 1;193(5):542-51. doi: 10.1164/rccm.201505-1040OC.
11. de Koning H, van der Aalst C, Haaf K ten, Oudkerk M, Liu S, Mansfield A, et al. PL02.05 Effects of Volume CT Lung Cancer Screening: Mortality Results of the NELSON Randomised-Controlled Population Based Trial. Journal of Thoracic Oncology Plenary sessions Vol 13, issue 10, supplement , S185, Oct 2018. doi: 10.1016/j.jtho.2018.08.012
12. Pastorino U, Silva M, Sestini S, Sabia F, Boeri M, Cantarutti A, et al. Prolonged lung cancer screening reduced 10-year mortality in the MILD trial: new confirmation of lung cancer screening efficacy. Ann Oncol. 2019 Jul 1;30(7):1162-1169. doi: 10.1093/annonc/mdz117.
13. Becker N, Motsch E, Gross ML, Eigentopf A, Heussel CP, Dienemann H, et al. Randomized Study on Early Detection of Lung Cancer with MSCT in Germany: Results of the First 3 Years of Follow-up After Randomization. J Thorac Oncol. 2015 Jun;10(6):890-6. doi: 10.1097/JTO.0000000000000530.
14. Field JK, Duffy SW, Baldwin DR, Whynes DK, Devaraj A, Brain KE, et al. UK Lung Cancer RCT Pilot Screening Trial: baseline findings from the screening arm provide evidence for the potential implementation of lung cancer screening. Thorax. 2016 Feb;71(2):161-70. doi: 10.1136/thoraxjnl-2015-207140.
15. Ledson M, Grundy S, Arvanitis R, Timoney M, Gaynor E, Field J. S12 The liverpool healthy lung project (lhlp) – seeking out lung disease. Thorax 2017 Dec; Vol 72 issue suppl 3:A10.2-A11. doi: 10.1136/thoraxjnl-2017-210983.18.

16. Cassidy A, Myles JP, van Tongeren M, Page RD, Liloglou T, Duffy SW, et al. The LLP risk model: an individual risk prediction model for lung cancer. Br J Cancer. 2008 Jan 29;98(2):270-6. doi: 10.1038/sj.bjc.6604158.
17. Kauczor HU, Baird AM, Blum TG, Bonomo L, Bostantzoglou C, Burghuber O, et al. ESR/ERS statement paper on lung cancer screening. Eur Radiol. 2020 Jun;30(6):3277-3294. doi: 10.1007/s00330-020-06727-7.
18. Pinsky PF. Lung cancer screening with low-dose CT: a world-wide view. Transl Lung Cancer Res. 2018 Jun;7(3):234-242. doi: 10.21037/tlcr.2018.05.12.
19. Moyer VA. Screening for lung cancer: U.S. preventive services task force recommendation statement. Ann Intern Med. 2014 Mar 4;160(5):330-8. doi: 10.7326/M13-2771.
20. Wood DE, Kazerooni EA, Baum SL, Eapen GA, Ettinger DS, Hou L, et al. Lung Cancer Screening, Version 3.2018, NCCN Clinical Practice Guidelines in Oncology. J Natl Compr Canc Netw. 2018 Apr;16(4):412-441. doi: 10.6004/jnccn.2018.0020.
21. Brenner DJ. Radiation Risks Potentially Associated with Low-Dose CT Screening of Adult Smokers for Lung Cancer. Radiology. 2004 May;231(2):440-5. doi: 10.1148/radiol.2312030880.
22. Horeweg N, van Rosmalen J, Heuvelmans MA, van der Aalst CN, Vliegenthart R, Sholten ET, et al. Lung cancer probability in patients with CT-detected pulmonary nodules: a prespecified analysis of data from the NELSON trial of low-dose CT screening. Lancet Oncol. 2014 Nov;15(12):1332-41. doi: 10.1016/S1470-2045(14)70389-4.
23. Walter JE, Heuvelmans MA, Dorrius M, Oudkerk M. Low-dose lung cancer screening: nodule measurement and management. Precision Cancer Medicine. 2:24– 24. doi: 10.21037/pcm.2019.07.03.
24. Kauczor HU, Bonomo L, Gaga M, Nackaerts K, Peled N, Prokop M, et al. ESR/ERS white paper on lung cancer screening. Eur Respir J. 2015 Jul;46(1):28-39. doi: 10.1183/09031936.00033015.
25. van Klaveren RJ, Oudkerk M, Prokop M, Scholten ET, Nackaerts K, Vernhout R, et al. Management of Lung Nodules Detected by Volume CT Scanning. N Engl J Med. 2009 Dec 3;361(23):2221-9. doi: 10.1056/NEJMoa0906085.
26. Parker MS, Groves RC, Kusmirek JE, et al. Lung Cancer Screening. Thieme 2009. doi: 10.1055/b-006-149764.
27. Wu GX, Raz DJ, Brown L, Sun V. Psychological Burden Associated With Lung Cancer Screening: A Systematic Review. Clin Lung Cancer. 2016 Sep;17(5):315-324. doi: 10.1016/j.cllc.2016.03.007.
28. Morgan L, Choi H, Reid M, Khawaja A, Mazzone PJ. Frequency of incidental findings and subsequent evaluation in low-dose computed tomographic scans for lung cancer screening. Ann Am Thorac Soc. 2017 Sep;14(9):1450-1456. doi: 10.1513/AnnalsATS.201612-1023OC.
29. Gaudio C, Tanzilli A, Mei M, Moretti A, Barillà F, Varveri A, et al. Concomitant screening of coronary artery disease and lung cancer with a new ultrafast-low-dose Computed Tomography protocol: A pilot randomised trial. Sci Rep. 2019 Sep 25;9(1):13872. doi: 10.1038/s41598-019-50407-6.
30. Marshall D, Simpson KN, Earle CC, Chu CW. Potential cost-effectiveness of one-time screening for lung cancer (LC) in a high risk cohort. Lung Cancer. 2001 Jun;32(3):227-36. doi: 10.1016/s0169-5002(00)00239-7.
31. Wisnivesky JP, Mushlin AI, Sicherman N, Henschke C. The Cost-Effectiveness of Low-Dose CT Screening for Lung Cancer: Preliminary Results of Baseline Screening. Chest. 2003 Aug;124(2):614-21. doi: 10.1378/chest.124.2.614.
32. Mahadevia PJ, Fleisher LA, Frick KD, Eng J, Goodman SN, Powe NR. Lung Cancer Screening With Helical Computed Tomography in Older Adult Smokers: A Decision and Cost-effectiveness Analysis. JAMA. 2003;289(3):313-322. doi:10.1001/jama.289.3.313.

33. Manser R, Dalton A, Carter R, Byrnes G, Elwood M, Campbell DA. Cost-effectiveness analysis of screening for lung cancer with low dose spiral CT (computed tomography) in the Australian setting. Lung Cancer. 2005 May;48(2):171-85. doi: 10.1016/j.lungcan.2004.11.001.
34. Black WC, Gareen IF, Soneji SS, Sicks JD, Keeler EB, Aberle DR, et al. Cost-Effectiveness of CT Screening in the National Lung Screening Trial. N Engl J Med. 2014 Nov 6;371(19):1793-802. doi: 10.1056/NEJMoa1312547.
35. Pataky R, Phillips N, Peacock S, Coldman AJ. Cost-effectiveness of population-based mammography screening strategies by age range and frequency. Journal of Cancer Policy. 2014 Dec 1;2(4):97–102. 10.1016/j.jcpo.2014.09.001
36. Hinde S, Crilly T, Balata H, Bartlett R, Crilly J, Barber P, et al. The cost-effectiveness of the Manchester 'lung health checks', a community-based lung cancer low-dose CT screening pilot. Lung Cancer. 2018 Dec;126:119-124. doi: 10.1016/j.lungcan.2018.10.029.
37. Dicken V, Bornemann L, Moltz JH, Peitgen HO, Zaim S, Scheuring U. Comparison of volumetric and linear serial ct assessments of lung metastases in renal cell carcinoma patients in a clinical phase IIB study. Acad Radiol. 2015 May;22(5):619-25. doi: 10.1016/j.acra.2014.12.018.
38. Han D, Heuvelmans MA, Oudkerk M. Volume versus diameter assessment of small pulmonary nodules in CT lung cancer screening. Translational Lung Cancer Research. 2017 Feb;6(1):52–61. doi: 10.21037/tlcr.2017.01.05.
39. Devaraj A, van Ginneken B, Nair A, Baldwin D. Use of Volumetry for Lung Nodule Management: Theory and Practice. Radiology. 2017 Sep;284(3):630-644. doi: 10.1148/radiol.2017151022.
40. Detterbeck FC, Lewis SZ, Diekemper R, Addrizzo-Harris D, Alberts WM. Executive Summary: Diagnosis and management of lung cancer, 3rd ed: American College of Chest Physicians evidence-based clinical practice guidelines. Chest. 2013 May;143(5 Suppl):7S-37S. doi: 10.1378/chest.12-2377.
41. Callister MEJ, Baldwin DR, Akram AR, Barnard S, Cane P, Draffan S et al. British Thoracic Society guidelines for the investigation and management of pulmonary nodules. Thorax. 2015 Aug;70 Suppl 2:ii1-ii54. doi: 10.1136/thoraxjnl-2015-207168.
42. MacMahon H, Naidich DP, Goo JM, Lee KS, Leung ANC, Mayo JY et al. Guidelines for Management of Incidental Pulmonary Nodules Detected on CT Images: From the Fleischner Society 2017. Radiology. 2017 Jul;284(1):228-243. doi: 10.1148/radiol.2017161659.
43. American College of Radiology Committee on Lung-RADS®. Lung-RADS Assessment Categories 2022. Available at https://www.acr.org/-/media/ACR/Files/RADS/Lung-RADS/Lung-RADS-2022.pdf.
44. Wood DE, Kazerooni EA, Aberle D, Bergman A, Brown LM, Eapen GE et al. NCCN Guidelines Insights: Lung Cancer Screening, Version 1.2022. JNCCN 2022 July; 20(7): 754-764. doi: 10.6004/jnccn.2022.0036.
45. Boll DT, Gilkeson RC, Fleiter TR, Blackham KA, Duerk JL, Lewin JS. (2004) Volumetric Assessment of Pulmonary Nodules with ECG-Gated MDCT. American AJR Am J Roentgenol. 183(5):1217-23. doi: 10.2214/ajr.183.5.1831217.
46. Pinto EG, Penha D, Hochhegger B, Monaghan C, Marchiori E, Taborda-Barata L et al. Incidental chest findings on coronary CT angiography: a pictorial essay and management proposal. J Bras Pneumol. 2022 May 13;48(4):e20220015. doi: 10.36416/1806-3756/e20220015.
47. Pinto EG, Penha D, Ravara S, Monaghan C, Hochhegger B, Marchiori E et al. Factors influencing the outcome of volumetry tools for pulmonary nodule analysis: a systematic review and attempted meta-analysis. doi: 10.1186/s13244-023-01480-z
48. Pinto EG, Penha D, Hochhegger B, Monaghan C, Marchiori E, Taborda-Barata L et al. The impact of cardiopulmonary hemodynamic factors in volumetry for pulmonary nodule management. BMC Med Imaging. 2022 Mar 18;22(1):49. doi: 10.1186/s12880-022-00774-w.

49. Pinto EG, Penha D, Hochhegger B, Monaghan C, Marchiori E, Taborda-Barata L et al. Variability of pulmonary nodule volumetry on coronary CT angiograms. Medicine (Baltimore). 2022 Sep 2;101(35):e30332. doi: 10.1097/MD.0000000000030332.
50. Bartlett E, Kemp SV, Rawal B, Devaraj A et al. Defining growth in small pulmonary nodules using volumetry: results from a "coffee-break" CT study and implications for current nodule management guidelines. Eur Radiol. 2022 Mar;32(3):1912-1920. doi: 10.1007/s00330-021-08302-0.
51. Paks M, Leong P, Einsiedel P, Irving LB, Steinfort DP, Pascoe DM et al. Ultralow dose CT for follow-up of solid pulmonary nodules: A pilot single-center study using Bland-Altman analysis. Medicine (Baltimore). 2018 Aug;97(34):e12019. doi: 10.1097/MD.0000000000012019.
52. Hwang EJ, Goo JM, Kim HY, Yi J, Kim Y. Optimum diameter threshold for lung nodules at baseline lung cancer screening with low-dose chest CT: exploration of results from the Korean Lung Cancer Screening Project. Eur Radiol. 2021 Sep;31(9):7202-7212. doi: 10.1007/s00330-021-07827-8.
53. Werner S, Gast R, Grimmer R, Wimmer A, Horger M. Accuracy and Reproducibility of a Software Prototype for Semi-Automated Computer-Aided Volumetry of the solid and subsolid Components of part-solid Pulmonary Nodules. Rofo. 2022 Mar;194(3):296-305. doi: 10.1055/a-1656-9834.
54. Cohen JG, Kim H, Park S bin, van Ginneken B, Ferretti GR, Lee CH, et al. Comparison of the effects of model-based iterative reconstruction and filtered back projection algorithms on software measurements in pulmonary subsolid nodules. Eur Radiol. 2017 Aug;27(8):3266-3274. doi: 10.1007/s00330-016-4716-5.
55. Moser JB, Mak SM, McNulty WH, Padley S, Nair A, Shah PL, et al. The influence of inspiratory effort and emphysema on pulmonary nodule volumetry reproducibility. Clin Radiol. 2017 Nov;72(11):925-929. doi: 10.1016/j.crad.2017.06.117.
56. Sui X, Meinel FG, Song W, Xu X, Wang Z, Wang Y, et al. Detection and size measurements of pulmonary nodules in ultra-low-dose CT with iterative reconstruction compared to low dose CT. Eur J Radiol. 2016 Mar;85(3):564-70. doi: 10.1016/j.ejrad.2015.12.013.
57. Kim H, Park CM, Woo S, Lee SM, Lee HJ, Yoo CG, et al. Pure and Part-Solid Pulmonary Ground-Glass Nodules: Measurement Variability of Volume and Mass in Nodules with a Solid Portion Less than or Equal to 5 mm. Radiology. 2013 Nov;269(2):585-93. doi: 10.1148/radiology.13121849.
58. Hein PA, Romano VC, Rogalla P, Klessen C, Lembcke A, Bornemann L, et al. Variability of Semiautomated Lung Nodule Volumetry on Ultralow-Dose CT: Comparison with Nodule Volumetry on Standard-Dose CT. J Digit Imaging. 2010 Feb;23(1):8-17. doi: 10.1007/s10278-008-9157-5.
59. Hoop B, Gietema H, Ginneken B, Zanen P, Groenewegen G, Prokop M, et al. A comparison of six software packages for evaluation of solid lung nodules using semi-automated volumetry: What is the minimum increase in size to detect growth in repeated CT examinations. Eur Radiol. 2009 Apr;19(4):800-8. doi: 10.1007/s00330-008-1229-x.
60. Hein P, Romano V, Rogalla P, Klessen C, Lembcke A, Dicken V, et al. Linear and Volume Measurements of Pulmonary Nodules at Different CT Dose Levels – Intrascan and Interscan Analysis. Rofo. 2009 Jan;181(1):24-31. doi: 10.1055/s-2008-1027874.
61. Rampinelli C, de Fiori E, Raimondi S, Veronesi G, Bellomi M. In Vivo Repeatability of Automated Volume Calculations of Small Pulmonary Nodules With CT. AJR Am J Roentgenol. 2009 Jun;192(6):1657-61. doi: 10.2214/AJR.08.1825.
62. Vogel MN, Vonthein R, Schmücker S, Maksimovich O, Bethge W, Dicken V, et al. Automated pulmonary nodule volumetry with an optimized algorithm. Accuracy at different slice thicknesses compared to unidimensional and bidimensional measurements. Rofo. 2008 Sep;180(9):791-7. doi: 10.1055/s-2008-1027562.
63. Gietema HA, Schaefer-Prokop CM, Mali WPTM, Groenewegen G, Prokop M. Pulmonary Nodules: Interscan Variability of Semiautomated Volume Measurements

with Multisection CT—Influence of Inspiration Level, Nodule Size, and Segmentation Performance. Radiology. 2007 Dec;245(3):888-94. doi: 10.1148/radiol.2452061054.
64. Petrou M, Quint LE, Nan B, Baker LH. Pulmonary nodule volumetric measurement variability as a function of CT slice thickness and nodule morphology. AJR Am J Roentgenol. 2007 Feb;188(2):306-12. doi: 10.2214/AJR.05.1063.
65. Wormanns D, Kohl G, Klotz E, Marheine A, Beyer F, Heindel W, et al. Volumetric measurements of pulmonary nodules at multi-row detector CT: in vivo reproducibility. Eur Radiol. 2004 Jan;14(1):86-92. doi: 10.1007/s00330-003-2132-0.

9. Appendix

9.1. The impact of cardiopulmonary hemodynamic factors in volumetry for pulmonary nodule management

Guedes Pinto et al. BMC Medical Imaging (2022) 22:49
https://doi.org/10.1186/s12880-022-00774-w

BMC Medical Imaging

RESEARCH Open Access

The impact of cardiopulmonary hemodynamic factors in volumetry for pulmonary nodule management

Erique Guedes Pinto[1*], Diana Penha[1,2], Bruno Hochhegger[3], Colin Monaghan[2], Edson Marchiori[4], Luís Taborda-Barata[1] and Klaus Irion[5]

Abstract

Background: The acceptance of coronary CT angiogram (CCTA) scans in the management of stable angina has led to an exponential increase in studies performed and reported incidental findings, including pulmonary nodules (PN). Using low-dose CT scans, volumetry tools are used in growth assessment and risk stratification of PN between 5 and 8 mm in diameter. Volumetry of PN could also benefit from the increased temporal resolution of CCTA scans, potentially expediting clinical decisions when an incidental PN is first detected on a CCTA scan, and allow for better resource management and planning in a Radiology department. This study aims to investigate how cardiopulmonary hemodynamic factors impact the volumetry of PN using CCTA scans. These factors include the cardiac phase, vascular distance from the main pulmonary artery (MPA) to the nodule, difference of the MPA diameter between systole and diastole, nodule location, and cardiomegaly presence.

Materials and methods: Two readers reviewed all CCTA scans performed from 2016 to 2019 in a tertiary hospital and detected PN measuring between 5 and 8 mm in diameter. Each observer measured each nodule using two different software packages and in systole and diastole. A multiple linear regression model was applied, and inter-observer and inter-software agreement were assessed using intraclass correlation.

Results: A total of 195 nodules from 107 patients were included in this retrospective, cross-sectional and observational study. The regression model identified the vascular distance ($p < 0.001$), the difference of the MPA diameter between systole and diastole ($p < 0.001$), and the location within the lower or posterior thirds of the field of view ($p < 0.001$ each) as affecting the volume measurement. The cardiac phase was not significant in the model. There was a very high inter-observer agreement but no reasonable inter-software agreement between measurements.

Conclusions: PN volumetry using CCTA scans seems to be sensitive to cardiopulmonary hemodynamic changes independently of the cardiac phase. These might also be relevant to non-gated scans, such as during PN follow-up. The cardiopulmonary hemodynamic changes are a new limiting factor to PN volumetry. In addition, when a patient experiences an acute or deteriorating cardiopulmonary disease during PN follow-up, these hemodynamic changes could affect the PN growth estimation.

Keywords: Cardiac-gated imaging techniques [E01.370.350.130.500, Lung neoplasms [C04.588.894.797.520, Pulmonary circulation [G09.330.100.770, Radiographic image interpretation, computer-assisted [E01.158.600.680

*Correspondence: ericguedespinto@gmail.com
[1] Universidade da Beira Interior, Covilhã, Portugal
Full list of author information is available at the end of the article

Keypoints

1. Cardiopulmonary hemodynamic factors affect volumetry for pulmonary nodule management.
2. The impact of hemodynamic changes in volumetry measurements is not related to the cardiac cycle phase, making them relevant even in non-gated scans.
3. During follow-up of a pulmonary nodule, hemodynamic changes (such as decompensated heart failure) could potentially impact growth estimation.

Background

The introduction of coronary CT angiograms (CCTA) in the diagnosis and management of stable coronary artery disease (CAD) has improved clinical outcomes and reduced the need for invasive coronary angiography [1]. As a result, CCTA is now established as a first-line examination for stable CAD [1, 2]. This has exponentially increased the number of CCTA examinations performed and the associated incidental findings [3].

Pulmonary nodules (PN) are among the most common incidental extracardiac findings on CCTA (up to 28% of scans) and require follow-up, even if only rarely malignant [3–5].

Several scientific societies have published guidelines and recommendations for PN management [6]. Small solid PNs are considered benign and do not require follow-up (e.g., smaller than 5 mm in diameter according to the British Thoracic Society (BTS) [7, 8] or 6 mm according to the Fleischner Society [9], the International Early Lung Cancer Action Program (I-ELCAP) [10], and the American College of Radiology (ACR, Lung-Rads) [11]. An exception is the National Comprehensive Cancer Network (NCCN), which recommends that nodules < 5 mm be followed up until the patient is no longer a candidate for definitive treatment [12]. Larger PN have a higher risk of malignancy, as evidenced by the Dutch-Belgian Lung Cancer Screening (NELSON) trial and I-ELCAP [10, 13].

In solid non-calcified PN between 5 and 8 mm in size, the growth rate is a better discriminator between benign and malignant pathology than size or morphological features [10]. The time required for a PN to double in volume at its specific growth rate is called the volume doubling time (VDT). Follow-up studies of PNs using low-dose CT scans (LD-CT) show that VDT is usually shorter than 30 days (e.g., inflammatory changes) or longer than 400 days (e.g., hamartomas) for benign pathology. In contrast, VDT tends to be between 30 and 400 days for malignant pathology [10, 14]. The further apart the two measurements are, the more reliable the growth estimate is. This is especially true for slow-growing lesions (VDT of 400 days), where intrinsic variability in the measurement may overshadow the actual growth of the lesion. However, even fast-growing (VDT of 180 days) 6 mm PN may have overlapping volume measurements with stable 6 mm PN if the follow-up period is less than three months [10].

Choosing the right time for follow-up is important. The Fleischner Society recommends waiting 6–12 months if there is a solid solitary PN with a diameter of 6–8 mm (100–250 mm^3), or 3–6 months if there are multiple solid nodules with a diameter greater the 6 mm (> 100 mm^3) [9].

PN follow-up is done using LD-CT scans. Suppose the PN is incidentally detected on a chest CT examination with a different protocol (e.g., CCTA). In that case, an LD-CT study should be requested as soon as possible and used as the baseline [15]. This raises the possibility of delaying the final diagnosis and justifies the use of institutional alert systems for actionable findings (such as PN), which are neither universal nor foolproof [16]. Using the initial CCTA scan as the baseline for growth assessment would allow better planning and resource management in a radiology department and reduce patient radiation exposure. Compared with LD-CT scans, the increased temporal resolution of CCTA could also improve the robustness of the measurement to cardiac motion and breathing artifacts, which are known to affect PN volumetry through available software tools [17].

All major scientific societies currently recommend automatic or semiautomatic volumetry tools for PN growth estimation, despite known limiting factors related to the nodule, adjacent structures, scanning protocol, or equipment [17]. Boll et al. published the only other study of PN volumetry in ECG-gated CT scans and suggested that cardiovascular motion, as resulting from the interaction of the cardiac cycle phase, location, and mean size of a PN, may influence PN volumetry [18].

Methods

This study aims to investigate how factors known to be related to the cardiopulmonary circulation, namely the cardiac cycle phase during image acquisition, the distance between the MPA and the PN, change in diameter of the MPA between systole and diastole, location of the PN (concerning hydrostatic pressure and vascular cross-sectional area), and presence of cardiomegaly, affect the results of volumetry tools currently in clinical use so that we can better understand their potential applications and limitations.

The Institutional Research Committee Review Board approved this retrospective study (cross-sectional, observational, analytical) and waived the requirement for

written informed consent because of the exclusive use of existing data.

Study sample

The study sample included all consecutive CCTA examinations performed at a tertiary cardiothoracic center from 2016 to 2019. All scans were performed with the same equipment (Somatom Definition Flash; Siemens). The imaging protocol used for the CCTA examinations is shown in Table 1.

The inclusion criteria comprise scans showing at least one solid non-calcified PN with a long-axis diameter between 5 and 8 mm. Exclusion criteria include the absence of an adequate systolic or diastolic phase archived in the hospital's picture archiving and communication system (PACS), defined as 30–40% for systole and 70–80% for diastole; or if the PN was not shown in the field of view (FOV) of both systole and diastole.

Readers and measurements

Two cardiothoracic radiologists with 10 (reader 1) and 5 (reader 2) years of experience identified and measured solid non-calcified PNs according to the protocol described in Fig. 1 and using the Carestream Vue PACS v 11.4.01.1011 (Carestream Health, Inc, Rochester, NY; tool 1) and Syngo via VB20 (Siemens Healthineers AG, Erlangen, Germany; tool 2) commercially available volumetric software packages based on region-growing algorithms. Both these tools performed semiautomatic segmentation by placing one seed point in the center of the nodule. The readers did not correct the resulting segmentation.

If the two readers disagreed on whether an appearance was a true nodule, a consensus decision was made between the two readers and another cardiothoracic radiologist with more than 25 years of experience.

For each nodule identified, the following information was recorded: reader; software package used; patient age and sex; failed segmentation of the nodule, defined as three consecutive failed attempts; nodule segmentation appropriateness, defined as complete PN inclusion with the exclusion of adjacent structures; semiautomatic volume measurement; long- and short-axis diameters in the axial plane, measured manually and semiautomatically, and rounded to one decimal place; distance from the MPA, at the level of the pulmonary valve, to the nodule (vascular distance) measured using curved plane reconstruction (Fig. 1); location of the PN in the axial (anterior; middle; posterior) and coronal plane (superior; middle; inferior); the diameter of the MPA in systole and diastole, measured at the level of the pulmonary valve and in the axial plane; and the presence of cardiomegaly.

Statistical analysis

Data were analyzed using SPSS software (ver. 26.0; IBM Corporation, Armonk, NY, USA).

The inter-quartile range (IQR) method detected outliers in volume measurements. Outliers and cases where segmentation failed were excluded from further analysis.

The average of long- and short-axis manually measured diameters (average diameter) was calculated for all included cases according to the recommendations of the Fleischner Society [9]. In addition, a continuous variable representing the difference of the MPA diameter between systole and diastole measured in the axial plane and at the level of the pulmonary valve was calculated for all nodules.

A multiple linear regression model using a stepwise automatic selection of significant variables was used to predict volume measures based on the reader, software package, cardiac cycle phase, appropriateness of segmentation, average diameter, vascular distance, difference of the MPA diameter between systole and diastole, location of the PN in both axial and coronal planes, presence of cardiomegaly, age, and sex.

The intraclass correlation coefficient (ICC) with an absolute agreement-type two-way mixed model was used to assess inter-observer and inter-software agreement.

Table 1 Imaging protocol for coronary CT angiogram (CCTA)

CCTA Imaging protocol parameters	
Range	From the carina to the apex of the heart
Respiratory phase	Inspiration, breath-hold
Contrast enhancement	75–95 ml of Niopam 370 (iopamidol), at 5–7 ml/s
Image reconstruction	2 mm thickness, 0.75 mm overlap
Kernels	B20f smooth/mediastinum, B60f sharp/lung
Acquisition parameters	Peak kilovoltage (kVp) between 100 and 120 kV; current modulation (CareDose 4D) with 320 mAs as reference
Average acquisition time	1–2 s

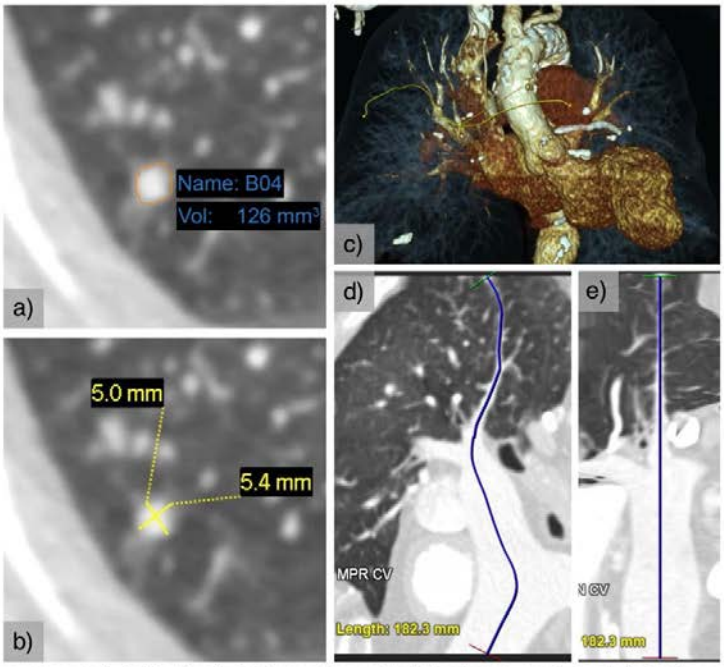

Fig. 1 **a** Volume measurement using the volumetry tool; **b** manual long- and short-diameter measurement using electronic calipers; **c**–**e** tracking the vascular distance between the proximal MPA (at the level of the pulmonary valve) to the nodule

Results

Of a total of 5973 CCTA scans performed, 4478 scans were excluded because either a systolic or diastolic phase was missing from PACS. In addition, 1357 scans were excluded because there were no qualifying solid PN in both systolic and diastolic FOV, and 31 scans were excluded after a consensus decision because they did not represent true nodules. Of the remaining 107 CCTA scans, a total of 195 solid, non-calcified nodules were identified with a long-axis diameter between 5 and 8 mm.

The mean age of the patients was 67.8 years, and the male to female ratio was 1.38 (Table 2).

Each PN was measured by each reader for systole and diastole and, using each software tool, resulting in a total of 1560 measurements (8 measurements per nodule).

Nodule segmentation failed in 11 measurements (1.41%) using the Carestream Vue PACS software package and 15 measurements (1.92%) using the Syngo via software package. However, the segmentation was

Table 2 Patient demographics and indications for CCTA

Patient characteristics	(N = 107)
Age (years): M ± SD	67.8 ± 11.7
Sex: n (%)	
Male	62 (57.9%)
Female	45 (42.1%)
Male to Female ratio	1.38
Indication for the CCTA examination: n (%)	
Acute or chronic chest pain	47 (43.9%)
Hypertension	16 (14.9%)
Diabetes Mellitus	13 (12.1%)
Abnormal or equivocal stress test	9 (8.4%)
Dyspnea	8 (7.4%)
Pre-operative	5 (4.7%)
Abnormal ECG	3 (2.8%)
Congestive heart failure	3 (2.8%)
Palpitations	3 (2.8%)

M mean, *SD* standard deviation

considered appropriate more often using the Syngo via software package (n = 685; 87.8%) than the Carestream Vue PACS software package (n = 623; 79.9%).

A total of 204 measurements were identified as outliers using the IQR method and removed from further analysis. The outliers' mean volume and standard deviation were 586.8 ± 1500.8 mm^3, with a minimum of 159 mm^3 and a maximum of 13,300 mm^3.

Nodules were more frequently identified in the upper third (49.2%) in the axial plane, and between the middle (39.5%) and posterior (40.5%) thirds of the FOV, in the coronal plane.

Descriptive statistical analysis is provided in Table 3.

The results of the regression model are presented in Table 4. The model explains 55.3% of the variation in volume measurement ($R^2 = 0.553$) and yields significant results ($F_{8,1313} = 202.785$, $p < 0.001$), without significant autocorrelation (DW = 1.871) or multicollinearity (VIF < 2).

The results show that the volume measurement increases with the average diameter (B = 24.10; CI_{95} [22.66, 25.54], $p < 0.001$); with the increasing difference of the MPA diameter between systole and diastole (B = 2.26; CI_{95} [1.52, 2.99], $p < 0.001$); when it is in the lower third (B = 13.03; CI_{95} [9.00, 17.06], $p < 0.001$) compared to the upper (reference) in the coronal plane; and when it is in the posterior third (B = 8.94; CI_{95}

Table 3 Descriptive statistics of quantitative variables

N = 1322	M ± SD	Min	Q1	Q2	Q3	Max
Volume (mm^3)	43.527 ± 30.065	2.0	22.0	34.1	58.1	152.0
Automatic long-axis diameter (mm)	6.375 ± 1.697	3.9	5.2	6	7.2	13.0
Automatic short-axis diameter (mm)	5.386 ± 1.104	2.9	4.7	5.3	6	7.7
Manual long-axis diameter (mm)	6.101 ± 1.001	4.3	5.2	6.5	7.1	8.5
Manual short-axis diameter (mm)	4.255 ± 0.789	2.9	3.9	4.2	4.7	6.5
Average diameter (mm)	5.178 ± 0.773	3.5	4.4	5.5	5.9	7.5
Vascular distance (cm)	18.405 ± 3.178	10.6	16.0	18.4	20.7	26.4
Difference of the MPA diameter between systole and diastole (mm)	2.295 ± 1.522	0.1	1.0	2.0	3.3	6.3

MPA main pulmonary artery

Table 4 Parameter estimates for the prediction of Volume

Variable	B	95% CI	t	p	Effect size
(Constant)	−37.40	[−48.82, −25.98]	−6.426	***< 0.001	0.030
Appropriate segmentation	−32.69	[−37.17, −28.20]	−14.291	***< 0.001	0.135
Average diameter	24.10	[22.66, 25.54]	32.824	***< 0.001	0.451
Vascular distance	−0.98	[−1.42, −0.54]	−4.368	***< 0.001	0.014
Difference of the MPA diameter between systole and diastole	2.26	[1.52, 2.99]	6.019	***< 0.001	0.027
Lower third (coronal)	13.38	[9.84, 16.93]	7.410	***< 0.001	0.040
Posterior third (axial)	7.87	[5.46, 10.29]	6.407	***< 0.001	0.030
Sex (male as reference)	−3.45	[−5.79, −1.11]	−2.895	**0.004	0.006
Cardiomegaly	7.05	[2.59, 11.51]	3.103	**0.002	0.007
Excluded variables					
Cardiac cycle phase				0.348	
Reader				0.590	
Software package for Volumetry				0.341	
Middle third (axial)				0.978	
Middle third (coronal)				0.505	
Age				0.165	

MPA main pulmonary artery, *B* parameter coefficient, *CI* confidence interval, *t* t test

*** $p < 0.001$; ** $p < 0.01$; Effect size (partial eta square—$\hat{\zeta}^2$)

[5.64, 12.24], $p < 0.001$) compared to the anterior (reference) in the axial plane.

Volume measurement decreases when segmentation is considered appropriate ($B = -32.69$; CI_{95} [−48.82, −25.98], $p < 0.001$), and with increasing vascular distance ($B = -0.98$: CI_{95} [−1.42, −0.54], $p < 0.001$).

The effect size is larger for the average diameter ($\zeta^2 = 0.451$, large), followed by the appropriateness of segmentation ($\zeta^2 = 0.135$, intermediate to large), the location of the PN in the lower third ($\zeta^2 = 0.040$, small to intermediate) or the posterior third ($\zeta^2 = 0.030$, small) of the FOV, the difference of the MPA diameter between systole and diastole ($\zeta^2 = 0.027$, small) and for the distance between the MPA and the PN ($\zeta^2 = 0.014$, small).

The results also show a tendency for the nodule to be slightly larger in the presence of cardiomegaly ($B = 7.05$; CI_{95} [2.59, 11.51], $p = 0.002$) and somewhat smaller in women ($B = -3.45$; CI_{95} [−5.79, −1.11], $p = 0.004$), but with a negligible effect size.

The cardiac cycle phase is not statistically significant in our regression model ($p = 0.348$), and there was no statistically significant difference in volume measurements based on cardiac phase using multivariate tests ($F_{7,1518} = 0.428$, $p = 0.885$, Wilks' lambda (Λ) = 0.998, partial $\eta^2 = 0.002$).

Intraclass correlation analysis (Table 5) shows very high reliability between the two readers (ICC = 0.870; CI_{95} [0.850, 0.887]) with no statistically significant difference between them ($F_{1,764} = 0.561$, $p = 0.561$). There is no reasonable reliability between the two software packages (ICC = 0.059; CI_{95} [−0.083, 0.183], $p = 0.002$), and there is a statistically significant difference between the measurement made with the two software tools ($F_{1,760} = 9.473$, $p = 0.002$).

Table 5 ICC between readers and software tools, for Volume measurement

	ICC	(95% CI)	F	p
Between readers				
Global Sample	0.870	[0.850, 0.887]	0.561	0.454
Systole 30–40%	0.865	[0.834, 0.889]	0.682	0.409
Diastole 70–80%	0.965	[0.958, 0.972]	0.373	0.542
Between software packages				
Global sample	0.059	[−0.083, 0.183]	9.473	**0.002
Systole 30–40%	0.027	[−0.186, 0.203]	6.302	*0.012
Diastole 70–80%	0.545	[0.441, 0.630]	12.559	*** < 0.001

ICC intra class coefficient, *CI* confidence interval

*** $p < 0.001$; ** $p < 0.01$; * $p < 0.1$

Discussion

The true volume of in vivo pulmonary nodules is unknown, and even when those nodules are surgically excised, their volume changes because of the sudden stop in blood flow [17]. Therefore, it is our expectation that the blood flow inside and surrounding a given pulmonary nodule will be included in the segmentation result provided by the volumetry tool. In that sense, it is expected that an increase in the blood pressure felt inside the nodule will translate into an increase in the blood volume included in the segmentation.

Our study identified factors related to cardiopulmonary circulation, namely the location of the PN, the difference of the MPA diameter between systole and diastole, and vascular distance between the MPA and the PN, which were statistically associated with the measurements of volumetry tools.

These results could be explained by the propagation of vascular pressure from the heart to the nodule through the complex arterial and capillary network. Assuming the pressure difference at the MPA between systole and diastole, one might expect a similar pressure difference at the capillaries surrounding the PN and that the cardiac cycle phase during acquisition would also be important. However, our results do not support this intuition nor corroborate earlier results from Boll et al. [18]. This is only the second study investigating PN volumetry using ECG-gated scans to the best of our knowledge. The significant dependence of volume measurement on the cardiac cycle phase, reported previously, has not yet been independently validated. Differences between our study and the former include larger sample size, number of detector rows of the CT scanner (128 vs. 16 slices), and current and updated segmentation algorithms in clinical use. The independence of volume measurement from the cardiac cycle phase means that our data cannot be used to recommend any particular cardiac phase for PN volumetry on CCTA scans. It could also suggest that these hemodynamic effects could be seen in non-gated scans (such as LD-CT). The high temporal resolution of CCTA scans accounts for their sensibility to momentary cardiopulmonary hemodynamic changes (subtle differences between two phases in a single cardiac cycle). These momentary changes could be used to model clinically significant hemodynamic changes that a patient may experience when suffering from an acute or progressing cardiopulmonary disease and could be extreme enough to affect the nodule's growth estimation. The overlap of demographic characteristics and risk factors in patients evaluated for CAD or PN follow-up makes this area of research clinically relevant.

A physiological model of cardiopulmonary hemodynamics should consider that the total time required for

the pressure wave to reach the PN (transit time) depends on the complex interaction between vascular and hydrostatic pressures, vascular resistance, the distance the blood travels between leaving the right ventricle and reaching the nodule (vascular distance), and the cross-sectional area of the vessels along the way. All these factors may affect the transit time for every PN differently so that the pressure peak reaches each PN at a different cardiac cycle phase.

The dynamic change of the intravascular pressure felt around or inside the PN could change the blood volume included in the segmentation result and consequently the volume measurement. If the change to the segmentation volume is not consistent between follow-up scans, the VDT will be either under- or overestimated.

During PN follow-up, events such as the onset of pleural effusion related to congestive heart failure could alter the PN position, vascular distance (as the aerated lung parenchyma is displaced by the volume of pleural effusion), and intravascular pressure, potentially impacting subsequent volume measurements.

Chronic thromboembolism and vasculitis are associated with increased resistance and tortuosity of the distal pulmonary vessels, affecting the propagation of the intra-vascular pressure wave, and the pressure magnitude. Clinically, these hemodynamic changes can lead to pulmonary hypertension and ultimately right ventricular dysfunction. This phenomenon increases the diameter of the MPA in both systole and diastole, but predominantly in the later, as can be seen on CT, reducing the diameter difference between both cardiac phases. In contrast, pulmonary valvular regurgitation would increase this difference by predominantly reducing the diastolic pressure [19].

Changes in hydrostatic pressure (anteroposterior gradient in a patient in decubitus position on the CT scanner), changes in the vessels' cross-sectional luminal area (craniocaudal gradient), and the vascular distance further explain the significance of the location of the nodule in our model.

Cardiomegaly was also significant in our model but had negligible effect size. One possible explanation is the increased pressure in the left atria with retrograde capillary recruitment around the PN [20]. The potential influence of sex is also difficult to explain and has a negligible effect size but may be related to a higher vessel density in women than in men, as suggested in a recent study [21].

The volume measurement is unsurprisingly strongly related to the average diameter, as both relate to a different aspect (i.e., volume and diameter) of the same characteristic (i.e., size). Likewise, the volume is also related to the appropriateness of the nodule segmentation with a moderate effect size. In clinical practice, cases considered inadequate will tend to overestimate the volume (e.g., the inclusion of the bronchial wall in segmentation) and should be manually corrected. By including this variable in the model, we can minimize inter-observer variability by avoiding manual correction of the semiautomatic segmentation results but still be able to distinguish its effect from the effect attributable to cardiopulmonary hemodynamic factors.

As expected, the inter-observer agreement is very high globally but even higher in diastole, which could be related to minimizing cardiac motion using ECG-gating, as suggested by Boll et al. [18].

No reasonable inter-software agreement can be assumed, which exposes the differences in segmentation performance across different software packages, and reinforces the current recommendations that the same software package should be used throughout the follow-up period [22].

CCTA scans allow multiple independent measurements of a PN (at different phases of the cardiac cycle) in a single acquisition, controlling for most other factors (such as the absence of true growth). In this way, it is similar to the coffee-break study design, which also assumes a lack of true growth (zero-change datasets). However, the latter is more useful in phantom studies because of the increased radiation exposure [23]. Nevertheless, investigating the effect of these hemodynamic changes on PN volumetry would not be feasible with a coffee-break study design using non-gated scans (zero-change even for hemodynamic changes) and would be very inefficient in a longitudinal study (because we cannot assume the absence of true growth over time and the true volume of a PN is unknown).

We propose future research into the variability of the volume measurement in CCTA scans since growth estimation is the most critical application of volumetry in PN between 5 and 8 mm.

A limitation of the present study is the low percentage of cases included in the study from the large study sample, which is due to the large number of CCTA scans with missing systolic or diastolic phases in PACS. This is related to the department approach of sending only the most diagnostically relevant phases for archiving. Nevertheless, to our knowledge, this study represents the largest published series on PN volumetry in ECG-gated CT scans and using current and updated volumetry tools in clinical use. Another limitation of the study is the lack of information on risk factors such as smoking. Given the substantial overlap between lung cancer and CAD risk factors, we assume that their prevalence is high in the study population. We realize that the model simplifies the complex mechanisms of cardiopulmonary hemodynamics and does not attempt

to address the systemic bronchial arteries or the regulatory mechanisms of ventilation and perfusion. Other non-hemodynamic factors may also influence the measurement, like the distribution of the nodules along the airways, which may also be confounded with the vascular distance.

Conclusion

Our data show that the studied factors related to cardiopulmonary hemodynamics influence the results of volumetry tools applied to PN between 5 and 8 mm. Because the cardiac cycle phase is not statistically significant in our model, there is no optimal phase that could control this effect, but more importantly, this raises the possibility of the effect also being relevant to non-gated CT scans.

The vascular distance between the MPA and the PN and the diameter difference of the MPA between systole and diastole are related to cardiac function and resistance in the pulmonary circulation. Therefore, these factors may change between the baseline and the follow-up evaluations (e.g., decompensated heart failure) and affect the growth estimation of a PN.

The inter-observer reliability of the volumetry tools is very high, which is the motivation for automatic and semiautomatic volumetry software packages.

The study design based on ECG-gated scans seems suited to study the impact of momentary changes in the cardiopulmonary circulation on PN volumetry and is likely a good model for the potentially more extreme hemodynamic changes that a patient can experience between scans.

Abbreviations

ACR: American College of Radiology; BTS: British Thoracic Society; CAD: Coronary artery disease; CCTA: Coronary CT angiography; ECG: Electrocardiogram; FOV: Field of view; I-ELCAP: International Early Lung Cancer Action Program; LD-CT: Low-dose CT scan; NELSON: Dutch-Belgian Lung Cancer Screening trial; NCCN: National Comprehensive Cancer Network; MPA: Main pulmonary artery; PACS: Picture archiving and communication system; PN: Pulmonary nodule; VDT: Volume doubling time.

Acknowledgements

For statistical support—Prof. Paulo Pereira.

Authors' contributions

Study conception and design: EGP, DP, KI. Data acquisition, analysis, and interpretation: EGP, DP, KI. Manuscript preparation: EGP, DP, KI. Manuscript editing: EGP, DP, BH, CM, EM, LTB, KI. All authors read and approved the final manuscript.

Funding

No funds, grants, or other support were received.

Availability of data and materials

The datasets used and analyzed during the current study are available from the corresponding author on reasonable request.

Declarations

Ethics approval and consent to participate

The study project was approved by the head of the Research & Innovation Committee of the Liverpool Heart and Chest Hospital, Dr. Bashir Matata, at the Research Committee meeting on 12/07/2019. The Liverpool Heart and Chest Hospital Institutional review board approved this study along with Informed consent waiver due to the use of existing clinical data. The study was conducted in accordance with the spirit and letter of the Helsinki Declaration, the Good Clinical Practice (GCP) recommendations, and the applicable legal protocols and regulations.

Consent for publication

Not applicable.

Competing interests

The authors declare that they have no competing interests.

Author details

[1]Universidade da Beira Interior, Covilhã, Portugal. [2]Imaging Department, Liverpool Heart and Chest Hospital NHS Foundation Trust: Liverpool, Liverpool, UK. [3]Pontifical Catholic University of Rio Grande Do Sul, Porto Alegre, Brazil. [4]Federal University of Rio de Janeiro, Rio de Janeiro, Brazil. [5]Imaging Department, University of Manchester, Manchester, UK.

Received: 2 November 2021 Accepted: 10 March 2022
Published online: 18 March 2022

References

1. Tzolos E, Newby DE. Coronary computed tomography angiography improving outcomes in patients with chest pain. Curr Cardiovasc Imaging Rep. 2019;12(5):1–10.
2. Moss AJ, Williams MC, Newby DE, Nicol ED. The Updated NICE Guidelines: cardiac CT as the first-line test for coronary artery disease. Curr Cardiovasc Imaging Rep. 2017;10(5):15.
3. Scholtz J-E, Lu MT, Hedgire S, Meyersohn NM, Oliveira GR, Prabhakar AM, et al. Incidental pulmonary nodules in emergent coronary CT angiography for suspected acute coronary syndrome: impact of revised 2017 Fleischner Society Guidelines. J Cardiovasc Comput Tomogr. 2018;12(1):28–33.
4. Ramanathan S, Ladumor SB, Francis W, Allam AA, Alkuwari M. Incidental non-cardiac findings in coronary computed tomography angiography: is it worth reporting? J Clin Imaging Sci. 2019;9(40):40.
5. Goehler A, McMahon PM, Lumish HS, Wu CC, Munshi V, Gilmore M, et al. Cost-effectiveness of follow-up of pulmonary nodules incidentally detected on cardiac computed tomographic angiography in patients with suspected coronary artery disease. Circulation. 2014;130(8):668–75.
6. Goo JM. MTE 27.02 pulmonary nodule guidelines: how do we decide between the IELCAP, ACCP, NCCN, Fleischner Society, BTS, and lung-RADS? J Thorac Oncol. 2017;12(11):S1654–5.
7. Callister MEJ, Baldwin DR, Akram AR, Barnard S, Cane P, Draffan J, et al. British Thoracic Society guidelines for the investigation and management of pulmonary nodules: accredited by NICE. Thorax. 2015;70(Suppl 2):ii1–54.
8. Graham RNJ, Baldwin DR, Callister MEJ, Gleeson FV. Return of the pulmonary nodule: the radiologist's key role in implementing the 2015 BTS guidelines on the investigation and management of pulmonary nodules. Br J Radiol. 2016;89(1059):20150776.
9. MacMahon H, Naidich DP, Goo JM, Lee KS, Leung ANCC, Mayo JR, et al. Guidelines for management of incidental pulmonary nodules detected on CT images: from the Fleischner Society 2017. Radiology. 2017;284(1):228–43.
10. Henschke CI, Yip R, Shaham D, Zulueta JJ, Aguayo SM, Reeves AP, et al. The regimen of computed tomography screening for lung cancer: lessons learned over 25 years from the International Early Lung Cancer Action Program. J Thorac Imaging. 2021;36(1):6–23.
11. Chelala L, Hossain R, Kazerooni E, Christensen J, Dyer D, White CS. Lung-RADS version 1.1: challenges and a look ahead, from the AJR special

series on radiology reporting and data systems. Am J Roentgenol. 2021;216:1411–22.
12. Wood DE, Kazerooni EA, Baum SL, Eapen GA, Ettinger DS, Hou L, et al. Lung cancer screening, version 3.2018, NCCN clinical practice guidelines in oncology. J Natl Compr Cancer Netw. 2018;16(4):412–41.
13. Walter JE, Heuvelmans MA, de Bock GH, Yousaf-Khan U, Groen HJM, van der Aalst CM, et al. Relationship between the number of new nodules and lung cancer probability in incidence screening rounds of CT lung cancer screening: the NELSON study. Lung Cancer. 2018;125:103–8.
14. Baldwin DR, Devaraj A. Lung cancer risk in new pulmonary nodules: implications for CT screening and nodule management. Lancet Oncol. 2016;17(7):849–50.
15. Bueno J, Landeras L, Chung JH. Updated Fleischner Society Guidelines for managing incidental pulmonary nodules: common questions and challenging scenarios. Radiographics. 2018;38(5):1337–50.
16. Watura C, Desai SR. Radiology report alerts - are emailed 'Fail-Safe' alerts acknowledged and acted upon? Int J Med Inform. 2020;133:104028.
17. Devaraj A, van Ginneken B, Nair A, Baldwin D. Use of volumetry for lung nodule management: theory and practice. Radiology. 2017;284(3):630–44.
18. Boll DT, Gilkeson RC, Fleiter TR, Blackham KA, Duerk JL, Lewin JS. Volumetric assessment of pulmonary nodules with ECG-gated MDCT. Am J Roentgenol. 2004;183(5):1217–23.
19. Helmberger M, Pienn M, Urschler M, Kullnig P, Stollberger R, Kovacs G, et al. Quantification of tortuosity and fractal dimension of the lung vessels in pulmonary hypertension patients. PLoS ONE. 2014;9(1):e87515.
20. Taylor BJ, Kjaergaard J, Snyder EM, Olson TP, Johnson BD. Pulmonary capillary recruitment in response to hypoxia in healthy humans: a possible role for hypoxic pulmonary venoconstriction? Respir Physiol Neurobiol. 2011;177(2):98–107.
21. Pienn M, Burgard C, Payer C, Avian A, Urschler M, Stollberger R, et al. Healthy lung vessel morphology derived from thoracic computed tomography. Front Physiol. 2018;9:346.
22. Soo E, Edey AJ, Mak SM, Moser J, Mohammadi S, Rodrigues T, et al. Impact of choice of volumetry software and nodule management guidelines on recall rates in lung cancer screening. Eur J Radiol. 2019;120:108646.
23. Talwar A, Willaime JMY, Pickup LC, Enescu M, Boukerroui D, Hickes W, et al. Pulmonary nodules: Assessing the imaging biomarkers of malignancy in a "coffee-break." Eur J Radiol. 2018;101:82–6.

Publisher's Note

9.2. Variability of pulmonary nodule volumetry on coronary CT angiograms

Observational Study

Medicine

OPEN

Variability of pulmonary nodule volumetry on coronary CT angiograms

Erique Pinto, MD, EBIR[a,*], Diana Penha, MD[a,b], Bruno Hochhegger, MD, PhD[c], Colin Monaghan, HCPC[d], Edson Marchiori, MD, PhD[e,f], Luís Taborda-Barata, MD, PhD[g], Klaus Irion, MD, PhD[h]

Abstract

This study aims to investigate the variability of pulmonary nodule (PN) volumetry on multiphase coronary CT angiograms (CCTA).

Two radiologists reviewed 5973 CCTA scans in this cross-sectional study to detect incidental solid noncalcified PNs measuring between 5 and 8 mm. Each radiologist measured the nodules' diameters and volume, in systole and diastole, using 2 commercially available software packages to analyze PNs.

Bland-Altman analysis was applied between different observers, software packages, and cardiac phases. Bland-Altman subanalysis for the systolic and diastolic datasets were also performed.

A total of 195 PNs were detected within the inclusion criteria and measured in systole and diastole. Bland-Altman analysis was used to test the variability of volumetry between cardiac phases ([–47.0%; 52.3%]), software packages ([–50.2%; 68.2%]), and observers ([–14.5%; 27.8%]). The inter-observer variability of the systolic and diastolic subsets was [–13.6%; 31.4%] and [–13.9%; 19.7%], respectively.

Using diastolic volume measurements, the variability of PN volumetry on CCTA scans is similar to the reported variability of volumetry on low-dose CT scans. Therefore, growth estimation of PNs on CCTA scans could be feasible.

Abbreviations: CAD = Coronary artery disease, CCTA = Coronary CT angiography, CI95 = 95% Confidence interval, CT = Computerized Tomography, ECG = Electrocardiogram, FOV = Field of view, kVp = Peak kilovoltage, LD-CT = Low-dose CT, LOA = Limits of agreement, PN = Pulmonary nodule, VDT = Volume doubling time.

Key words: coronary CT angiogram, lung cancer, pulmonary nodule, incidental finding, volumetry, volume doubling time.

1. Introduction

Most scientific societies now recognize Coronary CT angiogram (CCTA) as a first-line examination in diagnosing and clinically managing stable coronary artery disease (CAD).[1,2] CCTA has replaced invasive coronary angiography in diagnosing CAD and improved clinical outcomes for these patients.[3–8] However, the increasing number of CCTA scans performed led to an increase in reported incidental extracardiac findings, with pulmonary nodules (PNs) being the most common (up to 28% of scans).[9–11]

The Fleischner Society recommends low-dose chest CT (LD-CT) follow-up of incidental solid, noncalcified PNs measuring between 5 and 8 mm since the growth rate is a better marker for malignancy than size, calcifications, and morphological characteristics.[12–14] As such, incidental PNs detected in CCTA scans and between 5 and 8 mm in diameter should have an LD-CT scan as soon as possible.[12] We use dedicated volumetry tools to calculate the volume doubling time (VDT) and estimate the growth rate. When the VDT is shorter than 30 or longer than 400 days, the PN is more likely related to benign pathology (inflammatory causes or hamartomas, respectively). In comparison, a VDT between 30 and 400 days is suspicious for malignancy.[15] However, these tools suffer from numerous known limiting factors, including the specific software package, nodule's size, contact to other structures, use of contrast agent, slice thickness, slice overlap, "kernel," degree of chest expansion, motion artifacts, and many others.[15–20] In addition, factors related to cardiac function have also been suggested but not conclusively studied.[21]

Some authors have suggested that CCTA could be useful in lung cancer screening, given the considerable overlap of risk factors with CAD.[22] Compared to LD-CT, the higher temporal resolution and electrocardiogram (ECG)-gating makes CCTA scans more robust to motion and breathing artifacts. Likewise, estimating growth from previous CCTA scans could expedite the diagnosis and decision-making while allowing for better resource management in radiology departments. However, growth estimation by PN volumetry is related to the measurement variability, as it impacts the optimal waiting time between

The authors have no conflicts of interest to disclose.

The datasets generated during and/or analyzed during the current study are available from the corresponding author on reasonable request.

[a]Universidade da Beira Interior Faculdade de Ciências da Saúde, Covilha, Portugal, [b]Imaging Department, Liverpool Heart and Chest Hospital NHS Foundation Trust, Liverpool, United Kingdom, [c]Pontificia Universidade Catolica do Rio Grande do Sul, Porto Alegre, Brazil, [d]Radiology Department, Liverpool Heart and Chest Hospital NHS Foundation Trust, Liverpool, United Kingdom, [e]Universidade Federal do Rio de Janeiro Faculdade de Medicina, Rio DE Janeiro, RJ, Brazil, [f]Universidade Federal Fluminense Faculdade de Medicina, Niterói, RJ, Brazil, [g]Universidade da Beira Interior, Covilhã, Portugal, [h]Imaging Department, Manchester University NHS Foundation Trust, Manchester, United Kingdom.

*Correspondence: Erique Pinto, MD, EBIR, Rua Luís DE Camões, nº 102, lt 8, 3º esq, 1300–356 Lisbon, Portugal. (e-mail: ericguedespinto@gmail.com).

How to cite this article: Pinto E, Penha D, Hochhegger B, Monaghan C, Marchiori E, Taborda-Barata L, Irion K. Variability of pulmonary nodule volumetry on coronary CT angiograms. Medicine 2022;101:335(e30332).

Received: 15 February 2022 / Received in final form: 16 July 2022 / Accepted: 19 July 2022

http://dx.doi.org/10.1097/MD.0000000000030332

follow-up scans.[23] As such, a higher variability increases the overlap between benign and malignant pathology, reducing the discriminating power of volumetry (Fig. 1). The reported inter-scan variability of PN volumetry on LD-CT is around 25%, meaning that an increase in volume above 25% has a 95% likelihood of actual growth.[24,25] Recently, Bartlett et al published their results on nonmetastatic PNs (28–150 mm^3) and proposed that a threshold of 15% of volume increase could be more appropriate and that closer surveillance may be justifiable.[26]

Current guidelines and recommendations regarding the optimal waiting time between follow-up scans assume this variability of 25% for volumetry tools on LD-CT.[23] For PN volumetry to apply to CCTA scans, its variability must be within these limits; otherwise, the current recommended waiting times would not be optimal. We found no published reports related to the variability of PN volumetry on ECG-gated CT scans.

This study aims to investigate the variability of PN volumetry on CCTA scans when applied to incidental solid PNs between 5 and 8 mm in diameter.

2. Methods

The Institutional Research Committee Review Board approved this retrospective cross-sectional study (observational, analytical) and waived the requirement for written informed consent due to the use of existing clinical data.

2.1. Study sample

The study sample includes consecutive patients who underwent a CCTA scan between January 1, 2016, and December 31, 2019, in our institution. All patients had one or more CCTA scans performed on the same equipment (Somatom Definition Flash; Siemens). Images were acquired during inspiration and contrast injection (75–95 mL of Niopam 370, at 5–7 mL/s), with anatomical coverage from the carina through the cardiac apex. Acquisition parameters include peak kilovoltage (kVp) between 100–120 kV; current modulation (CareDose 4D) with 320 mAs as reference; average acquisition time of 1–2 seconds; collimation of 128 × 0.6 mm; and pitch of 3.4. Reconstruction parameters include 2 mm and 0.75 mm overlapping slices through the prescribed range, with a B20f algorithm and field of view (FOV) of 22 cm.

The study's inclusion criteria comprise scans with one or more incidental solid, noncalcified PN within the FOV in systole and diastole, measuring between 5 and 8 mm in long-axis diameter. Exclusion criteria comprise the absence of systolic (30–40%) or diastolic phase (70–80% of the cardiac cycle) in the archive; or when one of the cardiac phases did not present the PN in its FOV.

2.2. Observers and measurements

Two cardiothoracic radiologists with 10 (observer 1) and 5 years of experience (observer 2) identified nodules fitting the eligibility criteria within the study sample. In addition, a consensus decision between both observers and a third chest radiologist (with >25 years of experience) resolved disagreements regarding whether an appearance met the inclusion criteria.

Each observer measured each nodule using 2 different PN volumetry software packages in systole and diastole. The software

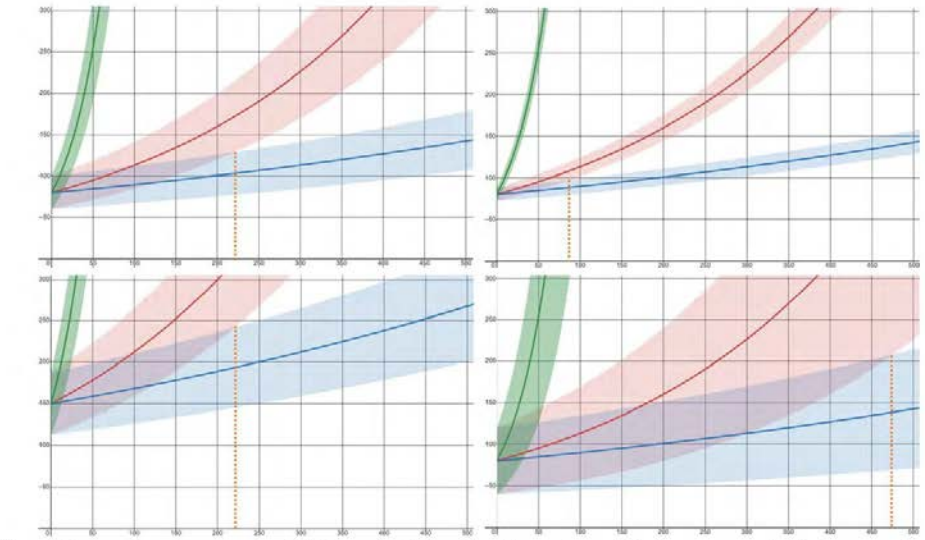

Figure 1. The importance of measurement variability in growth estimation. All graphs present expected volume measurements of 3 pulmonary nodules with different growth-rates [i.e., VDT = 30 days, as in inflammatory changes (green); VDT = 250 days, as in malignancy (red); and VDT = 600 days, as in benign pathology (blue)]. The shaded areas represent possible volume measurements over time given the different measurement variability values [left (top and bottom)—25%; top right—10%, and bottom right—50%]. Volume measurements in overlapping shaded areas cannot be confidently attributed to 1 growth rate or another. The starting volume of a nodule [top left—80 cc^3; bottom left—150 cc^3] does not change the optimal waiting time between follow-up scans for a confident discrimination between suspicious and benign pathology (dashed orange line), but the measurement variability can significantly shorten (top right) or extend it (bottom right).

packages used were Carestream Vue PACS v 11.4.01.1011 (Carestream Health, Inc, Rochester, NY) and Syngo via VB20 (Siemens Healthineers AG, Erlangen, Germany), as tool 1 and tool2, respectively.

Both tools performed semiautomatic segmentation by placing 1 seed point in the middle of the nodule. The observers did not correct the resulting segmentation. Still, they recorded the adequacy of the segmentation as "inadequate" if 3 consecutive segmentation attempts had failed or when the segmentation did not adequately represent the nodule. Also recorded were the observer's initials; software package used; cardiac phase; long-axis diameter of the nodule; location of the nodule in axial and coronal planes; and nodule volume calculated using the volumetry tool.

2.3. Statistical analysis

The data were analyzed using SPSS software (ver. 26.0; IBM Corporation).

Descriptive statistical analysis of the included nodules was performed.

All cases with inadequate nodule segmentation were excluded from further analysis.

The association of volume measurements was tested using Kendall tau correlation coefficients (τ) between different cardiac phases, software packages and observers.

The Bland-Altman analysis is a well-known statistical tool for method comparison and has been used previously to study the variability of PN volumetry.[27] Volume measurement agreement was tested by Bland-Altman analysis and plots. In addition, further inter-observer analyses of the systolic and diastolic data subsets were performed.

The estimation of the limits of agreement (LOA) in the Bland-Altman analysis used the nonparametric quartile analysis after the exclusion of normality of the differences of measurements. Possible reasons for this non-normal distribution include the presence of a natural limit (i.e., volume must be a positive number) and the restriction of the nodules' diameter between 5 and 8mm (i.e., sorted by diameter).

3. Results

Of a total of 5973 candidate CCTA scans performed between 2016 and 2019, 4478 were excluded for not having both a systolic and diastolic phase in the archive. Of the remaining 1495 scans, 1357 were excluded for not having qualifying solid PNs in both systolic and diastolic phases, and 31 scans were excluded after consensus decision (as not representing true nodules).

From the 107 scans included, a total of 195 nodules were identified with a manual long-axis measurement between 5 and 8 mm. The mean age of the patients was 67.8 years, with a male to female ratio of 1.34 (Table 1). Nodules were more frequently identified in the upper thirds of the FOV in the coronal plane (49.2%) and between the middle (39.5%) and posterior (40.5%) thirds in the axial plane.

For each nodule, each set of volume measurements was repeated by each observer, for systole and diastole, and using each software package, resulting in a total of 1560 volume measurements (8 measurements per nodule). Figure 2 provides an example of measurement. The quality of the nodule segmentation was considered inadequate in more cases using 1 software package (tool 1; n = 157; 20.1%) than the other (tool 2; n = 95; 12.2%).

The mean volume was close to 50mm^3 with a median of 35mm^3, ranging from 10.4 to 400 mm^3 (Table 2).

The volume measurements of the solid PN show a very strong association between systole and diastole, with a Kendall tau correlation coefficient (τ) of 0.812 (CI_{95} = [0.785; 0.838], df = 645, P < .0001); between software packages with a τ = 0.744 (CI_{95} = [0.714; 0.771], df = 616, P < .0001); and between different observers, with a τ = 0.942 (CI_{95} = [0.916; 0.957], df = 682, P < .0001) globally; τ = 0.928 (CI_{95} = [0.874; 0.955], df = 338, P < .0001) for the systolic dataset; and τ = 0.956 (CI_{95} = [0.931; 0.971], df = 344, P < .0001) for the diastolic dataset.

The Bland-Altman plots show an increase in the differences' variability as the measurement's magnitude increases, particularly for different cardiac phases and software packages. The estimated LOA of the percent Bland-Altman plots are [−47.0%; 52.3%], between phases of the cardiac cycle, and [−50.1%; 68.2%] between software packages (Fig. 3 and Table 3), with no significant bias. The estimated LOA of the percent Bland-Altman plots between different observers are [−14.5%; 27.8%] globally, [−13.6%; 31.4%] for the systolic dataset and [−13.9%; 19.7%] for the diastolic dataset.

Table 1

Demographics of the sample population.

		(n = 195)
Age (yrs): M ± SD		67.8 ± 11.7
Gender: n (%)	Male	112 (57.4)
	Female	83 (42.6)

M = Mean, SD = standard deviation

4. Discussion

Growth estimation is feasible using PN volumetry on the diastolic phase of CCTA scans. Conversely, comparing volume measurements from different cardiac phases could be as unreliable as using different volumetry tools (similar measurement variability), implying a lower discriminating power between benign and malignant pathology.

For the Bland-Altman analyses, we defined the a priori LOA as a difference of ±25% in volume, according to the previously reported variability of PN volumetry in LD-CT scans, which form the basis of recommendations for waiting time between follow-up scans.[15,23,28]

In the study's results, the shapes of the Bland-Altman plots for different software tools and cardiac phases show that the difference in volume increases proportionally with their mean.[27] Therefore, the variability is assumed to be relative or proportional (represented as a volume percentage). However, this proportionality is less obvious between different observers with larger nodules. For example, for PNs larger than 65.6 mm^3, the estimated LOA between observers vary between −8.6 mm^3 and 15.9 mm^3, which will be <25% of their volume. The proportionality seems to apply for smaller nodules, so the percentage Bland-Altman analysis is still relevant with the estimated LOA ([−14.45%; 27.77%]) much closer but outside the a priori LOA. However, in the inter-observer subanalysis specific for diastolic measurements, the estimated LOA ([−13.92%; 19.66%]) are well within the a priori LOA. The lower variability seen in diastole is likely related to less cardiac motion when compared with systole and the higher temporal resolution compared to LD-CT scans. In addition, the low interobserver variability is an expected benefit of semiautomatic volumetry tools.[15]

Identified limitations of the present study include (1) the large portion of excluded candidate CCTA scans, which was due to departmental protocol not to archive, per default, both systolic and diastolic phases; (2) the disproportionate representation of smaller nodules in comparison to larger ones; and (3) the non-normal distribution of the differences between measurements, which implied a nonparametric statistical approach.

To the best of our knowledge, this is only the second (and largest) study to focus on PN volumetry in ECG-gated CT scans

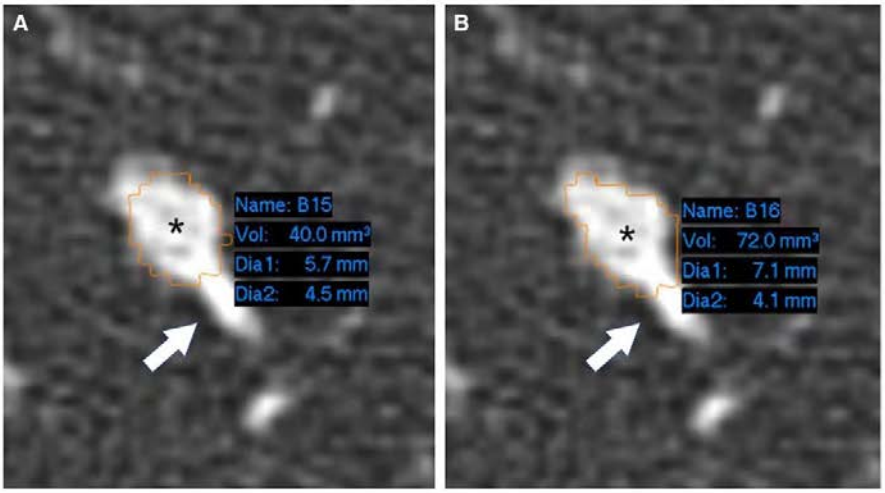

Figure 2. Example of a nodule included in the study measured in systole (A) and diastole (B). The seed points (*) were placed in the nodule center, and the yellow lines show the semiautomatic segmentation result, which was not corrected and considered adequate by both observers. Notice the small vessel (arrows) approaching the nodule, which was excluded from the segmentation in both instances. The volume measured in diastole was 80% greater than in systole.

Table 2

Descriptive statistical analysis of volume measurements in the sample population and at different phases of the cardiac cycle, using different software packages and by different observers.

Volume	n	Mean (mm^3)	SD (mm^3)	Q_1 (mm^3)	Median (mm^3)	Q_3 (mm^3)
Sample population						
	1237	63.282	68.039	24.5	38	89
Between systole and diastole						
Systole	645	51.99	46.11	23.375	36	62
Diastole	645	50.836	44.947	23.3	35.5	60.4
Difference	645	−1.154	13.13	−3.6	−0.5	1.7
Between different software packages						
Tool 1	616	47.108	38.438	23.3	34.5	59.8
Tool 2	616	48.807	42.257	22	35	59
Difference	616	1.699	15.942	−3.25	−2.0	6.7
Between different observers						
Observer 1	642	53.62	46.993	24	36.6	62.9
Observer 2	642	52.91	47.172	23.4	36.2	62
Difference	642	−0.701	8.723	0	0	0
Between different observers (systolic dataset)						
Observer 1	318	44.668	29.936	23.4	34.9	59
Observer 2	318	43.751	29.583	23	34.05	58
Difference	318	−0.917	9.911	0	0	0
Between different observers (diastolic dataset)						
Observer 1	322	43.862	29.316	23	34.6	57.2
Observer 2	322	43.019	28.611	23	34	55
Difference	322	−0.842	6.806	0	0	0

Q_1 = first quartile, Q_3 = third quartile, SD = standard deviation.

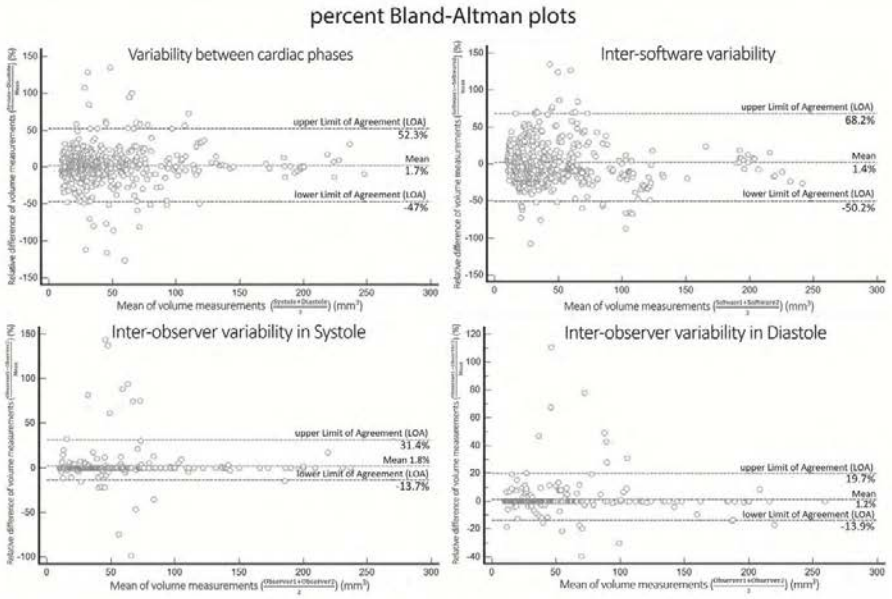

Figure 3. Relative (percent) Bland-Altman plots, with estimated limits of agreement, when comparing volume measurements between systole and diastole (top left corner), different software packages (top right corner), and different observers (bottom). Interobserver subanalysis is presented for the systolic (bottom left corner) and diastolic datasets separately (bottom right corner).

Table 3

Results of the Bland-Altman analysis.

	Bland-Altman (mm³)			Percent Bland-Altman (%)		
	Bias	lower LOA	Upper LOA	Bias	lower LOA	Upper LOA
Between systole and diastole	1.15	−24.91	36.78	1.73	−47.02	52.29
Between software packages	1.7	−39	34.08	1.35	−50.16	68.21
Between observers	0.7	−6.2	17.39	1.49	−14.45	27.77
Between observers (systolic dataset)	0.88	−4.7	24.47	1.75	−13.63	31.36
Between observers (diastolic dataset)	0.53	−8.58	15.85	1.23	−13.92	19.66

LOA = estimated limits of agreement.

after Boll et al suggested that factors related to the pulmonary circulation (cardiac phase and cardiac motion) could influence nodule segmentation.[21] It is also the first study to measure the in vivo variability of PN volumetry on CCTA, which is the main requirement for growth estimation. Therefore, our conclusions still need to be reproduced and validated independently, and further research is needed with a larger sample size before volumetry of PN in CCTA scans becomes useful for growth estimation between 2 CCTA scans. Further research should also compare in vivo volume measurements between CCTA in diastole and LD-CT, before growth of PN can be estimated by comparing CCTA and LD-CT scans (as used in Lung cancer screening), since significant protocol differences exist.

The increased variability of volume measurements between cardiac phases could model the effect of hemodynamic changes often seen between follow-up scans, like the acute onset of heart failure or pleural effusion. Such events are likely more significant than the relatively small intrascan changes seen between systole and diastole. Since the actual in vivo volume of a PN is unknown, a common approach in studies on PN volumetry is to use "coffee-break" studies, where the PN is scanned twice in a short time frame (typically minutes), thus excluding any real growth. In this way, measurement variability explains any volume difference.[15,26,27] However, the impact of such hemodynamically significant events is difficult to study directly since the absence of growth cannot be assumed over any substantial period. In addition, the extra radiation and time demands of "coffee-break" studies make them more suited to phantom studies. On the other hand, CCTA scans allow several opportunities to measure the volume of a PN at different cardiac phases and within a single scan (i.e., no growth occurred), thus providing a tool better suited for clinical research.

5. Conclusions

The interobserver variability of PN volumetry on CCTA scans was comparable to the reported for LD-CT only in diastole. As such, growth estimation of PN between 2 CCTA scans could be feasible using diastolic measurements. However, using systolic volume measurements or comparing volume measurements from systole and diastole implies a higher variability, which could lower the discriminating power of PN volumetry.

Acknowledgments

We would like to acknowledge Prof Paulo Pereira for statistical support.

References

[1] Al-Mallah MH, Aljizeeri A, Villines TC, et al. Cardiac computed tomography in current cardiology guidelines. J Cardiovasc Comput Tomogr. 2015;9:514–23.
[2] Knuuti J, Wijns W, Saraste A, et al. 2019 ESC guidelines for the diagnosis and management of chronic coronary syndromes. Eur Heart J. 2020;41:407–77.
[3] Tzolos E, Newby DE. Coronary computed tomography angiography improving outcomes in patients with chest pain. Curr Cardiovasc Imaging Rep. 2019;12:15.
[4] Taron J, Foldyna B, Mayrhofer T, et al. Risk stratification with the use of coronary computed tomographic angiography in patients with nonobstructive coronary artery disease. JACC Cardiovasc Imaging. 2021;14:2186–95.
[5] Vij A, Kassab K, Chawla H, et al. Invasive therapy versus conservative therapy for patients with stable coronary artery disease: an updated meta-analysis. Clin Cardiol. 2021;44:675–82.
[6] Maron DJ, Hochman JS, Reynolds HR, et al. Initial invasive or conservative strategy for stable coronary disease. N Engl J Med. 2020;382:1395–407.
[7] Leipsic JA, Achenbach S. The ISCHEMIA trial: implication for cardiac imaging in 2020 and beyond. Radiol Cardiothorac Imaging. 2020;2:e200021.
[8] Newby DE, Adamson PD, Berry C, et al; SCOT-HEART Investigators. Coronary CT angiography and 5-year risk of myocardial infarction. N Engl J Med. 2018;379:924–33.
[9] Ramanathan S, Ladumor SB, Francis W, et al. Incidental non-cardiac findings in coronary computed tomography angiography: is it worth reporting? J Clin Imaging Sci. 2019;9:40.
[10] Kay FU, Canan A, Abbara S. Common incidental findings on cardiac CT: a systematic review. Curr Cardiovasc Imaging Rep. 2019;12.
[11] Williams MC, Hunter A, Shah AS, et al. Impact of noncardiac findings in patients undergoing CT coronary angiography: a substudy of the Scottish computed tomography of the heart (SCOT-HEART) trial. Eur Radiol. 2018;28:2639–46.
[12] Bueno J, Landeras L, Chung JH. Updated Fleischner society guidelines for managing incidental pulmonary nodules: common questions and challenging scenarios. RadioGraphics. 2018;38:1337–50.
[13] Walter JE, Heuvelmans MA, de Jong PA, et al. Occurrence and lung cancer probability of new solid nodules at incidence screening with low-dose CT: analysis of data from the randomised, controlled NELSON trial. Lancet Oncol. 2016;17:907–16.
[14] MacMahon H, Naidich DP, Goo JM, et al. Guidelines for management of incidental pulmonary nodules detected on CT images: from the Fleischner society 2017. Radiology. 2017;284:228–43.
[15] Devaraj A, van Ginneken B, Nair A, et al. Use of volumetry for lung nodule management: theory and practice. Radiology. 2017;284:630–44.
[16] Soo E, Edey AJ, Mak SM, et al. Impact of choice of volumetry software and nodule management guidelines on recall rates in lung cancer screening. Eur J Radiol. 2019;120:108646.
[17] Honda O, Johkoh T, Sumikawa H, et al. Pulmonary nodules: 3D volumetric measurement with multidetector CT - effect of intravenous contrast medium. Radiology. 2007;245:881–7.
[18] Christe A, Bronnimann A, Vock P, et al. Volumetric analysis of lung nodules in computed tomography (CT): comparison of two different segmentation algorithm softwares and two different reconstruction filters on automated volume calculation. Acta Radiol. 2014;55:54–61.
[19] Ravenel JG, Leue WM, Nietert PJ, et al. Pulmonary nodule volume: Effects of reconstruction parameters on automated measurements - a phantom study. Radiology. 2008;247:400–8.
[20] Petrou M, Quint LE, Nan B, et al. Pulmonary nodule volumetric measurement variability as a function of CT slice thickness and nodule morphology. Am J Roentgenol 2007;188:306–12.
[21] Boll DT, Gilkeson RC, Fleiter TR, et al. Volumetric assessment of pulmonary nodules with ECG-Gated MDCT. Am J Roentgenol. 2004;183:1217–23.
[22] Robertson J, Nicholls S, Bardin P, et al. Incidental pulmonary nodules are common on CT coronary angiogram and have a significant cost impact. Heart Lung Circ. 2019;28:295–301.
[23] Heuvelmans MA, Oudkerk M, De Bock GH, et al. Optimisation of volume-doubling time cutoff for fast-growing lung nodules in CT lung cancer screening reduces false-positive referrals. Eur Radiol. 2013;23:1836–45.
[24] Wormanns D, Kohl G, Klotz E, et al. Volumetric measurements of pulmonary nodules at multi-row detector CT: in vivo reproducibility. Eur Radiol. 2004;14:86–92.
[25] Gietema HA, Schaefer-Prokop CM, Mali WPTM, et al. Pulmonary nodules: interscan variability of semiautomated volume measurements with multisection CT—influence of inspiration level, nodule size, and segmentation performance. Radiology. 2007;245:888–94.
[26] Bartlett EC, Kemp SV, Rawal B, et al. Defining growth in small pulmonary nodules using volumetry: results from a "coffee-break" CT study and implications for current nodule management guidelines. Eur Radiol. 2022;32:1912–20.
[27] Talwar A, Willaime JMY, Pickup LC, et al. Pulmonary nodules: assessing the imaging biomarkers of malignancy in a "coffee-break". Eur J Radiol. 2018;101:82–6.
[28] Giavarina D. Understanding bland Altman analysis. Biochem Medica 2015;25:141–51.

9.3. Incidental chest findings on coronary CT angiography: a pictorial essay and management proposal

J Bras Pneumol. 2022;48(4):e20220015
https://dx.doi.org/10.36416/1806-3756/e20220015

Incidental chest findings on coronary CT angiography: a pictorial essay and management proposal

Erique Pinto[1], Diana Penha[1,2], Bruno Hochhegger[3], Colin Monaghan[2], Edson Marchiori[4,5], Luís Taborda-Barata[1], Klaus Irion[2]

1. Faculdade de Ciências da Saúde, Universidade da Beira Interior, Covilhã, Portugal.
2. Imaging Department, Liverpool Heart and Chest Hospital NHS Foundation Trust, Liverpool, United Kingdom.
3. Pontifícia Universidade Católica do Rio Grande do Sul, Porto Alegre (RS) Brasil.
4. Faculdade de Medicina, Universidade Federal do Rio de Janeiro, Rio de Janeiro (RJ) Brasil.
5. Faculdade de Medicina, Universidade Federal Fluminense, Niterói (RJ) Brasil.

Submitted: 18 January 2022.
Accepted: 7 March 2022.

Study carried out at the Liverpool Heart and Chest Hospital, NHS Foundation Trust, Liverpool, United Kingdom.

ABSTRACT

Many health systems have been using coronary CT angiography (CCTA) as a first-line examination for ischaemic heart disease patients in various countries. The rising number of CCTA examinations has led to a significant increase in the number of reported incidental extracardiac findings, mainly in the chest. Pulmonary nodules are the most common incidental findings on CCTA scans, as there is a substantial overlap of risk factors between the population seeking to exclude ischaemic heart disease and those at risk of developing lung cancer (i.e., advanced age and smoking habits). However, most incidental findings are clinically insignificant and actively pursuing them could be cost-prohibitive and submit the patient to unnecessary and potentially harmful examinations. Furthermore, there is little consensus regarding when to report or actively exclude these findings and how to manage them, that is, when to trigger an alert or to immediately refer the patient to a pulmonologist, a thoracic surgeon or a multidisciplinary team. This pictorial essay discusses the current literature on this topic and is illustrated with a review of CCTA scans. We also propose a checklist organised by organ and system, recommending actions to raise awareness of pulmonologists, thoracic surgeons, cardiologists and radiologists regarding the most significant and actionable incidental findings on CCTA scans.

Keywords: Incidental findings; Cardiac-gated imaging techniques; Coronary angiography; Lung neoplasms.

INTRODUCTION

Coronary CT angiography (CCTA) has recently been included in the guidelines for the diagnosis and management of coronary artery disease by several international cardiological societies, such as the American Heart Association/American College of Cardiology, the European Society of Cardiology and the European Association for Cardio-Thoracic Surgery.[1] In addition, the National Institute for Health and Care Excellence also recommends CCTA as a first-line test for evaluating stable angina based on cost-effectiveness and diagnostic accuracy.[2,3]

Numerous incidental findings (IFs) can be documented by CCTA, despite the small field of view (FOV) and optimised protocol for cardiac anatomy and function. A systematic review by Kay et al.[4] reported IFs in 45% of CCTA scans (7-100%).

Most IFs are clinically insignificant and pursuing them can add unnecessary costs and occasionally harmful evaluations. However, some IFs might present an alternative explanation for symptoms often misinterpreted as ischaemic heart disease (IHD).[5] In addition, the opportunity for dual screening (i.e., screening for IHD and lung cancer) in a population that shares risk factors of both diseases (e.g., advanced age and smoking habits) is appealing and could be achieved by using the full FOV.[6]

CCTA services have been successfully implemented worldwide, being most often the result of a partnership between radiologists and cardiologists. However, the service provision, multidisciplinary support, referral pathways and even access to relevant clinical information or previous examinations are very dependent on local practice, expertise and resources.[2] Therefore, clear guidelines for reporting and managing IFs are challenging to be implemented, but the need for multidisciplinary collaboration, including pulmonologists and thoracic surgeons, is widely recognised.

This pictorial essay reviews the most common IFs on CCTA scans, organised by organ and structure (Table 1) and discusses their clinical significance and proposed management.

Lung

IFs of the lung are the most common ones, with pulmonary nodules (PNs) or masses occurring in 14% to 38% of CCTA scans.[4,5] Multiple international societies provide guidelines for investigating and managing PNs that exceed 5 mm in diameter (or 80 mm^3 in volume) or show suspicious features.[7-11] Suspicious

Correspondence to:
Erique Pinto. Rua Luís de Camões, 102, lt 8, 3º esq, 1300-356, Lisboa, Portugal.
Tel: 44 749290-9500 or 351 96 1174460. E-mail: ericguedespinto@gmail.com
Financial support: None.

Table 1. Checklist of incidental findings on coronary CT angiography per organ/system.

- Lung
  - Solid pulmonary nodule
    - < 5 mm or < 80 mm^3 with no suspicious features (e.g., granulomas, IPLNs)
      - → Reporting is optional, and no follow-up is required
    - > 5 mm, previously unknown or with suspicious features
      - → Report and alert the respiratory team
      - 5-8 mm → Baseline LDCT and provide an LDCT follow-up schedule
        - 5-6 mm: LDCT within one year
        - 6-8 mm: LDCT within three months
      - > 8 mm or > 300 mm^3 → Assess the risk of cancer (Brock model)
        - < 10% risk of cancer: baseline LCDT and follow-up LDCT within one year
        - ≥ 10% risk of cancer: referral to lung cancer MDT
  - Subsolid pulmonary nodule
    - ≥ 5 mm → Report to and alert the respiratory team
      - → Baseline LDCT and provide a follow-up schedule within three months
      - Stable after ≥ 3 months: assess the risk of cancer (Brock model)
        - < 10% risk of cancer: follow-up LDCT within one year
        - ≥ 10% risk of cancer: referral to lung cancer MDT
      - Growing or altered morphology → Referral to lung cancer MDT
  - Pulmonary emboli → Report and urgent referral to the respiratory team
  - ILAs → Report to and alert the respiratory team
    - In the presence of respiratory symptoms, physiological abnormalities, gas transfer abnormalities and extensive CT changes → Referral to the respiratory team/ILD MDT meeting
    - In the presence of risk factors for progression → Follow-up may be appropriate even after exclusion of ILD (the optimal interval for follow-up CT scanning is unknown)
  - Infection/Consolidation
    - → Report and referral to the respiratory team if not already under their care
    - → CT reassessment after therapy
  - Emphysema → Report and grade severity
  - Bronchiectasis, atelectasis → Report
- Pleura
  - Pneumothorax (rare) → Report and urgent referral to the medical emergency team
  - Pleural plaques → Report
    - in lung cancer patients: differentiate pleural plaques from pleural metastases
    - in asbestos exposure: assess signs suspicious for mesothelioma
  - Pleural effusion → Report
    - in cardiac patients it may be related to heart failure: trigger an alert
- Mediastinum
  - Pneumomediastinum (rare) → Report and urgent referral to the medical emergency team
  - Mediastinal nodule or mass → Report
    - if presenting suspicious features → Referral to the cardiothoracic surgical team
    - if benign-looking → Suggest annual CT follow-up or MRI characterisation
  - Aorta and pulmonary vessels → Report abnormalities in the context of the patient's cardiovascular disease
  - Lymphadenopathy → Report
    - if suspicious features or absence of an explaining disease to justify lymphadenopathy → Consider providing a follow-up schedule or suggest further characterisation with PET-CT or biopsy
  - Oesophageal hiatus hernia → Report
    - In the presence of heartburn (confounding symptom) → Referral to gastrointestinal evaluation
- Chest wall
  - Bone
    - 'Do not touch' lesions → Report but no follow-up required
    - Degenerative bony changes → Report (may cause atypical chest pain)
    - Suspicious bone lesions → Report and trigger an alert
  - Skin, subcutaneous and muscle lesions → Report new or previously undiagnosed lesions
  - Breast → Report new or previously undiagnosed lesions and alert breast team

Continue...▶

Table 1. Checklist of incidental findings on coronary CT angiography per organ/system. (Continued...)

Upper abdomen
Liver
Simple hepatic cysts → Reporting is optional, and no follow-up is required
Other focal parenchymal lesions → Report if previously undiagnosed and suggest further evaluation with triple-phase CT or MRI
Biliary system
Abnormal appearance of the gallbladder wall, biliary obstruction or pneumobilia → Report and suggest further evaluation
Gallstones → Reporting is optional, and no follow-up is required
Adrenal glands, pancreas, stomach and spleen
Any cystic or solid lesions, or splenomegaly → Report and suggest further evaluation if previously undiagnosed
Kidneys
Simple or minimally complex renal cysts (Bosniak I and II) → Reporting is optional, and no follow-up is required
Complex renal cysts → Report and suggest further evaluation
Solid renal masses → Report and trigger an alert
Peritoneum
Nodules, infiltrative masses, haziness, ascites, peritoneal thickening or implants → Report, alert and suggest further evaluation
Lymphadenopathy → Report and suggest further evaluation

IPLNs: intrapulmonary lymph nodes; LDCT: low-dose CT; MDT: multidisciplinary team; ILAs: interstitial lung abnormalities; and ILD: interstitial lung disease.

features of malignancy in PNs include the diameter-volume ratio, growth, distance from the pleura (if more than 10 mm), spiculation, ground-glass appearance, pleural indentation, vascular convergence, circumference-diameter ratio (roundness), upper lobe location, presence of air bronchogram, presence of lymphadenopathy and cavity wall thickness. Benign features include some patterns of nodule calcification (diffuse, central, laminated or popcorn pattern), smooth border, cavitation, satellite lesions and perifissural location.[8]

The British Thoracic Society[8,9] recommends the Brock model for estimating the risk of lung cancer in any solid nodule greater than 8 mm in diameter (or 300 mm^3 in volume) and in subsolid nodules larger than 5 mm if they are stable after three months. The decision between CT surveillance or further characterisation (i.e., PET-CT, biopsy, excision or non-surgical treatment) depends on this risk estimate, so the report should include it.[9] However, physicians should note that the Brock model was validated for low-dose CT scans and not for CCTA scans.[12,13] For solid, noncalcified PNs measuring between 5 and 8 mm in diameter, their growth rate is better at distinguishing malignancy from benign pathology than are morphological features. Because of this, the Fleischner Society recommends performing a baseline low-dose chest CT as soon as possible and a subsequent follow-up low-dose chest CT for any indeterminate PNs between 5 and 8 mm in diameter.[10,11]

The prevalence of IFs of malignancy in all patients undergoing CCTA is small (estimated at 0.7%), and most of them (72%) will be lung cancer (primary or secondary).[4,5] Even in patients with known cancer elsewhere, incidental small PNs are often benign and should not preclude treatment for the primary malignancy until proven to be metastases. Likewise, second primary lung cancer may have a better prognosis than may metastatic lung cancer and still be a candidate for treatment. The report should include any incidental and previously undocumented lung lesions larger than 5 mm and a proposed follow-up schedule. Lesions larger than 8 mm in diameter, growing or presenting suspicious features (Figure 1), should trigger an alert and referral for a lung cancer team so that they can be reviewed by a pulmonologist, an oncologist and a thoracic surgeon.[11]

Pulmonary emboli (Figure 2) are rare, identified in just 0.2% of CCTA scans, but should be reported and trigger an urgent referral, as the patient will benefit from a timely start of therapy.[14]

Pulmonary consolidation should trigger a referral to the respiratory team and a post-treatment imaging reassessment, as the differential diagnosis is vast and includes infection, alveolar haemorrhage, organising pneumonia and malignancy, among others.[15]

Interstitial lung abnormalities (ILAs) are imaging findings potentially compatible with interstitial lung disease (ILD) in patients with no prior history of ILD.[16] These findings are unexpected and incidental, common in the older (above 60 years of age) smoking population (4-9%). ILAs are often asymptomatic but may be related to mild ILD with potential functional impairment, risk of progressing disease and increased mortality risk.[17] Some imaging patterns, such as subpleural reticulations, basal predominance and honeycombing, are more strongly associated with progression.[16] Others, such as centrilobular nodules, are less likely to progress. Likewise, imaging patterns of pulmonary fibrosis are related to increased all-cause

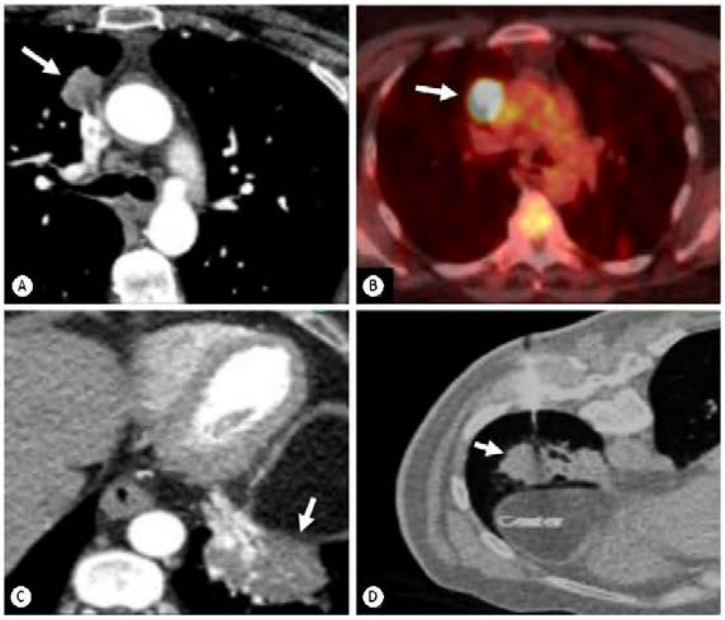

Figure 1. In A, an axial CT scan with a mediastinal window setting shows an incidental 20-mm nodule (arrow) in the right upper lobe. As per the British Thoracic Society guidelines,[8,9] this finding requires further evaluation and therefore was highlighted in the report. In B, a PET-CT scan of the same patient showed a standardised uptake value (SUV) of 12. This lesion was confirmed as a metastasis from a previously unknown melanoma on histology. In C, an axial CT scan with a mediastinal window setting shows an incidental left basal consolidation (arrow) and atelectasis in another patient. This area demonstrated an increased uptake (SUV = 3.4) on PET-CT (in D) and was proven to be an adenocarcinoma on histology. The staging after the multidisciplinary team meeting was T3N1M0.

Figure 2. CT scans of a patient with acute chest pain and cardiac arrest. In A, an axial scan with a mediastinal window setting shows bilateral pulmonary emboli with the biggest thrombus occluding the left lower lobar artery (arrow). In B, a scan shows that the patient had an infarct of the left anterior descending coronary artery's territory with perfusion defects of the mid-cavity and apical walls (arrows). In C, a left ventricular thrombus in the apex (arrow) is also noted.

mortality. There are no clear guidelines for reporting or managing ILAs. Still, the Fleischner Society proposes that patients with respiratory symptoms, physiological abnormalities, gas transfer abnormalities and extensive CT changes should be referred for pulmonary evaluation and to a respective multidisciplinary team if available (Figure 3).[16] Follow-up of ILAs may still be appropriate after the exclusion of ILD but in the presence of risk factors for progression, even if the optimal interval for follow-up CT scanning is unknown.[16,18]

Other findings in the lung parenchyma include bronchial wall thickening in patients with COPD, emphysema, bronchiectasis and atelectasis (Figure 4).[4]

Intrapulmonary lymph nodes (IPLNs) are common on chest CT (prevalence of up to 66%) but under-represented on IF studies and do not require follow-up. The morphological criteria for IPLNs (Figure 5) are solid, homogeneous and noncalcified nodules with less than 12 mm in diameter. IPLNs may have an oval, lentiform,

or triangular shape, have regular and smooth margins, and be located primarily in the middle or lower lobes within 15 mm of the pleura.[19] Half of the cases show a connection between IPLNs and the pleura. In addition, IPLNs may present single or multiple attachments with veins but not with arteries, which can be useful in differentiating adenocarcinomas from IPLNs.[19]

Pleural space

Pleural effusion should be reported and related to heart failure in cardiac patients. Pleural plaques (Figure 6) are also common and under-reported IFs, linked to asbestos exposure and increased risk of mesothelioma.[5] The report should differentiate them from pleural metastases in patients with lung cancer. In addition, the presence of pleural plaques is also a marker for increased mortality in a history of asbestos exposure, and the report should document them for surveillance and legal compensation.[4,5,20]

Pneumothorax is rarely seen or reported on CCTA scans, likely because of the reduced FOV of CCTA scans and the outpatient setting. However, its clinical presentation can range from asymptomatic to life-threatening, and, when present, it should be reported and the patient should urgently be referred to the respiratory team or emergency room.

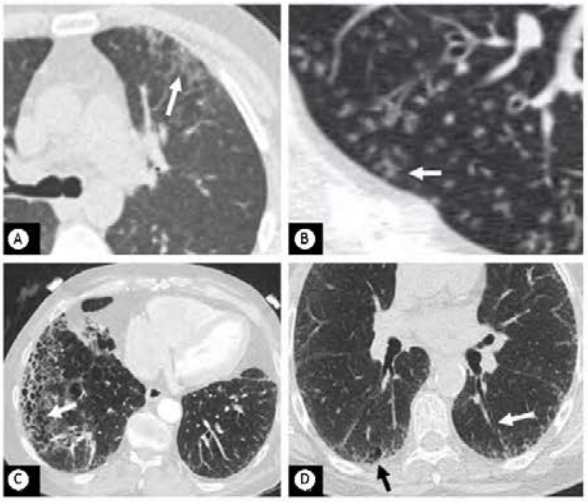

Figure 3. CT scans of a patient with atypical chest pain. Subpleural ground-glass opacities in the left upper lobe (arrow in A) and focal areas with tree-in-bud pattern (arrow in B) in the right lower lobe are seen. The patient was diagnosed with a lower tract respiratory infection. In another patient with a history of previous severe right lower lobe pneumonia, opening the field of view (FOV) allowed the visualisation of interstitial lung changes in the right lower lobe with asymmetric subpleural honeycombing and ground-glass patterns and bronchiectasis (arrow in C), residual to the previous infection. Likewise, using a large FOV in another patient, the scan shows the incidental finding of ILD (in D), characterised by subpleural reticulation with honeycombing (black arrow) and traction bronchiectasis (white arrow) affecting the lower lobes. These were further investigated with HRCT, and the diagnosis of the multidisciplinary team was probable usual interstitial pneumonia.

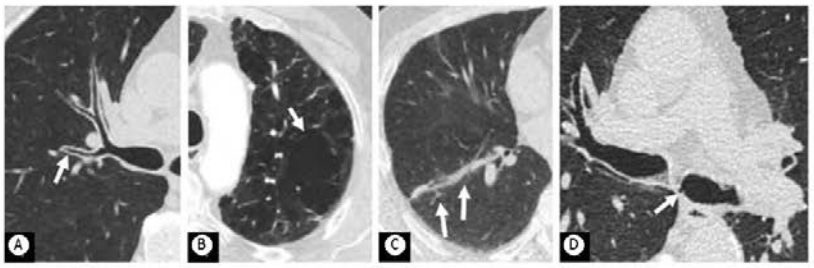

Figure 4. CT scans of a current smoker diagnosed with COPD, using the calcium score acquisition with a large field of view show bronchial thickening noted mainly in the lobar (arrow) and central segmental bronchi (in A) and centrilobular and paraseptal emphysema, forming a left upper lobe emphysematous bulla (arrow in B). Likewise, in another patient with COPD, an axial image shows linear atelectasis in the left lower lobe and mucous plugging (arrows in C). In D, a bronchial diverticulum is seen at the origin of the left main bronchus (arrow).

Mediastinum

Mediastinal lesions have a comprehensive list of differential diagnoses, including benign pathology (e.g., pericardial, bronchogenic or oesophageal duplication cysts; diving goitre) and malignancy (e.g., thymoma, thyroid malignancy, germ cell tumours, neurogenic tumours, oesophageal cancer and lymphoma; Figures 7 and 8).[4,5,21]

Most lesions in the anterior mediastinum will have attenuation compatible with a soft tissue lesion, with larger lesions more likely representing early-stage thymic epithelial tumours and smaller lesions likely expressing benign cysts.[22] On follow-up evaluation, most lesions are stable or slowly growing, and the absence of growth cannot distinguish between benignity and malignancy. While long-term follow-up may be appropriate, a purely cystic lesion is most commonly a benign thymic cyst and does not need follow-up. Thoracic MRI scanning is far superior to CT in distinguishing simple or complex cystic lesions from solid lesions, identifying fatty, cystic or necrotic components within solid lesions, as well as septations or soft tissue components within cystic lesions. In addition, MRI may be appropriate to alleviate patient anxiety.[22]

Mediastinal teratoma is the most common mediastinal germ cell tumour. Mature teratomas usually present multiple densities, including fat, cystic spaces, homogeneous soft tissue and calcification. Conversely, immature teratomas usually present as solid heterogeneous lesions. Mature and most immature teratomas are benign but some immature teratomas may have a malignant germ cell tumour component and even mature teratomas may undergo malignant transformation of non-germ cell components (usually squamous component).

Both inflammatory and malignant diseases may cause mediastinal lymphadenopathy. Examples of the former include tuberculosis, fungal infection, sarcoidosis,

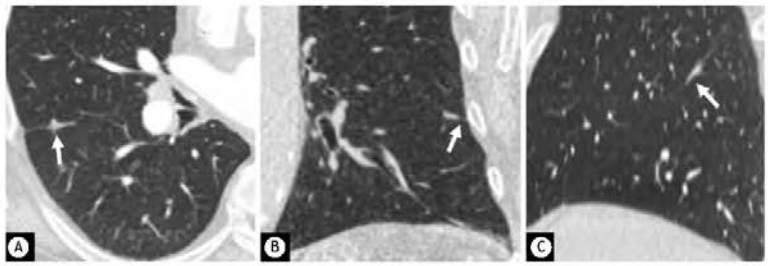

Figure 5. In A, an axial CT scan using the full field of view shows an oval-shaped, lentiform nodule in contact with the fissure (arrow). Coronal (in B) and sagittal (in C) CT scans show that the nodule adopts a more triangular shape and a linear contact with the fissure and adjacent pleura (arrows). These findings meet the criteria for benign intrapulmonary lymph nodes, and no follow-up is required.

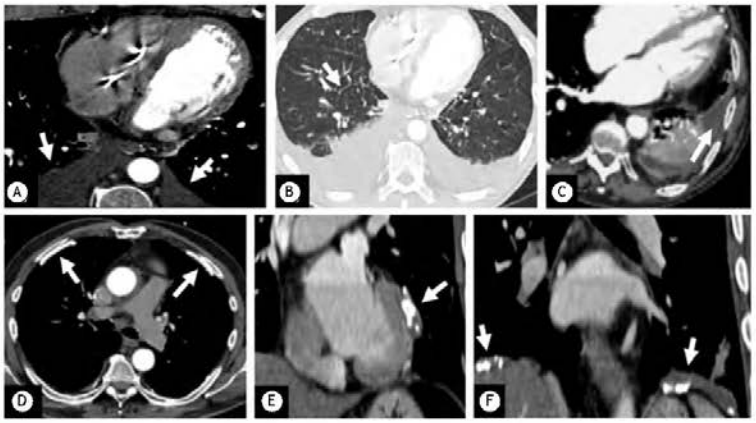

Figure 6. In A, bilateral pleural effusion (arrows) can be seen in the cardiac field of view (FOV) on a CT scan. In a reconstructed, wider FOV with a lung window setting (in B), the effusions are confirmed, and signs of pulmonary oedema with interlobular thickening (arrow) are also seen. In another patient, incidental left pleural effusion can be noted in C. The pleural layers were enhanced and showed areas of focal nodular thickening (arrows in D). Mesothelioma was diagnosed in this patient after further evaluation. CT scans of a patient with known exposure to asbestos reveal bilateral calcified pleural plaques (arrows), including the mediastinal (arrows in E) and diaphragmatic layers (arrows in F).

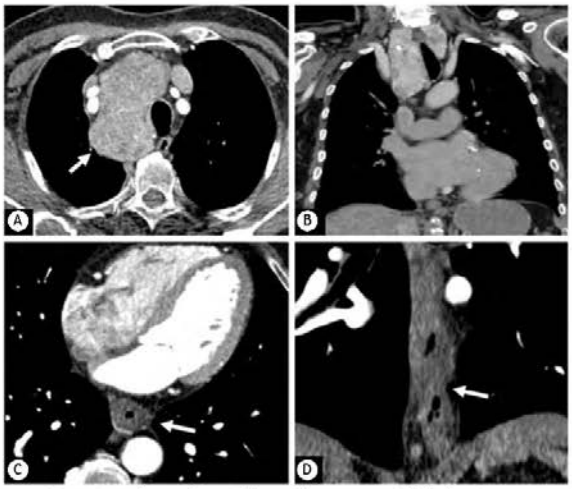

Figure 7. Coronary CT angiography performed for graft assessment (full chest coverage with wide field of view) shows an incidental finding of an anterior and heterogeneous mid-mediastinal soft-tissue mass (arrow in A), corresponding to diving goitre with a deviation of the trachea also depicted in a coronal view (in B). This patient was referred to the neck team for medical and surgical evaluation. Life-threatening severe complications, such as airway obstruction and neurovascular compression, can arise suddenly in these cases, usually secondary to intrathyroidal bleeding from trauma or infection. In another patient, axial (in C) and coronal (in D) scans show circumferential irregular thickening of the thoracic oesophagus (arrow) with adjacent enlarged lymph nodes. The patient was immediately referred to the upper gastrointestinal team, and upper endoscopy was performed. An adenocarcinoma was confirmed on histology.

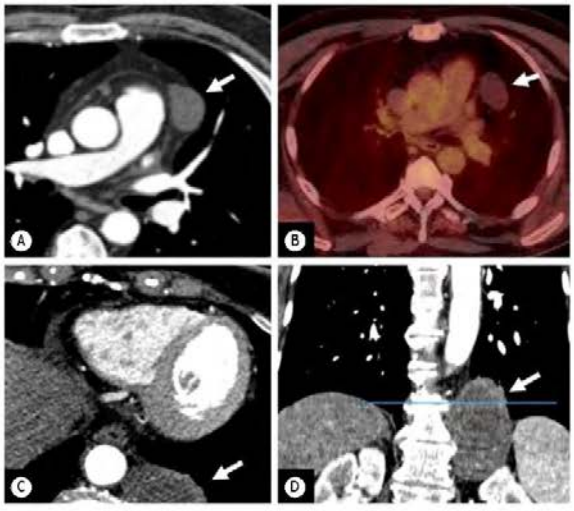

Figure 8. In A, an axial CT scan with a mediastinal window setting shows the incidental finding of a rounded lesion with fluid density (arrow). In B, a PET-CT scan shows that the lesion has no uptake (arrow) and is likely to represent a benign pericardial cyst. Surgical resection or percutaneous drainage is reserved for symptomatic individuals when complications are observed or when the diagnosis is uncertain. In another patient, an axial CT scan shows a heterogeneous left retrocrural mass (arrow in C) seen in the cardiac field of view. In D, a coronal CT scan confirms the left paraspinal location (arrow) of the lesion that was later confirmed as a neurogenic tumour. This finding requires an alert on the report as the patient will benefit from further evaluation and treatment.

silicosis, drug reactions, amyloidosis, Castleman's disease, ILD and COPD. Examples of the latter include lung cancer, lymphoproliferative disease and metastases (Figure 9). The criteria for lymphadenopathy include a short-axis diameter larger than 10 mm, changes to its usual ovoid shape or usual attenuation, coalescence

with adjacent enlarged lymph nodes or an invasive behaviour into the surrounding mediastinal fat.[19] Mediastinal lymph node enlargement is the third most common IF reported in the literature (1.7%) after lung nodules and parenchymal abnormalities.[4,19,23]

In the absence of suspicious features, lymph nodes smaller than 15 mm in the short-axis are overwhelmingly reactive lymph nodes and, if few, do not need follow-up.[21] The shape and number of lymph nodes, the presence of a fatty hilum, enhancement or calcifications, as well as previous history of diseases potentially explaining the enlarged lymph nodes are also important when considering follow-up or further characterisation with PET-CT or biopsy.[21]

Abnormalities of the aorta (Figure 10) and pulmonary arteries should be considered an integral part of the cardiac or coronary assessment in the context of the cardiovascular disease being evaluated, such as in cases of congenital abnormalities or pre-transcatheter aortic valve replacement.

Oesophageal hiatus hernia is very common and may cause chest pain (heartburn) as a confounding symptom behind the CCTA request. These patients will benefit from gastrointestinal evaluation and treatment.[4]

Similarly to pneumothorax, pneumomediastinum is infrequent and under-represented in systematic reviews of IFs on CCTA. However, these should be reported and trigger an urgent referral to the respiratory team or emergency department.

Chest wall

Degenerative bony changes are widespread in older patients and could cause atypical chest pain.[5] Metastatic disease, multiple myeloma, lymphoma, and leukaemia account for more than 99% of malignant bone lesions in the chest wall. Therefore, the report should distinguish them from common benign bony lesions (e.g., bone islands and haemangiomas) that do not require further assessment.[24]

The skin, muscles and subcutaneous fat tissue are sometimes the site of metastases and should be reviewed.[5] Despite the low predictive value for breast lesions on CCTA, it may be the first study to demonstrate a previously undiagnosed lesion. Incidental breast lesions first detected on CCTA prove to be cancer in 24-70% of the cases; therefore, any breast lesion not previously demonstrated to be benign (Figure 11) should be reported and trigger an alert for an appointment and further evaluation with a specialist.[25]

Abdominal cavity

A CCTA study usually includes some slices through the upper abdomen. The most common abdominal IFs are simple hepatic cysts, reported in 5% of CCTA scans as lesions with uniform fluid attenuation, no visible wall and no contrast enhancement.[5] These are benign and require no further imaging. However, the complete characterisation of focal liver lesions is often impossible to be obtained from a CCTA scan and may require a targeted protocol (e.g., triple-phase CT scan or liver MRI).[26] Hence, the report should include any new focal liver lesion apart from simple cysts, and further characterisation should be suggested. Likewise, biliary obstruction, pneumobilia and focal or diffuse thickening of the gallbladder wall should be alerted if previously undiagnosed. Renal cysts are also common and frequently benign IFs that do not require follow-up in the absence of suspicious features (e.g., septations, internal density, enhancement, calcification, and solid

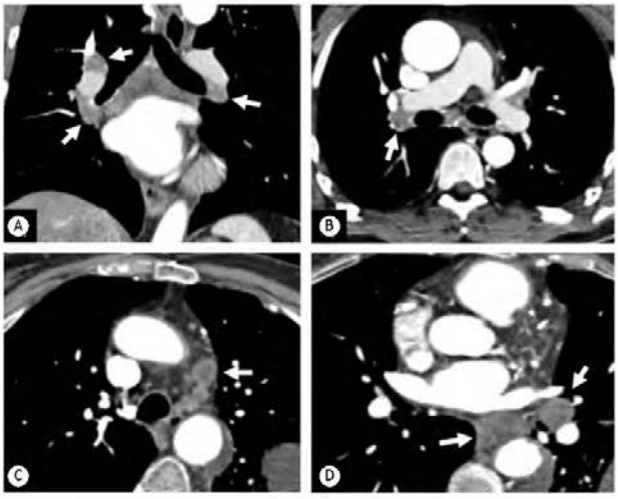

Figure 9. Coronal (in A) and axial (in B) CT scans show bilateral enlarged hilar lymph nodes (arrows), the biggest of them in the right hilum measuring 15 mm in the short axis. EBUS confirmed sarcoidosis. CT scans of another patient (in C and D) present several mediastinal and left hilar lymph nodes with a hypodense centre. The report alerted these findings, and EBUS later confirmed metastatic small cell carcinoma.

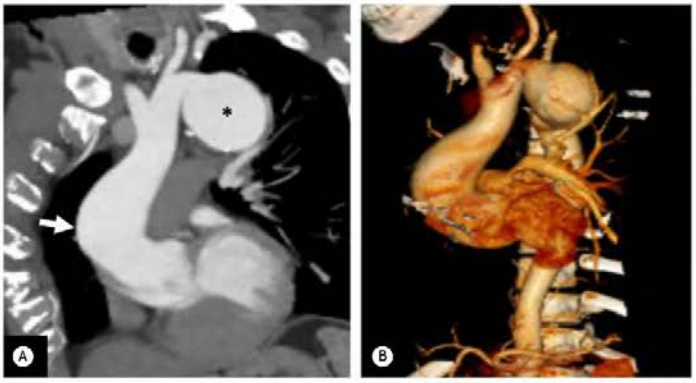

Figure 10. In A, coronal maximum-intensity projection reconstruction of the thoracic aorta of a young patient admitted with chest pain shows an incidental finding of an ascending aorta aneurysm (arrow) with distal aortic arch coarctation and a proximal descending saccular thoracic aorta aneurysm (asterisk). The congenital anatomical change and aneurysm are depicted in the 3D reconstruction (in B). The clinical information provided referred to a bicuspid aortic valve, which justified tailoring the imaging protocol to include the aortic arch.

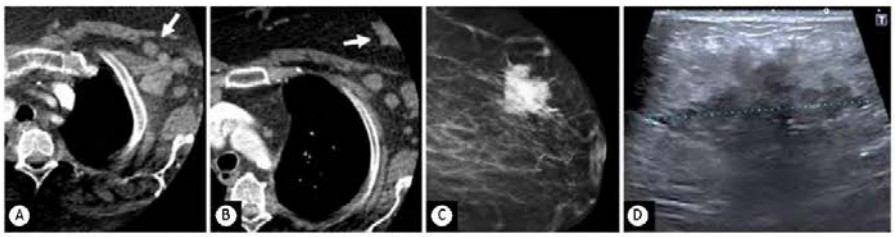

Figure 11. Axial CT images show an incidental finding of multiple left axillary adenopathy (arrow in A) and a left breast mass, partially included in the cardiac field of view (arrow in B). In C, a mammogram showed a suspicious spiculated lesion with a significant amount of microcalcifications. In D, the lesion was confirmed malignant on ultrasound-guided biopsy.

components). However, any solid renal nodule or mass should be reported and further characterised.[5,27]

Coverage of the adrenal glands, pancreas, spleen, and stomach are limited to the FOV and the patient's anatomy. However, any previously undiagnosed solid or cystic mass in these organs, splenomegaly, peritoneal disease (e.g., nodules, haziness and omental cake) and ascites should also be reported and further evaluated.[28,29]

FINAL CONSIDERATIONS

Clinically significant IFs are common in the evaluation of IHD using CCTA. Although their detection has the potential for additional costs and patient harm, it also presents opportunities for intervening to benefit patients. Therefore, radiologists and cardiologists reporting CCTA findings should be familiar with IFs.

AUTHOR CONTRIBUTIONS

EP and DP: study conception and design, data collection, drafting and review of the manuscript. CM, EM, BH, KI and LTB: review of the manuscript. All authors read and approved the final version of the manuscript.

CONFLICT OF INTEREST

None declared.

REFERENCES

1. Knuuti J, Wijns W, Saraste A, Capodanno D, Barbato E, Funck-Brentano C, et al. 2019 ESC Guidelines for the diagnosis and management of chronic coronary syndromes [published correction appears in Eur Heart J. 2020 Nov 21;41(44):4242]. Eur Heart J. 2020;41(3):407-477. https://doi.org/10.1093/eurheartj/ehz425
2. Tzolos E, Newby DE. Coronary Computed Tomography Angiography Improving Outcomes in Patients with Chest Pain. Curr Cardiovasc Imaging Rep. 2019;12:15. https://doi.org/10.1007/s12410-019-9492-6
3. Moss AJ, Williams MC, Newby DE, Nicol ED. The Updated NICE Guidelines: Cardiac CT as the First-Line Test for Coronary Artery Disease. Curr Cardiovasc Imaging Rep. 2017;10(5):15. https://doi.org/10.1007/s12410-017-9412-6

4. Kay FU, Canan A, Abbara S. Common Incidental Findings on Cardiac CT: a Systematic Review. Curr Cardiovasc Imaging Rep. 2019;12(6):21. doi: 10.1007/s12410-019-9494-4 https://doi.org/10.1007/s12410-019-9494-4
5. Macmillan MT, Williams MC. Incidental Non-cardiac Findings in Cardiovascular Imaging. Curr Treat Options Cardiovasc Med. 2018;20(12):93. https://doi.org/10.1007/s11936-018-0700-5
6. Chao H, Shan H, Homayounieh F, Singh R, Khera RD, Guo H, et al. Deep learning predicts cardiovascular disease risks from lung cancer screening low dose computed tomography. Nat Commun. 2021;12(1):2963. https://doi.org/10.1038/s41467-021-23235-4
7. Ito M, Miyata Y, Okada M. Management pathways for solitary pulmonary nodules. J Thorac Dis. 2018;10(Suppl 7):S860-S866. https://doi.org/10.21037/jtd.2018.01.07
8. Graham RN, Baldwin DR, Callister ME, Gleeson FV. Return of the pulmonary nodule: the radiologist's key role in implementing the 2015 BTS guidelines on the investigation and management of pulmonary nodules. Br J Radiol. 2016;89(1059):20150776. https://doi.org/10.1259/bjr.20150776
9. Callister ME, Baldwin DR, Akram AR, Barnard S, Cane P, Draffan J, et al. British Thoracic Society guidelines for the investigation and management of pulmonary nodules [published correction appears in Thorax. 2015 Dec;70(12):1188]. Thorax. 2015;70 Suppl 2:ii1-ii54. https://doi.org/10.1136/thoraxjnl-2015-207168
10. MacMahon H, Naidich DP, Goo JM, Lee KS, Leung ANC, Mayo JR, et al. Guidelines for Management of Incidental Pulmonary Nodules Detected on CT Images: From the Fleischner Society 2017. Radiology. 2017;284(1):228-243. https://doi.org/10.1148/radiol.2017161659
11. Bueno J, Landeras L, Chung JH. Updated Fleischner Society Guidelines for Managing Incidental Pulmonary Nodules: Common Questions and Challenging Scenarios. Radiographics. 2018;38(5):1337-1350. https://doi.org/10.1148/rg.2018180017
12. Fox AH, Tanner NT. Approaches to lung nodule risk assessment: clinician intuition versus prediction models. J Thorac Dis. 2020;12(6):3296-3302. https://doi.org/10.21037/jtd.2020.03.68
13. Nair VS, Sundaram V, Desai M, Gould MK. Accuracy of Models to Identify Lung Nodule Cancer Risk in the National Lung Screening Trial. Am J Respir Crit Care Med. 2018;197(9):1220-1223. https://doi.org/10.1164/rccm.201708-1632LE
14. Williams MC, Hunter A, Shah ASV, Dreisbach J, Weir McCall JR, Macmillan MT, et al. Impact of noncardiac findings in patients undergoing CT coronary angiography: a substudy of the Scottish computed tomography of the heart (SCOT-HEART) trial. Eur Radiol. 2018;28(6):2639-2646. https://doi.org/10.1007/s00330-017-5181-5
15. Munden RF, Black WC, Hartman TE, MacMahon H, Ko JP, Dyer DS, et al. Managing Incidental Findings on Thoracic CT: Lung Findings. A White Paper of the ACR Incidental Findings Committee. J Am Coll Radiol. 2021;18(9):1267-1279. https://doi.org/10.1016/j.jacr.2021.04.014
16. Hatabu H, Hunninghake GM, Richeldi L, Brown KK, Wells AU, Remy-Jardin M, et al. Interstitial lung abnormalities detected incidentally on CT: a Position Paper from the Fleischner Society. Lancet Respir Med. 2020;8(7):726-737. https://doi.org/10.1016/S2213-2600(20)30168-5
17. Putman RK, Hatabu H, Araki T, Gudmundsson G, Gao W, Nishino M, et al. Association Between Interstitial Lung Abnormalities and All-Cause Mortality. JAMA. 2016;315(7):672-681. https://doi.org/10.1001/jama.2016.0518
18. Putman RK, Gudmundsson G, Axelsson GT, Hida T, Honda O, Araki T, et al. Imaging Patterns Are Associated with Interstitial Lung Abnormality Progression and Mortality. Am J Respir Crit Care Med. 2019;200(2):175-183. https://doi.org/10.1164/rccm.201809-1652OC
19. Schreuder A, Jacobs C, Scholten ET, van Ginneken B, Schaefer-Prokop CM, Prokop M. Typical CT Features of Intrapulmonary Lymph Nodes: A Review. Radiol Cardiothorac Imaging. 2020;2(4):e190159. https://doi.org/10.1148/ryct.2020190159
20. Mazzei MA, Contorni F, Gentili F, Guerrini S, Mazzei FG, Pinto A, et al. Incidental and Underreported Pleural Plaques at Chest CT: Do Not Miss Them-Asbestos Exposure Still Exists. Biomed Res Int. 2017;2017:6797826. https://doi.org/10.1155/2017/6797826
21. Munden RF, Carter BW, Chiles C, MacMahon H, Black WC, Ko JP, et al. Managing Incidental Findings on Thoracic CT: Mediastinal and Cardiovascular Findings. A White Paper of the ACR Incidental Findings Committee. J Am Coll Radiol. 2018;15(8):1087-1096. https://doi.org/10.1016/j.jacr.2018.04.029
22. Yoon SH. Management of incidental anterior mediastinal lesions: summary of relevant studies. Mediastinum. 2018;3:9. https://doi.org/10.21037/med.2019.03.01
23. Nin CS, de Souza VV, do Amaral RH, Schuhmacher Neto R, Alves GR, Marchiori E, et al. Thoracic lymphadenopathy in benign diseases: A state of the art review. Respir Med. 2016;112:10-17. https://doi.org/10.1016/j.rmed.2016.01.021
24. Bernard S, Walker E, Raghavan M. An Approach to the Evaluation of Incidentally Identified Bone Lesions Encountered on Imaging Studies. AJR Am J Roentgenol. 2017;208(5):960-970. https://doi.org/10.2214/AJR.16.17434
25. Son JH, Jung HK, Song JW, Baek HJ, Doo KW, Kim W, et al. Incidentally detected breast lesions on chest CT with US correlation: a pictorial essay. Diagn Interv Radiol. 2016;22(6):514-518. https://doi.org/10.5152/dir.2016.15539
26. Gore RM, Pickhardt PJ, Mortele KJ, Fishman EK, Horowitz JM, Fimmel CJ, et al. Management of Incidental Liver Lesions on CT: A White Paper of the ACR Incidental Findings Committee. J Am Coll Radiol. 2017;14(11):1429-1437. https://doi.org/10.1016/j.jacr.2017.07.018
27. Herts BR, Silverman SG, Hindman NM, Uzzo RG, Hartman RP, Israel GM, et al. Management of the Incidental Renal Mass on CT: A White Paper of the ACR Incidental Findings Committee. J Am Coll Radiol. 2018;15(2):264-273. https://doi.org/10.1016/j.jacr.2017.04.028
28. Megibow AJ, Baker ME, Morgan DE, Kamel IR, Sahani DV, Newman E, et al. Management of Incidental Pancreatic Cysts: A White Paper of the ACR Incidental Findings Committee. J Am Coll Radiol. 2017;14(7):911-923. https://doi.org/10.1016/j.jacr.2017.03.010
29. Mayo-Smith WW, Song JH, Boland GL, Francis IR, Israel GM, Mazzaglia PJ, et al. Management of Incidental Adrenal Masses: A White Paper of the ACR Incidental Findings Committee. J Am Coll Radiol. 2017;14(8):1038-1044. https://doi.org/10.1016/j.jacr.2017.05.001

9.4. Influencing factors in pulmonary nodule volumetry tools: Systematic review and attempted meta-analysis

Guedes Pinto *et al. Insights into Imaging* (2023) 14:152
https://doi.org/10.1186/s13244-023-01480-z

Insights into Imaging

CRITICAL REVIEW Open Access

Factors influencing the outcome of volumetry tools for pulmonary nodule analysis: a systematic review and attempted meta-analysis

Erique Guedes Pinto[1*], Diana Penha[1,2], Sofia Ravara[1], Colin Monaghan[2], Bruno Hochhegger[3], Edson Marchiori[4,5], Luís Taborda-Barata[1] and Klaus Irion[6]

Abstract

Abstract Health systems worldwide are implementing lung cancer screening programmes to identify early-stage lung cancer and maximise patient survival. Volumetry is recommended for follow-up of pulmonary nodules and outperforms other measurement methods. However, volumetry is known to be influenced by multiple factors. The objectives of this systematic review (PROSPERO CRD42022370233) are to summarise the current knowledge regarding factors that influence volumetry tools used in the analysis of pulmonary nodules, assess for significant clinical impact, identify gaps in current knowledge and suggest future research. Five databases (Medline, Scopus, Journals@Ovid, Embase and Emcare) were searched on the 21st of September, 2022, and 137 original research studies were included, explicitly testing the potential impact of influencing factors on the outcome of volumetry tools. The summary of these studies is tabulated, and a narrative review is provided. A subset of studies (n = 16) reporting clinical significance were selected, and their results were combined, if appropriate, using meta-analysis. Factors with clinical significance include the segmentation algorithm, quality of the segmentation, slice thickness, the level of inspiration for solid nodules, and the reconstruction algorithm and kernel in subsolid nodules. Although there is a large body of evidence in this field, it is unclear how to apply the results from these studies in clinical practice as most studies do not test for clinical relevance. The meta-analysis did not improve our understanding due to the small number and heterogeneity of studies testing for clinical significance.

Critical relevance statement Many studies have investigated the influencing factors of pulmonary nodule volumetry, but only 11% of these questioned their clinical relevance in their management. The heterogeneity among these studies presents a challenge in consolidating results and clinical application of the evidence.

Key points

- Factors influencing the volumetry of pulmonary nodules have been extensively investigated.
- Just 11% of studies test clinical significance (wrongly diagnosing growth).
- Nodule size interacts with most other influencing factors (especially for smaller nodules).
- Heterogeneity among studies makes comparison and consolidation of results challenging.
- Future research should focus on clinical applicability, screening, and updated technology.

*Correspondence:
Erique Guedes Pinto
ericguedespinto@gmail.com
Full list of author information is available at the end of the article

Keywords Systematic review, Screening, Cancer, Lung cancer, Computed tomography, Spiral

Graphical abstract

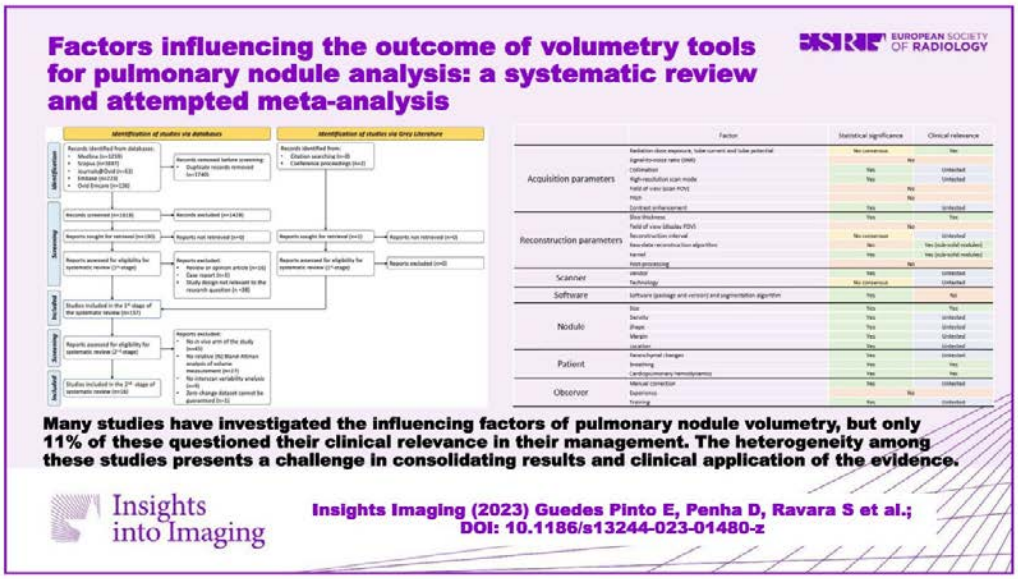

Introduction

Health systems worldwide are implementing Lung Cancer Screening programmes (LCS) to identify early-stage lung cancer and maximise patient survival. However, false positive findings presenting as mostly benign, small, non-calcified pulmonary nodules are present in 22–51% of participants, which may cause morbidity and undermines the cost-effectiveness of LCS [1, 2].

Before the Dutch-Belgian randomised lung cancer screening (NELSON) trial, any pulmonary nodule was considered potentially malignant until proven stable for two years. This trial linked the risk of malignancy to the nodule's size, with small nodules (≤ 100 mm^3 in volume or ≤ 5 mm in diameter) having a low risk of cancer (0.4%), while large nodules (>300 mm^3 or >10 mm) see this risk raise to 16.9%. The risk of malignancy for medium-sized nodules depends on their growth rate, increasing from 0.8% for nodules with a volume doubling time (VDT) ≥ 600 days to 9.9% for nodules with a VDT <400 days [1].

Volumetry has consistently outperformed other methods of measuring pulmonary nodules and has been recommended by several international scientific societies for their follow-up [1, 3, 4]. However, the growth curves based on volumetry are highly variable and influenced by multiple known factors [5, 6]. These influencing factors can be related to the scanner, acquisition (e.g., radiation dose exposure, slice thickness) and reconstruction parameters (e.g., kernel), software package, nodule (e.g., size, shape, location), patient (e.g., breathing, comorbidities) or even to the observer (e.g., experience and training). The consistent use of the same scanner, protocol, and software during the follow-up of a pulmonary nodule reduces measurement variability. Still, it is often impractical, such as in cases of equipment failure, critical software upgrades, or the patient moving house.

The primary objective of this systematic review is to summarise the current knowledge regarding the factors that influence the outcome of volumetry tools dedicated to pulmonary nodules. The secondary objectives are to assess the clinical significance of the evidence, identify gaps in current knowledge and suggest future research.

Methods

The protocol and search strategy were registered with PROSPERO with the registration number CRD42022370233.

The authors defined the primary and secondary research questions as "What factors influence the outcome of volumetry tools dedicated to pulmonary nodules?" and "What is the clinical significance of their effect?" respectively.

The authors searched the following databases on the 21st of September 2022: MEDLINE, SCOPUS, Journals@Ovid, Embase, and Ovid Emcare, using the query: (((Volume OR Volumetry OR Volumetric) AND (lung OR pulmonary) AND (nodule OR nodules)).

Eligibility criteria

The inclusion criteria were defined as follows:

- Original research studies using dedicated volumetry tools in solid or part-solid pulmonary nodules.
- Study design explicitly tests the potential impact of influencing factors on these tools' outcomes (i.e., volume, segmentation quality).

The exclusion criteria were defined as follows:

- Case reports reviews, or opinion articles.
- Study design exclusively investigating ground-glass opacities (GGOs), using a dedicated (i.e., less generalisable) segmentation algorithm.

The authors excluded duplicate records using the Rayyan online tool (Perdue University).

Assessment of methodological quality

The quality of the included studies was assessed independently by two authors (chest radiologists with over five years of experience in LCS) based on the revised Quality Assessment of Diagnostic Accuracy Studies (QUADAS-2), and all disagreement was resolved through discussion with a third chest radiologist. The risk of bias was rated as high, low, or unclear.

Data extraction

Both authors agreed on the final list of reports and retrieved the respective full articles.

Non-English articles (i.e., Chinese, German) were translated using an online service (www.translated.com).

The authors then screened the complete reference lists of all included articles for additional pertinent entries. Grey literature reports were used to identify potential candidate studies.

The variables collected included: population, nodule features, statistical methodology, influencing factor(s), outcome variable, observed effect(s), interactions between different influencing factors, and the statistical significance of relevant tests.

Statistical analysis and data presentation

To assess the evidence for clinical significance, we selected all in vivo studies reporting interscan variability using relative Bland–Altman analysis. The variables collected at this stage included: influencing factor(s), systematic bias, Limits of Agreement (LOA), and sub-group analysis. The LOA were deduced from the standard deviation and systematic bias if needed. When appropriate, the authors synthesised LOA and systematic bias from groups of studies using the inverse-variance method with a random-effects model (SPSS v26 [IBM, Armonk, NY, USA]).

The heterogeneity between the primary studies was assessed using the heterogeneity variance (τ^2) and Forest plots. The Deeks' funnel plot was planned to determine study asymmetry and potential publication bias if comparing more than ten studies.

Missing values were excluded after an unsuccessful attempt to contact the corresponding author of the primary study.

Results

The search returned 1259 (MEDLINE), 1697 (SCOPUS), 53 (Journals@Ovid), 223 (Embase), and 126 (Emcare) results from 1960 to 2022. The PRISMA flow diagram is presented in Fig. 1.

After the study selection and critical appraisal, the first stage of the systematic review included a cohort of 137 studies. A consolidated summary of results is presented in Table 1, and the complete list of the summarised results is provided as Additional file 1: Table S1.

The second stage of the review identified a cohort of 16 studies, summarising their results in Table 2. Meta-analysis was attempted in two study groups, with results presented as Additional file 1 (Table S3 and Figures S1 and S2). Funnel plots were not performed since the minimum of 10 studies was unmet.

Influencing factors related to the scanner

Acquisition parameters

Radiation dose exposure, tube current, and tube potential Minimising radiation dose exposure is essential to LCS and can be done by manipulating tube current and potential, often interchangeably. The interaction between

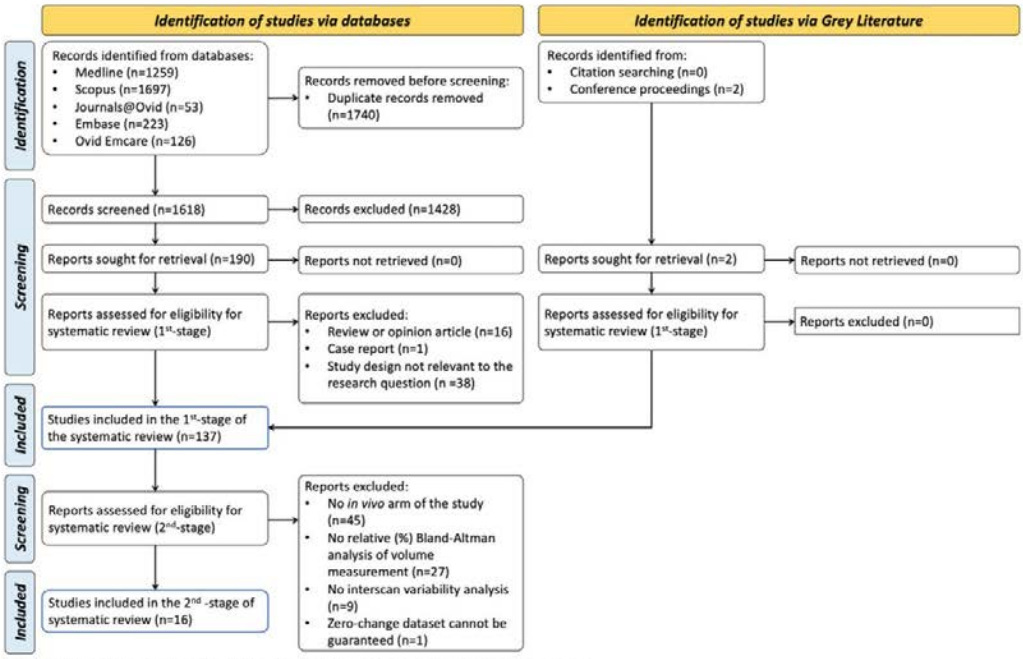

Fig. 1 Prisma flow diagram describing the results of the search and selection process

dose exposure and tube current–time product (mAs) is linear and well understood. However, the interaction with tube potential is not, with a reduction of tube voltage from 100 to 80kVp resulting in a reduction of dose exposure in the order of 1.5 [23].

Several studies investigated the impact of radiation dose exposure, tube voltage, or tube current on the outcome of volumetry tools. Less than half of the studies showed a statistically significant difference in accuracy, and the vast majority concluded this difference to be clinically insignificant [13, 15, 24–38]. Some studies reported worsening segmentation quality with lower dose exposure [30] and reduced precision with lower dose exposure, tube current–time product, or tube voltage, limited to small 5 mm and non-solid nodules [28, 39–46].

The impact of radiation dose exposure on volumetry showed clinically significant differences between standard-dose (SDCT) vs low-dose (LDCT) [18] CT protocols and SDCT vs ultra-low-dose CT protocols (ULDCT) [15, 17], contradicting the consensus that reducing the radiation dose does not affect the outcome of volumetry. Studies comparing LDCT vs ULDCT did not confirm this result, thus supporting their use in LCS [10, 13]. Despite the acceptance of SDCT, LDCT and ULDCT protocols, their definition varies among authors, and the effective radiation dose depends on the patient's body weight. The estimated effective dose acceptable for LCS is 2 mSv [47].

The signal-to-noise ratio (SNR) is not an independent influencing factor [32, 48].

Collimation

The effect of collimation is statistically significant between thin ($\leq$0.75 mm) and thick ($\geq$1.5 mm) settings, with some authors recommending thinner [37, 38] while others recommend thicker [49, 50] settings for volumetry. However, the consensus considers collimation as not clinically significant.

High-resolution scan mode

The development of garnet detectors in CT scanners enabled the high-resolution scan mode, increasing the sampling per gantry rotation, spatial resolution, and image quality while reducing volume overestimation [51].

Table 1 Summary of studies included in the review

Factor	Statistical significance	Clinical relevance	Observations
Acquisition parameters			
Radiation dose exposure, tube current and tube potential	No consensus	Yes	Despite usually considered as non-significant, there are numerous contradictory study results, with some studies even showing inter-scan variability of volumetry measures in the realm of clinical relevance
Signal-to-noise ratio (SNR)	No		Not an independent factor
Collimation	Yes	Untested	Generally considered as clinically not relevant, but untested
High-resolution scan mode	Yes	Untested	Single study showing reduced volume overestimation of pulmonary nodules
Field of view (scan FOV)	No		
Pitch	No		Not significant unless using high pitch mode (pitch factor = 3) in small nodules (< 5 mm)
Contrast enhancement	Yes	Untested	Overestimates the volume of the pulmonary nodule
Reconstruction parameters			
Slice thickness	Yes	Yes	Thinner slice thickness improves accuracy, precision, and segmentation quality Should be thin enough to allow any nodule to be visible in ≥ 3 consecutive slices A thickness ≥ 2.5 mm is inadequate to detect 1 mm changes in nodule's diameter
Field of view (display FOV)	No		
Reconstruction interval	No consensus	Untested	Overlap (interval < thickness) improves accuracy and precision of volumetry in smaller nodules and thicker slices Likely not significant using 1 mm slice thickness
Raw-data reconstruction algorithm	No	Yes (sub-solid nodules)	Iterative reconstruction (IR) algorithms outperform filtered back projection (FBP) for small part-solid nodules and at lower tube currents improving performance of volumetry tools The noise reduction provided by IR is not uniform and less significant at the nodules' edges
Kernel	Yes	Yes (sub-solid nodules)	Sharp kernel improves volumetry performance in thin 1 mm slices Smooth kernel outperforms sharp kernel in thicker ≥ 2.5 mm slices
Post-processing	No		Image compression and vessel suppression considered as not significantly influencing volumetry of pulmonary nodules
CT scanner equipment			
Vendor	Yes	Untested	Only for small nodules not requiring follow-up
Technology	No consensus	Untested	Multi-detector CT, flat-panel, dual energy spectral CT
Software			
Software (package and version) and segmentation algorithm	Yes	No	The same software package and version should be consistently used through the follow-up of any pulmonary nodule
Nodule			
Size	Yes	Yes	Performance of volumetry tools is degraded in smaller nodules and considered unreliable for growth estimation of nodules < 5 mm
Density	Yes	Untested	Volumetry of non-solid nodules has worse accuracy and precision than for solid nodules

Table 1 (continued)

Factor	Statistical significance	Clinical relevance	Observations
Shape	Yes	Untested	Volumetry of nodules with irregular and spiculated shapes has lower accuracy and precision than volumetry of nodules with round, elongated, smooth or lobulated shapes
Margin	Yes	Untested	Volumetry of nodules with poorly defined margins have higher variability
Location	Yes	Untested	Attachment to surrounding structures (e.g., pleura, vessels, bronchial walls) degrades the performance of volumetry tools
Patient			
Parenchymal changes	Yes	Untested	Only with increased attenuation of surrounding parenchyma (e.g., ILD)
Breathing	Yes	Yes	Breathing artifacts are related to volume overestimation and increased measurement variability
Cardiopulmonary haemodynamics	Yes	Yes	Complex cardiopulmonary interactions affecting the amount of blood inside or around a nodule, leading to increased volume measurement variability
Observer			
Manual correction	Yes	Untested	Selectively correcting obvious segmentation errors improves the performance of volumetry tools
Experience	No		
Training	Yes	Untested	Training with the volumetry tool is important in unexperienced observers

Field-of-view (FOV)

The scanners' spatial resolution in the axial plane depends on the FOV and the matrix size. The scan FOV determines the amount of raw data acquired, but images can be later reconstructed with a different and smaller display FOV.

Several authors investigated the effect of changing the FOV (between 9.6 cm and 36 cm) and showed no statistically significant impact on volumetry [52–55].

Pitch

Likewise, the pitch parameter has no significant impact on volumetry within conventionally used values [36, 49, 53, 56], apart from improved repeatability with smaller pitch values (0.9 vs 1.2) [49]. However, the high pitch mode (i.e., pitch factor of 3) reduces the accuracy of volumetry in small (< 5 mm) solid nodules [56].

Contrast enhancement

Contrast enhancement overestimates the volume, possibly by increasing the attenuation of the nodules or adjacent structures [57–61]. Rampinelli et al. found volumetry comparable across different delay times (i.e., phases) in contrast-enhanced CT [58].

Reconstruction parameters

Slice thickness

Slice thickness has been investigated as an influencing factor of volumetry between 0.625 and 5 mm. Thinner slices resulted in statistically significant improvement in accuracy and precision in all but one study [19, 21, 31, 34, 36, 39, 44, 48–50, 52–55, 62–67]. In comparison, thicker slices are related to lower measurement agreement and reduced segmentation quality [52, 54, 66].

The slice thickness determines the scan's longitudinal (z-axis) spatial resolution. The difference between the higher axial and lower longitudinal spatial resolution explains why the FOV is insignificant while the slice thickness is, especially for thicker slices.

Increasing the slice thickness increases the volume of voxels along the z-axis. Larger voxels may increase the volume measurement, but surface voxels will also suffer more partial volume effects, increasing measurement variability [54]. Since smaller nodules have a higher ratio of surface to inner voxels, the volumetry of smaller nodules is more affected by slice thickness [21, 36, 49, 52].

The slice thickness should be thin enough to make any nodule visible in at least three consecutive slices [52].

Table 2 Summary of studies reporting percent Bland–Altman analysis of interscan variability

Ref.	Population	(n)	Independent variable/subgroup	Bias	$_{lower}$LOA	$_{upper}$LOA
[7]	Patients with known pulmonary nodules					
		100	Size: all	− 0,90%	− 16,40%	14,60%
		58	Size: 30–< 80 mm^3	− 0.3%	− 16.8%	16.2%
		42	Size: 80–150 mm^3	− 1.7%	− 15.5%	12.3%
[8]	Patients with pulmonary nodules detected on CCTA	195	Cardiac cycle phase (systole vs diastole)	2.65%	− 47.0%	52.3%
[9]	Patients with part− solid nodules	66	Kernel			
			Solid component segmentation	− 3.2%	− 45.0%	39.0%
			Whole nodule segmentation	13,00%	− 21.0%	46.0%
[10]	Patients under surveillance for < 2 mm solid nodules		Radiation dose exposure (LDCT vs. ULDCT)			
		170	all nodules	− 2.0%	− 18.0%	22.7%
		97	indeterminate nodules	− 6.0%	− 12.7%	21.9%
		68	BMI < 25	− 2.5%	− 17.5%	23.6%
		102	BMI > 25	− 1.0%	− 18.3%	20.8%
[11]	Patients with preoperative scans for subsolid nodules	66	Reconstruction algorithm: FBP vs. MBIR			
			solid component segmentation	6.3%	− 51.9%	64.6%
			whole nodule segmentation	3.2%	− 20.5%	27,00%
[12]	Patients with emphysema	88	Level of inspiration (end-inspiratory vs end-expiratory)	7,5%	− 24,1%	39,1%
[13]	Patients were enrolled prospectively	105	Radiation dose (LDCT vs. ULDCT with FBP or SAFIRE)			
			FBP	0.2%	− 20.0%	20.4%
			SAFIRE	0.3%	− 9.7%	10.4%
[14]	Patients with subsolid nodules	94	intraobserver (R1)	− 1,5%	− 17,3%	16,5%
			Intraobserver (R2)	0,4%	− 14,8%	18,5%
[15]	Patients retrospectively enrolled	202	Radiation dose exposure (SDCT vs. ULDCT)			
			Intraobserver (R1)	1.4%	− 25.1%	26.2%
			Intraobserver (R2)	1.9%	− 25.1%	28.9%
			Interobserver (R1 vs R2)	1.2%	− 25,0%	27.4%
			interobserver (R2 vs R1)	2.1%	− 23.9%	28.1%
[16]	Consecutive patients referred for known or suspected pulmonary metastases (3.3 mm—30 mm)	89	Software			
			Software A	0,0%	− 17,0%	17,0%
			Software B	0,0%	− 13,1%	13,1%
			Software C	0,0%	− 20,8%	20,8%
			Software D	0,0%	− 13,4%	13,4%
			Software E	0,0%	− 20,5%	20,5%
			Software F	0,0%	− 19,6%	19,6%
[17]	Patients on follow-up for lung cancer or scanned because of suspicious pulmonary nodules		Radiation dose exposure (SDCT vs. ULDCT)			
		229	Size: all			
			Intraobserver (R1)	1.5%	− 25.1%	28.1%
			Intraobserver (R2)	2,0%	− 26.4%	30.4%
			Interobserver (R1 vs R2)	1.3%	− 26.5%	29.1%
			interobserver (R2 vs R1)	2.2%	− 25.2%	29.6%
		153	size: < 10 mm			
			Intraobserver (R1)	2.3%	− 28.5%	33.1%
			Intraobserver (R2)	2.6%	− 29.4%	34.6%
			Interobserver (R1 vs R2)	1.9%	− 28.3%	32.1%
			Interobserver (R2 vs R1)	2.1%	− 29,10%	33.3%
		76	Size: ≥ 10 mm			
			Intraobserver (R1)	1.4%	− 18.6%	21.4%
			Intraobserver (R2)	0.4%	− 18.6%	19.4%
			Interobserver (R1 vs R2)	0.4%	− 17,00%	17.8%

Table 2 (continued)

Ref.	Population	(n)	Independent variable/subgroup	Bias	$_{lower}$LOA	$_{upper}$LOA
			Interobserver (R2 vs R1)	0.6%	− 18.4%	19.6%
[18]	Patients with known nodules were prospectively enrolled	83	Radiation dose: SDCT vs. LDCT			
			SDCT	12.8%	− 27.0%	40.0%
			LDCT	17.0%	− 38.0%	60.0%
[19]	Patients with contrast-enhanced chest CT	101	Slice thickness: 1 mm	− 0.1%	− 21.6%	20.3%
		101	Slice thickness: 3 mm	1.0%	− 15.4%	15.2%
		101	Slice thickness: 5 mm	1.6%	− 21.8%	27.6%
[20]	Patients with pulmonary metastases	218	Segmentation: all	1.3%	− 21.2%	23.8%
		106	Segmentation: complete	0.28%	− 11.9%	12.4%
		112	Segmentation: incomplete	1.61%	− 26.8%	30.0%
[21]	Patients with pulmonary metastases	96	Segmentation algorithm	0.0%	− 26.9%	26.9%
[22]	Patients with pulmonary metastases	151	Size: all	0.7%	− 20.4%	21.9%
		105	Size: < 10 mm	0.55%	− 19.3%	20.4%

The independent variable is the influencing factor (if any) that changes between measurements of each nodule (e.g., standard dose [SDCT], low-dose CT [LDCT] vs. ultra-low-dose CT [ULDCT])

Likewise, a thickness ≥ 2.5 mm is inadequate to detect 1 mm changes in diameter [63, 65].

Reconstruction interval

When the reconstruction interval is smaller than the slice thickness (i.e., overlap), the longitudinal spatial resolution improves independently of slice thickness [36, 55].

In a study by Gavrielides et al., the accuracy and precision of volumetry tools improved with 50% overlap, with significant cross-effects between reconstruction interval, slice thickness, nodule size, and radiation dose exposure [36]. Honda et al. reported that non-overlapping reconstructions were associated with volume overestimation in scans obtained with 2.5 mm and 3.75 mm slice thicknesses [54]. Eberhard et al. found no significant benefit of overlapping protocols when using a 1 mm slice thickness, arguing in favour of skipping them to improve LCS cost-effectiveness [68].

Raw-data reconstruction algorithm and kernel

CT image reconstruction involves converting the raw data to a sinogram (representing the number and angulation of photons as they hit the detectors) and then to a matrix of attenuation values, known as the image model. This process is called direct back-projection and results in significant blurring. In filtered back projection (FBP), filters (or kernels) are applied to the image model to reduce the blurring effect, provide smoothing or edge enhancement, and highlight certain features and anatomical components.

Most studies investigating the impact of kernels on volumetry have considered them statistically significant (10 out of 13 studies). High-spatial frequency (sharp) kernels, like lung or bone, improved accuracy, precision, and repeatability in most studies [36, 45, 49, 63]. In contrast, a single study reported increased repeatability with a low-spatial frequency (smooth) kernel [64]. Larici et al. investigated the interaction between kernel and slice thickness to conclude that a sharp kernel provides the best performance for volumetry in 1.25 mm slice thickness. A smooth kernel outperforms the sharp kernel in 2.5 mm slice thickness [66].

Several studies reported an overestimation of volume associated with the sharp kernel [54, 59, 64], especially in non-overlapping acquisition and solid nodules (or solid components of part-solid nodules) [54]. Conversely, volumetry of GGOs (or ground-glass components of part-solid nodules) results in higher estimates when using a smooth kernel [9].

In iterative reconstruction (IR), the scanner converts the image model into an artificial sinogram (forward projection). It then compares it to the original sinogram with each iteration, correcting random fluctuations in photon measurement. This process minimises noise and improves image quality at significantly lower radiation exposure [69]. However, this noise reduction is less significant at the edges of the pulmonary nodules, resulting in IR-specific measurement error for small nodules and lower doses or higher noise levels [25, 34].

Multiple studies investigated the influence of raw data reconstruction algorithms on volumetry tools [13, 24, 25, 28, 30, 32–34, 39–42, 51, 70–72], with the consensus being that IR outperforms FBP for small, part-solid nodules or at lower tube currents [28, 39–41], allowing IR-based protocols to replace FBP safely.

Recently, Kim et al. [73] investigated two deep learning (DL)-based raw-data reconstruction algorithms (Truefidelity and ClariCT.AI), showing improved accuracy against the adaptive statistical iterative reconstruction (ASiR) algorithm using LDCT and ULDCT.

The scientific literature often refers to raw-data reconstruction algorithms and kernels as just reconstruction algorithms, which could be confusing since the former is generally considered not to influence volumetry measurements. At the same time, the latter is known to do so [42].

Post-processing

Despite the earlier warning by Ko et al. regarding image compression [74], Santos et al. found no significant deterioration in the performance of volumetry tools within the limits proposed in the European Society of Radiology (ESR) position paper [75, 76].

The influence of vessel suppression on volumetry was investigated by Milanese et al. using commercially available software (ClearRead, Riverain, Miamisburg, OH, USA). The authors reported high measurement agreement with and without vessel suppression, although the rate of manual correction was unusually high (49/77, 75.4%) [77].

CT scanner equipment

CT scanner vendor

Comparing the performance of volumetry tools using different scanners showed good accuracy regardless of the scanner vendor [37]. Two later studies found a statistically significant difference between scanner vendors, but only for small nodules, which would not require follow-up according to current guidelines [26, 78].

CT scanner technology

Several studies have compared the performance of volumetry between different scanner technologies (e.g., single or multiple detectors, flat-panel, and dual-energy CT scanners) [19, 37, 55, 79, 80]. Das et al. reported increasing accuracy in volumetry with more detector rows [38], although Xie et al. did not confirm this [81].

Flat-panel scanners outperform multi-detector scanners in pulmonary nodule volumetry, especially in small nodules (< 5 mm) [82–85].

Mono-energetic reconstructions at 70 keV using dual-energy spectral CT are considered equivalent to conventional CT images acquired using 120 kVp, and several authors found no significant difference in volumetry accuracy between them [86–88]. In addition, mono-energetic reconstructions improved the repeatability of volumetry at the same radiation dose [87].

Influencing factors related to the software

Software package and segmentation algorithm

Several studies compared different software packages and different segmentation algorithms for pulmonary nodule volumetry, reporting statistically significant differences in all but one study [45, 83, 89–92] and even between different versions of the same software [93]. Adjusting the attenuation threshold, as some segmentation algorithms allow, also influences the volume measurement outcome [45, 55, 92].

Several international societies firmly recommend consistently using the same software package, version, and segmentation algorithm during follow-up [94].

Influencing factors related to the nodule

Nodule size

Volumetry is less performant for small nodules [10, 13, 16, 18, 21, 25, 28, 29, 31, 36–38, 40, 41, 45, 48–51, 53, 55, 56, 60, 63, 70, 72, 74, 78, 79, 81, 82, 89, 92, 93, 95–101], explained mainly by partial volume effects, and is considered unreliable for nodules < 5 mm in diameter [60, 102].

Multiple interactions between nodule size and other influencing factors are known, including collimation [31, 49], tube current [29, 41], reconstruction algorithm [29, 41, 51, 70, 72], kernel [36], reconstruction interval [36], slice thickness [20, 21, 31, 36, 48, 49, 53], scanner technology [41, 52, 82], software [16, 45, 89, 93], compression level [74], density [28, 41], and level of inspiration [16, 20].

Hwang et al. suggested that raising the threshold to 9 mm for starting follow-up would lead to a significant increase in specificity (i.e., from 91.7% to 96.7%) at the cost of only a modest decrease in sensitivity (i.e., from 96.2% to 94.2%). The impact of such a change to current recommendations would result in a 60% reduction of follow-up scans at the cost of delaying the diagnosis of 1.9% of lung cancer patients [103]. Volumetry tools should be robust to influencing factors for solid nodules ≥ 9 mm when using current LDCT protocols in LCS programmes.

Density

Published studies in the literature describe the density of a nodule as either a qualitative (e.g., solid, part-solid, ground-glass, calcified) or quantitative feature (i.e., in Hounsfield Units).

Non-solid nodules are more challenging to segment manually and using volumetry tools and present lower

accuracy and higher variability than solid nodules [11, 25, 26, 28, 36, 41, 45, 92].

Interactions between density and other influencing factors have been described, including nodule size [28, 36, 92], reconstruction algorithms [28, 41, 70], slice thickness [36], tube current [41], level of inspiration [104], and image compression [74]. Higher nodule density is correlated to larger volume [88].

Shape and margin

The shape of a pulmonary nodule can be round, elongated, smooth, lobulated, spiculated, or irregular.

An irregular or spiculated shape is associated with lower accuracy [62, 64] and precision [20] of volumetry tools. It is also associated with a lower volume measurement [78], lower segmentation quality [97, 105], and increased variability [21, 96, 97, 100, 106].

The ratio of surface to inner voxels increases in nodules with an irregular or spiculated shape (i.e., larger surface area), deteriorating the performance of volumetry tools due to partial volume effects [78, 100]. Therefore, volumetry of small (≤6 mm) pulmonary nodules with irregular or spiculated shapes (i.e., high-risk features for malignancy) may be unreliable and can justify an optional follow-up period [107].

The shape of a nodule also interacts with other influencing factors, such as the nodule's density [28], location, slice thickness, and kernel [64].

Several authors describe spiculation as a feature of the nodule's margin, which can be a source of confusion. We defined the margin as either well or poorly defined. In a study by Iwano et al., volume measurements of nodules with poorly defined margins had a significantly higher variability [108].

Location

Most authors categorise a nodule's location as either intra-parenchymal, juxta-pleural, juxta-fissural, or juxta-vascular [37, 38, 51, 64, 66, 96, 109, 110], with intra-parenchymal nodules further classified as either central or peripheric [74, 111, 112].

Attachments to adjacent structures (e.g., vessels, bronchial wall, and pleura) may result in the latter's inclusion, overestimating the volume and increasing the measurement variability [111, 112].

In a recent study by Guedes Pinto et al., the authors reported the location in both the axial (anterior, middle, or posterior) and coronal (upper, middle, lower) planes, additionally measuring the vascular distance along the pulmonary arteries, from the main pulmonary artery (MPA) to the nodule using multiplanar reformatting, which proved to be statistically significant [113]. Conversely, the location within a lobe [18] or segment [98] was not proven to be statistically significant.

Interactions have been reported between the location and software [111], shape [64], slice thickness [64, 66], kernel [64], tube current [66], and compression [74].

Influencing factors related to the patient

Parenchymal changes

Both global and regional parenchymal changes in emphysema patients (i.e., reduced parenchymal attenuation) have been investigated and found not significantly to affect pulmonary nodule volumetry (108. However, in diseases with increased parenchyma attenuation, like interstitial lung disease (ILD), the reduced contrast between nodule and surrounding parenchyma could deteriorate the performance of volumetry tools. In two phantom studies by Gavrielides et al., the difference in attenuation between a synthetic nodule and the background was statistically significant [39, 67]. Recently, Penha et al. reported that the quality of pulmonary nodule segmentation by volumetry tools decreases with increasing attenuation of the surrounding parenchyma [114].

Breathing

Breathing artefacts are related to overestimating volume and increased measurement variability of volumetry tools [12, 16, 20, 43, 99, 104, 115, 116]. This effect is most significant at the end of expiration and for smaller nodules but is considered unlikely to be clinically relevant [12, 16, 20, 115]. However, Goo et al. reported a volume overestimation of 23.1% from inspiration to expiration, interpreted as clinically significant [116].

The level of inspiration interacts with other influencing factors like the nodule size [16], density [104], and software package [16].

Cardiopulmonary haemodynamic factors

Studies designed with coronary CT angiography (CCTA) can compare the performance of volumetry tools at different cardiac phases in a single acquisition.

Boll et al. reported changes in volume measurement related to a complex interaction between the cardiac phase, location (i.e., pulmonary segments), and nodule size [98].

Guedes Pinto et al. investigated the impact of cardiopulmonary haemodynamic factors on volumetry tools, including the cardiac phase, calibre change of the MPA between systole and diastole, the vascular distance between the MPA and the nodule, and nodule's

location along the axial (related to hydrostatic pressure) and coronal plane (related to vascular section area), all statistically significant except the cardiac phase. The authors proposed a theoretical model where the volume of a given nodule is affected by the dynamic vascular pressure as blood travels from the heart to the nodule [113]. In another study by the same authors, the variability of volumetry vastly exceeded the criterion for clinical significance when comparing measurements in opposing cardiac phases (systole vs diastole [−47%, 52.3%]), with the lower variability seen when comparing two measurements in diastole ([−18.9%, 19.7%]) [8].

CCTA is not appropriate for LCS. However, there is considerable overlap in risk factors between coronary artery disease and lung cancer. Patients enrolled in LCS are also at risk of cardiovascular events, with some authors advocating a role for dual screening [113].

Influencing factors related to the observer

Manual correction, observer experience and training

The promise of (semi)automated tools is to reduce inter-observer variability by limiting the observer's influence in the measurement [102, 117]. Counter-intuitively, allowing manual correction of the segmentation improves the tool's performance [60, 102, 118]. This is explained because inadequately segmented nodules tend to be outliers (i.e., either including adjacent structures [113] or incompletely segmenting the nodule [20]), resulting in higher variability and lower observer agreement.

The outcome of volumetry tools is independent of observer experience (i.e., radiologists vs non-radiologists), even when manually correcting the segmentation result. However, in the un-experienced group of observers, training with the tool was statistically significant for volume measurements [119].

Regarding concerns of bias and excluded studies

The most common concern of bias in the included studies (Table 3) is the use of experimental algorithms [9, 28, 45, 53, 74, 89, 92, 117, 120–152], followed by the assumption of zero-change datasets over more extended periods, relying on the perceived stability of the nodules [80, 95, 152]. Two studies use non-consecutive or convenience sample techniques, possibly introducing selection bias [60, 71]. Still, others present an incomplete description of their methods, poorly defining their population or the statistical analysis [26, 72, 77, 93, 148, 152].

Several promising candidate studies were excluded after full-text analysis based on their choice of outcome (Additional file 1: Table S2). These outcomes include the risk of malignancy [1, 100, 103, 153–161], prognosis [162–167], growth [5, 67, 101, 112, 168–174], or comparison to other methods of measurement like diameter [100, 175], area [175], the diameter of an equivalent volume sphere [3] or manual segmentations (e.g., most of the recent research using DL-based segmentation).

Although these outcomes are clinically interesting, they are unrelated to our research questions.

Table 3 Assessment of bias of the primary studies

Specific concerns of bias	References
Experimental algorithm not commercially available	[9, 28, 45, 53, 74, 89, 92, 117, 120–152]
Assumption of zero-change dataset cannot be guaranteed	[80, 95, 152]
Inadequate description of statistical analysis	[72, 93, 148, 152]
Non-consecutive or convenience sample	[60, 71]
Study population is inadequately described	[26, 77]

Discussion

The influencing factors of volumetry tools have been investigated extensively. However, the possibility of wrongly diagnosing a nodule as stable or growing between follow-up scans has only been tested in a little over 10% of studies. Consolidating the results from different studies is difficult due to the heterogeneity, but an impact on clinical decision-making seems more likely in smaller nodules.

The contrast between nodule and surrounding lung parenchyma and the surface-to-inner voxel ratio are two key concepts in understanding how volumetry tools can be influenced.

Pulmonary nodule volumetry benefits from the contrast between the nodule and the surrounding well-aerated lung parenchyma. This contrast is decreased in sub-solid nodules when the surrounding parenchyma has increased attenuation (e.g., ILD, expiratory phase, contrast enhancement) or when the nodule contacts adjacent structures. Image reconstruction with different kernels and raw-data reconstruction algorithms may also expand or contract the segmentation by changing the attenuation value of the voxels.

Surface voxels contain both nodule tissue and surrounding parenchyma and suffer partial volume effects leading to measurement error and variability.

The surface-to-inner voxel ratio depends primarily on the size difference between the nodule and the voxel (i.e., how many voxels fit in the nodule). Still, it can also

be increased by an irregular shape or ill-defined nodule margin (i.e., increased surface area).

Reducing the slice thickness and measuring nodules of increasing size rapidly decreases the ratio of surface to inner voxels, improving the performance of volumetry tools.

Apart from these two key concepts, implementation details involved in the segmentation algorithms account for most of the remaining observed influence in volumetry tools.

Despite the large number of included studies in this review, comparing study results is problematic given a large number of influencing factors and heterogeneity in study design, outcomes, statistical analysis, nodule features and demographics. Additionally, multiple authors report statistically significant results while openly questioning their clinical relevance. Changing a factor that influences a volumetry tool may not be enough to change our assessment of nodule growth and clinical management. Therefore, using this evidence to support clinical decisions is challenging. We consider this a limitation of the evidence and a strong motivator for this review.

A clarification of clinical significance seems needed. The optimal waiting period for a follow-up scan is based on the inherent in vivo interscan measurement variability of volumetry tools, accepted as $\leq 25\%$ of total volume [6]. Higher measurement variability implies a longer time to distinguish real growth from measurement error. Therefore, we defined clinical significance as interscan variability $> 25\%$ of volume change since false-positive growth estimation would become more likely in this setting. We used this criterion to select a subset of all studies reporting interscan variability using Bland–Altman analysis (n = 16). Influencing factors investigated regarding their clinical relevance include radiation dose exposure, slice thickness, raw-data reconstruction algorithms, kernels, size, cardiac cycle phase, software package, segmentation algorithm, and level of inspiration.

We combined the results of two studies comparing SDCT vs ULDCT protocols [15, 17], and the synthesised result confirmed the primary studies' conclusions. We also combined the results in a second group (three studies) by disregarding sub-group analysis concerning size [7, 22] and quality of segmentation [20], with a synthesised result within the clinically acceptable a priori LOA, but losing the influence of the factors (i.e., size and quality of segmentation) under study. Due to significant population, outcome, and design heterogeneity, we could not combine other studies. Therefore, our attempted meta-analysis failed to advance the current knowledge meaningfully (Additional file 1: Table S3 and Figures S1 and S2).

Several other factors have been statistically shown to influence the outcome of volumetry tools. However, the clinical relevance of these findings still needs to be investigated (Table 1) and represents gaps in current knowledge and opportunities for future research.

Implications of the results for practice, policy, and future research

Findings from this review confirm the clinically significant impact of some known influencing factors on pulmonary nodule volumetry, including the segmentation algorithm, quality of the segmentation, slice thickness, the level of inspiration for solid nodules, and the reconstruction algorithm and kernel in subsolid nodules (Table 3).

Much of the evidence collected has yet to be tested for potential clinical significance and is thus open for future research.

A concern related to this systematic review is the long period of the included studies in a rapidly changing field, suggesting that this review may not reflect current performance. A comparison of recent (i.e., last five years) and older studies show an improving performance trend likely related to software and scanner technology innovations. In a recent study by Bartlett et al., the reported interscan variability was not clinically relevant ($_{95}$CI [−16.8%; 16%]) even for very small (30–80 mm^3) solid, non-metastatic and non-calcified pulmonary nodules (n = 58), suggesting that a shorter optimal waiting time may already be appropriate [7].

We propose a standard for future studies around the Bland–Altman analysis and restricted to nodules between 5 and 10 mm where growth estimation is useful. Such studies should investigate the persisting gaps in current knowledge, focusing on clinical applicability and currently available technology. Future research should also explore the cost and benefits of potential changes to current practices, like raising the threshold for follow-up or shortening the optimal waiting period in the follow-up schedule.

Abbreviations

CCTA	Coronary CT angiography
DL	Deep-learning
FBP	Filtered back-projection
FOV	Field of view
GGO	Ground-glass opacity
IR	Iterative reconstruction
LCS	Lung cancer screening
LDCT	Low-dose CT
LOA	Limits of agreement
QUADAS-2	Quality Assessment of Diagnostic Accuracy Studies tool
SDCT	Standard dose CT
SNR	Signal-to-noise ratio
ULDCT	Ultra-low-dose CT
VDT	Volume doubling time

Supplementary Information

The online version contains supplementary material available at https://doi.org/10.1186/s13244-023-01480-z.

Additional file 1: Supplementary Table S1. Studies included in the first stage of the systematic review [176–182]. **Supplementary Table S2.** Studies that seemed promising for inclusion during the screening phase but were later excluded [183, 184]. **Supplementary Table S3.** Results of the attempted meta-analysis of two sets of similar studies. **Supplementary Figures S1.** Forest plot of similar studies [15, 17]. **Supplementary Figures S2.** Forest plot of similar studies [7, 20, 22].

Author contributions

All authors critically revised the manuscript and approved it prior to submission. EGP, DP, and KI conceived this study and supervised all aspects of its implementation. EGP and DP collected the data and carried out the analysis of the data. All the authors contributed to the interpretation of the results and the proofreading of the manuscript. All authors read and approved the final manuscript.

Funding

The authors did not receive financial or non-financial support for this systematic review.

Availability of data and materials

All data extracted or synthesised and the analytic code used for the meta-analysis can be obtained from the corresponding author on reasonable request.

Declarations

Ethics approval and consent to participate

Not applicable.

Consent for publication

Not applicable.

Competing interests

The authors declare no competing interests.

Author details

[1]R. Marquês de Ávila E Bolama, Universidade da Beira Interior Faculdade de Ciências da Saúde, 6201-001 Covilhã, Portugal. [2]Liverpool Heart and Chest Hospital NHS Foundation Trust, Thomas Dr, Liverpool L14 3PE, UK. [3]University of Florida, Gainesville, FL 32611, USA. [4]Faculdade de Medicina, Universidade Federal Do Rio de Janeiro, Bloco K - Av. Carlos Chagas Filho, 373 - 2º Andar, Sala 49 - Cidade Universitária da Universidade Federal Do Rio de Janeiro, Rio de Janeiro - RJ 21044-020, Brasil. [5]Faculdade de Medicina, Universidade Federal Fluminense, Av. Marquês Do Paraná, 303 - Centro, Niterói - RJ 24220-000, Brasil. [6]Manchester University NHS Foundation Trust, Manchester Royal Infirmary, Oxford Rd, Manchester M13 9WL, UK.

Received: 18 April 2023 Accepted: 8 July 2023
Published online: 23 September 2023

References

1. Horeweg N, van Rosmalen J, Heuvelmans MA et al (2014) Lung cancer probability in patients with CT-detected pulmonary nodules: a prespecified analysis of data from the NELSON trial of low-dose CT screening. Lancet Oncol 15(12):1332–1341. https://doi.org/10.1016/S1470-2045(14)70389-4
2. Walter JE, Heuvelmans MA, Dorrius M, Oudkerk M (2019) Low-dose lung cancer screening: nodule measurement and management. Precis Cancer Med 2:24–24. https://doi.org/10.21037/pcm.2019.07.03
3. Dicken V, Bornemann L, Moltz JH, Peitgen HO, Zaim S, Scheuring U (2015) Comparison of volumetric and linear serial ct assessments of lung metastases in renal cell carcinoma patients in a clinical phase IIB study. Acad Radiol 22(5):619–625. https://doi.org/10.1016/j.acra.2014.12.018
4. Han D, Heuvelmans MA, Oudkerk M (2017) Volume versus diameter assessment of small pulmonary nodules in CT lung cancer screening. Transl Lung Cancer Res 6(1):52–61. https://doi.org/10.21037/tlcr.2017.01.05
5. Korst RJ, Lee BE, Krinsky GA, Rutledge JR (2011) The utility of automated volumetric growth analysis in a dedicated pulmonary nodule clinic. J Thorac Cardiovasc Surg 142(2):372–377. https://doi.org/10.1016/j.jtcvs.2011.04.015
6. Devaraj A, van Ginneken B, Nair A, Baldwin D (2017) use of volumetry for lung nodule management: theory and practice. Radiology 284(3):630–644. https://doi.org/10.1148/radiol.2017151022
7. Bartlett EC, Kemp S, Rawal B, Devaraj A (2022) Defining growth in small pulmonary nodules using volumetry: results from a "coffee-break" CT study and implications for current nodule management guidelines. Eur Radiol 32(3):1912–1920. https://doi.org/10.1007/s00330-021-08302-0
8. Pinto EG, Penha D, Hochhegger B et al (2022) Variability of pulmonary nodule volumetry on coronary CT angiograms. Medicine (Baltimore) 101(35):e30332. https://doi.org/10.1097/MD.0000000000030332
9. Werner S, Gast R, Grimmer R, Wimmer A, Horger M (2022) Accuracy and reproducibility of a software prototype for semi-automated computer-aided volumetry of the solid and subsolid components of part-solid pulmonary nodules. Rofo 194(3):296–305. https://doi.org/10.1055/a-1656-9834
10. Paks M, Leong P, Einsiedel P, Irving LB, Steinfort DP, Pascoe DM (2018) Ultralow dose CT for follow-up of solid pulmonary nodules. Medicine (Baltimore) 97(34):e12019. https://doi.org/10.1097/MD.0000000000012019
11. Cohen JG, Kim H, Park S et al (2017) Comparison of the effects of model-based iterative reconstruction and filtered back projection algorithms on software measurements in pulmonary subsolid nodules. Eur Radiol 27(8):3266–3274. https://doi.org/10.1007/s00330-016-4716-5
12. Moser JB, Mak SM, McNulty WH et al (2017) The influence of inspiratory effort and emphysema on pulmonary nodule volumetry reproducibility. Clin Radiol 72(11):925–929. https://doi.org/10.1016/j.crad.2017.06.117
13. Sui X, Meinel FG, Song W et al (2016) Detection and size measurements of pulmonary nodules in ultra-low-dose CT with iterative reconstruction compared to low dose CT. Eur J Radiol 85(3):564–570. https://doi.org/10.1016/j.ejrad.2015.12.013
14. Kim H, Park CM, Woo S et al (2013) Pure and part-solid pulmonary ground-glass nodules: measurement variability of volume and mass in nodules with a solid portion less than or equal to 5 mm. Radiology 269(2):585–593. https://doi.org/10.1148/radiology.13121849
15. Hein PA, Romano VC, Rogalla P et al (2010) Variability of semiautomated lung nodule volumetry on ultralow-dose CT: comparison with nodule volumetry on standard-dose CT. J Digit Imaging 23(1):8–17. https://doi.org/10.1007/s10278-008-9157-5
16. Hoop B, Gietema H, Ginneken B et al (2009) A comparison of six software packages for evaluation of solid lung nodules using semi-automated volumetry: What is the minimum increase in size to detect growth in repeated CT examinations. Eur Radiol 19(4):800–808. https://doi.org/10.1007/s00330-008-1229-x
17. Hein P, Romano V, Rogalla P et al (2009) Linear and volume measurements of pulmonary nodules at different CT dose levels – intrascan and interscan analysis. Rofo 181(1):24–31. https://doi.org/10.1055/s-2008-1027874
18. Rampinelli C, de Fiori E, Raimondi S, Veronesi G, Bellomi M (2009) In vivo repeatability of automated volume calculations of small pulmonary nodules with CT. AJR Am J Roentgenol 192(6):1657–1661. https://doi.org/10.2214/AJR.08.1825
19. Vogel MN, Vonthein R, Schmücker S et al (2008) Automated pulmonary nodule volumetry with an optimized algorithm. Accuracy at different slice thicknesses compared to unidimensional and bidimensional measurements. Rofo 180(9):791–797. https://doi.org/10.1055/s-2008-1027562
20. Gietema HA, Schaefer-Prokop CM, Mali WPTM, Groenewegen G, Prokop M (2007) Pulmonary nodules: interscan variability of semiautomated

volume measurements with multisection CT—influence of inspiration level, nodule size, and segmentation performance. Radiology 245(3):888–894. https://doi.org/10.1148/radiol.2452061054
21. Petrou M, Quint LE, Nan B, Baker LH (2007) Pulmonary nodule volumetric measurement variability as a function of CT slice thickness and nodule morphology. AJR Am J Roentgenol 188(2):306–312. https://doi.org/10.2214/AJR.05.1063
22. Wormanns D, Kohl G, Klotz E et al (2004) Volumetric measurements of pulmonary nodules at multi-row detector CT: in vivo reproducibility. Eur Radiol 14(1):86–92. https://doi.org/10.1007/s00330-003-2132-0
23. Lira D, Padole A, Kalra MK, Singh S (2015) Tube potential and CT radiation dose optimization. AJR Am J Roentgenol 204(1):W4-10. https://doi.org/10.2214/AJR.14.13281
24. Lee HN, Kim JI, Shin SY (2020) Measurement accuracy of lung nodule volumetry in a phantom study. Medicine (Baltimore) 99(23):e20543. https://doi.org/10.1097/MD.0000000000020543
25. Eberhard M, Stocker D, Milanese G et al (2019) Volumetric assessment of solid pulmonary nodules on ultralow-dose CT: a phantom study. J Thorac Dis 11(8):3515–3524. https://doi.org/10.21037/jtd.2019.08.12
26. Liu J, Qing H, Luo H et al (2019) Accuracy of pulmonary nodule volumetry at different exposure parameters in low-dose computed tomography. J Comput Assist Tomogr 43(6):926–930. https://doi.org/10.1097/RCT.0000000000000908
27. Jin S, Zhang B, Zhang L, Li S, Li S, Li P (2018) Lung nodules assessment in ultra-low-dose CT with iterative reconstruction compared to conventional dose CT. Quant Imaging Med Surg 8(5):480–490. https://doi.org/10.21037/qims.2018.06.05
28. Gavrielides MA, Berman BP, Supanich M et al (2017) Quantitative assessment of nonsolid pulmonary nodule volume with computed tomography in a phantom study. Quant Imaging Med Surg 7(6):623–635. https://doi.org/10.21037/qims.2017.12.07
29. Su D, Feng L, Jiang Y, Wang Y (2017) Effect of scanning and reconstruction parameters on three dimensional volume and CT value measurement of pulmonary nodules: a phantom study. Zhongguo Fei Ai Za Zhi 20(8):562–567. https://doi.org/10.3779/j.issn.1009-3419.2017.08.11
30. den Harder AM, Willemink MJ, van Hamersvelt RW et al (2016) Pulmonary nodule volumetry at different low computed tomography radiation dose levels with hybrid and model-based iterative reconstruction. J Comput Assist Tomogr 40(4):578–583. https://doi.org/10.1097/RCT.0000000000000408
31. Gavrielides MA, Li Q, Zeng R, Myers KJ, Sahiner B, Petrick N (2016) Volume estimation of multidensity nodules with thoracic computed tomography. J Med Imaging (Bellingham) 3(1):013504. https://doi.org/10.1117/1.JMI.3.1.013504
32. Young S, Kim HJG, Ko MM, Ko WW, Flores C, McNitt-Gray MF (2015) Variability in CT lung-nodule volumetry: effects of dose reduction and reconstruction methods. Med Phys 42(5):2679–2689. https://doi.org/10.1118/1.4918919
33. Kim H, Park CM, Song YS, Lee SM, Goo JM (2014) Influence of radiation dose and iterative reconstruction algorithms for measurement accuracy and reproducibility of pulmonary nodule volumetry: A phantom study. Eur J Radiol 83(5):848–857. https://doi.org/10.1016/j.ejrad.2014.01.025
34. Chen B, Barnhart H, Richard S, Robins M, Colsher J, Samei E (2013) Volumetric quantification of lung nodules in CT with iterative reconstruction (ASiR and MBIR). Med Phys 40(11):111902. https://doi.org/10.1118/1.4823463
35. Christe A, Szucs-Farkas Z, Huber A et al (2013) Optimal dose levels in screening chest ct for unimpaired detection and volumetry of lung nodules, with and without computer assisted detection at minimal patient radiation. PLoS One 8(12):e82919. https://doi.org/10.1371/journal.pone.0082919
36. Gavrielides MA, Zeng R, Myers KJ, Sahiner B, Petrick N (2013) Benefit of overlapping reconstruction for improving the quantitative assessment of CT lung nodule volume. Acad Radiol 20(2):173–180. https://doi.org/10.1016/j.acra.2012.08.014
37. Das M, Ley-Zaporozhan J, Gietema HA et al (2007) Accuracy of automated volumetry of pulmonary nodules across different multislice CT scanners. Eur Radiol 17(8):1979–1984. https://doi.org/10.1007/s00330-006-0562-1
38. Das M, Muhlenbruch G, Katoh M et al (2007) Automated volumetry of solid pulmonary nodules in a phantom. Invest Radiol 42(5):297–302. https://doi.org/10.1097/01.rli.0000258683.20123.c4
39. Gavrielides MA, Li Q, Zeng R et al (2019) Discrimination of pulmonary nodule volume change for low- and high-contrast tasks in a phantom CT study with low-dose protocols. Acad Radiol 26(7):937–948. https://doi.org/10.1016/j.acra.2018.09.006
40. Ohno Y, Yaguchi A, Okazaki T et al (2016) Comparative evaluation of newly developed model-based and commercially available hybrid-type iterative reconstruction methods and filter back projection method in terms of accuracy of computer-aided volumetry (CADv) for low-dose CT protocols in phantom study. Eur J Radiol 85(8):1375–1382. https://doi.org/10.1016/j.ejrad.2016.05.001
41. Doo KW, Kang EY, Yong HS, Woo OH, Lee KY, Oh YW (2014) Accuracy of lung nodule volumetry in low-dose CT with iterative reconstruction: an anthropomorphic thoracic phantom study. Br J Radiol 87(1041):20130644. https://doi.org/10.1259/bjr.20130644
42. Wielpütz MO, Lederlin M, Wroblewski J et al (2013) CT volumetry of artificial pulmonary nodules using an ex vivo lung phantom: Influence of exposure parameters and iterative reconstruction on reproducibility. Eur J Radiol 82(9):1577–1583. https://doi.org/10.1016/j.ejrad.2013.04.035
43. Tateishi U, Tsukagoshi S, Inokawa H, Okumura M, Moriyama N (2008) Fluctuation in measurements of pulmonary nodule under tidal volume ventilation on four-dimensional computed tomography: preliminary results. Eur Radiol 18(10):2132–2139. https://doi.org/10.1007/s00330-008-1002-1
44. Kuhnigk JM, Dicken V, Bornemann L et al (2006) Morphological segmentation and partial volume analysis for volumetry of solid pulmonary lesions in thoracic CT scans. IEEE Trans Med Imaging 25(4):417–434. https://doi.org/10.1109/TMI.2006.871547
45. Ko JP, Rusinek H, Jacobs EL et al (2003) Small pulmonary nodules: volume measurement at chest CT—phantom study. Radiology 228(3):864–870. https://doi.org/10.1148/radiol.2283020059
46. Kinnard LM, Gavrielides MA, Myers KJ, et al (2008) Volume error analysis for lung nodules attached to pulmonary vessels in an anthropomorphic thoracic phantom. In: Proceedings, Medical imaging: computer-aided diagnosis, vol 6915 (2008). https://doi.org/10.1117/12.773039
47. Larke FJ, Kruger RL, Cagnon CH et al (2011) Estimated radiation dose associated with low-dose chest CT of average-size participants in the National Lung Screening Trial. AJR Am J Roentgenol 197:1165–1169. https://doi.org/10.2214/AJR.11.6533
48. Diwakar M, Kumar M (2018) A review on CT image noise and its denoising. Biomed Signal Process Control 42:73–88. https://doi.org/10.1016/j.bspc.2018.01.010
49. Li Q, Gavrielides MA, Sahiner B, Myers KJ, Zeng R, Petrick N (2015) Statistical analysis of lung nodule volume measurements with CT in a large-scale phantom study. Med Phys 42(7):3932–3947. https://doi.org/10.1118/1.4921734
50. Bolte H, Riedel C, Knöß N et al (2007) Computed tomography-based lung nodule volumetry—do optimized reconstructions of routine protocols achieve similar accuracy, reproducibility and interobserver variability to that of special volumetry protocols? Rofo 179(3):276–281. https://doi.org/10.1055/s-2007-962929
51. Coenen A, Honda O, van der Jagt EJ, Tomiyama N (2013) Computer-assisted solid lung nodule 3D volumetry on CT: influence of scan mode and iterative reconstruction: a CT phantom study. Jpn J Radiol 31(10):677–684. https://doi.org/10.1007/s11604-013-0235-3
52. Ravenel JG, Leue WM, Nietert PJ, Miller J, Taylor KK, Silvestri GA (2008) Pulmonary nodule volume: effects of reconstruction parameters on automated measurements—a phantom study. Radiology 247(2):400–408. https://doi.org/10.1148/radiol.2472070868
53. Way TW, Chan HPP, Goodsitt MM et al (2008) Effect of CT scanning parameters on volumetric measurements of pulmonary nodules by 3D active contour segmentation: a phantom study. Phys Med Biol 53(5):1295–1312. https://doi.org/10.1088/0031-9155/53/5/009
54. Honda O, Sumikawa H, Johkoh T et al (2007) Computer-assisted lung nodule volumetry from multi-detector row CT: influence of image reconstruction parameters. Eur J Radiol 62(1):106–113. https://doi.org/10.1016/j.ejrad.2006.11.017

55. Goo JM, Tongdee T, Tongdee R, Yeo K, Hildebolt CF, Bae KT (2005) Volumetric measurement of synthetic lung nodules with multi-detector row CT: effect of various image reconstruction parameters and segmentation thresholds on measurement accuracy. Radiology 235(3):850–856. https://doi.org/10.1148/radiol.2353040737
56. Hwang SH, Oh YW, Ham SY, Kang EY, Lee KY (2015) Effect of the high-pitch mode in dual-source computed tomography on the accuracy of three-dimensional volumetry of solid pulmonary nodules: a phantom study. Korean J Radiol 16(3):641–647. https://doi.org/10.3348/kjr.2015.16.3.641
57. de Jong PA, Leiner T, Lammers JWJ, Gietema HA (2012) Can low-dose unenhanced chest ct be used for follow-up of lung nodules? AJR Am J Roentgenol 199(4):777–780. https://doi.org/10.2214/AJR.11.7577
58. Rampinelli C, Raimondi S, Padrenostro M et al (2010) Pulmonary nodules: contrast-enhanced volumetric variation at different CT scan delays. AJR Am J Roentgenol 195(1):149–154. https://doi.org/10.2214/AJR.09.3212
59. Honda O, Johkoh T, Sumikawa H et al (2007) Pulmonary nodules: 3D volumetric measurement with multidetector CT–effect of intravenous contrast medium. Radiology 245(3):881–887. https://doi.org/10.1148/radiol.2453062116
60. Goodman LR, Gulsun M, Washington L, Nagy PG, Piacsek KL (2006) Inherent variability of CT lung nodule measurements in vivo using semiautomated volumetric measurements. AJR Am J Roentgenol 186(4):989–994. https://doi.org/10.2214/AJR.04.1821
61. Mohamed HFA, Bülbül M, de Jong PA (2016) Pulmonary nodule follow-up: be careful with volumetry between contrast enhanced and unenhanced CT. Ann Transl Med 4(18):346. https://doi.org/10.21037/atm.2016.08.43
62. Petrick N, Kim HJG, Clunie D et al (2014) Comparison of 1D, 2D, and 3D nodule sizing methods by radiologists for spherical and complex nodules on thoracic CT phantom images. Acad Radiol 21(1):30–40. https://doi.org/10.1016/j.acra.2013.09.020
63. Yang R, Yu T, Wang Y, Wang Q (2012) Effects of different reconstruction parameters on CT volumetric measurement of pulmonary nodules. Zhongguo Fei Ai Za Zhi 15(2):72–77. https://doi.org/10.3779/j.issn.1009-3419.2012.02.02
64. Wang Y, de Bock GH, van Klaveren RJ et al (2010) Volumetric measurement of pulmonary nodules at low-dose chest CT: effect of reconstruction setting on measurement variability. Eur Radiol 20(5):1180–1187. https://doi.org/10.1007/s00330-009-1634-9
65. Nietert PJ, Ravenel JG, Leue WM et al (2009) Imprecision in automated volume measurements of pulmonary nodules and its effect on the level of uncertainty in volume doubling time estimation. Chest 135(6):1580–1587. https://doi.org/10.1378/chest.08-2040
66. Larici AR, Storto ML, Torge M et al (2008) Automated volumetry of pulmonary nodules on multidetector CT: influence of slice thickness, reconstruction algorithm and tube current. Preliminary results. Radiol Med 113(1):29–42. https://doi.org/10.1007/s11547-008-0231-3
67. Gavrielides MA, Li Q, Zeng R, et al. (2016) Detectable change of lung nodule volume with CT in a phantom study with high and low signal to background contrast. In: Proceedings, medical imaging 2016: physics of medical imaging, vol 9783; 978329 (2016). https://doi.org/10.1117/12.2217887
68. Eberhard M, Martini K, Euler A, Frauenfelder T (2022) Overlapping reconstructions in thin-section computed tomography. J Thorac Imaging 37(4):W56–W57. https://doi.org/10.1097/RTI.0000000000000631
69. Arndt C, Güttler F, Heinrich A, Bürckenmeyer F, Diamantis I, Teichgräber U (2021) Deep learning CT image reconstruction in clinical practice. Rofo 193(3):252–261. https://doi.org/10.1055/a-1248-2556
70. Kim SK, Kim C, Lee KY et al (2019) Accuracy of model-based iterative reconstruction for CT volumetry of part-solid nodules and solid nodules in comparison with filtered back projection and hybrid iterative reconstruction at various dose settings: an anthropomorphic chest phantom study. Korean J Radiol 20(7):1195–1206. https://doi.org/10.3348/kjr.2018.0893
71. Willemink MJ, Borstlap J, Takx RAP et al (2013) The effects of computed tomography with iterative reconstruction on solid pulmonary nodule volume quantification. PLoS One 8(2):e58053. https://doi.org/10.1371/journal.pone.0058053
72. Willemink MJ, Leiner T, Budde RPJJ et al (2012) Systematic error in lung nodule volumetry: effect of iterative reconstruction versus filtered back projection at different CT parameters. AJR Am J Roentgenol 199(6):1241–1246. https://doi.org/10.2214/AJR.12.8727
73. Kim C, Kwack T, Kim W, Cha J, Yang Z, Yong HS (2022) Accuracy of two deep learning-based reconstruction methods compared with an adaptive statistical iterative reconstruction method for solid and ground-glass nodule volumetry on low-dose and ultra-low-dose chest computed tomography: a phantom study. PLoS One 17(6):e0270122. https://doi.org/10.1371/journal.pone.0270122
74. Ko JP, Chang J, Bomsztyk E, Babb JS, Naidich DP, Rusinek H (2005) Effect of CT image compression on computer-assisted lung nodule volume measurement. Radiology 237(1):83–88. https://doi.org/10.1148/radiol.2371041079
75. dos Santos DP, Friese C, Borggrefe J, Mildenberger P, Mahringer-Kunz A, Kloeckner R (2020) The impact of irreversible image data compression on post-processing algorithms in computed tomography. Diagn Interv Radiol 26(1):22–27. https://doi.org/10.5152/dir.2019.18245120
76. (2011) Usability of irreversible image compression in radiological imaging. A position paper by the European Society of Radiology (ESR). Insights Imaging 2(2):103–115. https://doi.org/10.1007/s13244-011-0071-x.
77. Milanese G, Eberhard M, Martini K, Vittoria De Martini I, Frauenfelder T (2018) Vessel suppressed chest computed tomography for semi-automated volumetric measurements of solid pulmonary nodules. Eur J Radiol 101:97–102. https://doi.org/10.1016/j.ejrad.2018.02.020
78. Xie X, Willemink MJ, de Jong PA et al (2014) Small irregular pulmonary nodules in low-dose CT: observer detection sensitivity and volumetry accuracy. AJR Am J Roentgenol 202(3):W202–W209. https://doi.org/10.2214/AJR.13.10830
79. Xie X, Willemink MJ, Zhao Y et al (2013) Inter- and intrascanner variability of pulmonary nodule volumetry on low-dose 64-row CT: an anthropomorphic phantom study. Br J Radiol 86(1029):20130160. https://doi.org/10.1259/bjr.20130160
80. Marchianò A, Calabrò E, Civelli E et al (2009) Pulmonary nodules: volume repeatability at multidetector CT lung cancer screening. Radiology 251(3):919–925. https://doi.org/10.1148/radiol.2513081313
81. Xie X, Zhao Y, Snijder RA et al (2013) Sensitivity and accuracy of volumetry of pulmonary nodules on low-dose 16- and 64-row multi-detector CT: an anthropomorphic phantom study. Eur Radiol 23(1):139–147. https://doi.org/10.1007/s00330-012-2570-7
82. Marten K, Dullin C, Machann W et al (2009) Comparison of flat-panel-detector-based CT and multidetector-row CT in automated volumetry of pulmonary nodules using an anthropomorphic chest phantom. Br J Radiol 82(981):716–723. https://doi.org/10.1259/bjr/40733553
83. Obenauer S, Dullin C, Heuser M (2007) Flat panel detector-based volumetric computed tomography (fpVCT). Invest Radiol 42(5):291–296. https://doi.org/10.1097/01.rli.0000258663.13199.bf
84. Marten K, Funke M, Engelke C (2004) Flat panel detector-based volumetric CT: prototype evaluation with volumetry of small artificial nodules in a pulmonary phantom. J Thorac Imaging 19(3):156–163. https://doi.org/10.1097/01.rti.0000131591.12777.a8
85. Marten K, Engelke C, Grabbe E, Rummeny EJ (2004) Flat-panel detector-based computed tomography: accuracy of experimental growth rate assessment in pulmonary nodules. Rofo 176(5):752–757. https://doi.org/10.1055/s-2004-813020
86. He C, Liu J, Hu S et al (2020) Accuracy of pulmonary nodule volumetry using noise-optimized virtual monoenergetic image and nonlinear blending image algorithms in dual-energy computed tomography: a phantom study. J Comput Assist Tomogr 44(6):847–851. https://doi.org/10.1097/RCT.0000000000001102
87. Kim J, Lee KH, Kim J, Shin YJ, Lee KW (2019) Improved repeatability of subsolid nodule measurement in low-dose lung screening with monoenergetic images: a phantom study. Quant Imaging Med Surg 9(2):171–179. https://doi.org/10.21037/qims.2018.10.06
88. den Harder AM, Bangert F, van Hamersvelt RW et al (2017) The effects of iodine attenuation on pulmonary nodule volumetry using novel dual-layer computed tomography reconstructions. Eur Radiol 27(12):5244–5251. https://doi.org/10.1007/s00330-017-4938-1

89. Balagurunathan Y, Beers A, Kalpathy-Cramer J et al (2018) Semi-automated pulmonary nodule interval segmentation using the NLST data. Med Phys 45(3):1093–1107. https://doi.org/10.1002/mp.12766
90. Kalpathy-Cramer J, Zhao B, Goldgof D et al (2016) A comparison of lung nodule segmentation algorithms: methods and results from a multi-institutional study. J Digit Imaging 29(4):476–487. https://doi.org/10.1007/s10278-016-9859-z
91. Ashraf H, de Hoop B, Shaker SB et al (2010) Lung nodule volumetry: segmentation algorithms within the same software package cannot be used interchangeably. Eur Radiol 20(8):1878–1885. https://doi.org/10.1007/s00330-010-1749-z
92. Mullally W, Betke M, Wang J, Ko JP (2004) Segmentation of nodules on chest computed tomography for growth assessment. Med Phys 31(4):839–848. https://doi.org/10.1118/1.1656593
93. Rinaldi MF, Bartalena T, Braccaioli L et al (2010) Three-dimensional analysis of pulmonary nodules: variability of semiautomated volume measurements between different versions of the same software. Radiol Med 115(3):403–412. https://doi.org/10.1007/s11547-010-0511-6
94. MacMahon M, Naidich D, Lee KS et al (2017) Incidental pulmonary nodules detected on CT images: from the Fleischner Society 2017. Radiology 284(1):228–243. https://doi.org/10.1148/radiol.2017161659
95. Liang M, Yip R, Tang W et al (2017) Variation in screening CT–detected nodule volumetry as a function of size. AJR Am J Roentgenol 209(2):304–308. https://doi.org/10.2214/AJR.16.17159
96. Wang Y, van Klaveren RJ, van der Zaag-Loonen HJ et al (2008) Effect of nodule characteristics on variability of semiautomated volume measurements in pulmonary nodules detected in a lung cancer screening program. Radiology 248(2):625–631. https://doi.org/10.1148/radiol.2482070957
97. Gietema HA, Wang Y, Xu D et al (2006) Pulmonary nodules detected at lung cancer screening: interobserver variability of semiautomated volume measurements. Radiology 241(1):251–257. https://doi.org/10.1148/radiol.2411050860
98. Boll DT, Gilkeson RC, Fleiter TR, Blackham KA, Duerk JL, Lewin JS (2004) Volumetric assessment of pulmonary nodules with ECG-gated MDCT. AJR Am J Roentgenol 183(5):1217–1223. https://doi.org/10.2214/ajr.183.5.1831217
99. Kostis WJ, Yankelevitz DF, Reeves AP, Fluture SC, Henschke CI (2004) Small pulmonary nodules: reproducibility of three-dimensional volumetric measurement and estimation of time to follow-up CT. Radiology 231(2):446–452. https://doi.org/10.1148/radiol.2312030553
100. Hwang EJ, Goo JM, Kim J et al (2017) Development and validation of a prediction model for measurement variability of lung nodule volumetry in patients with pulmonary metastases. Eur Radiol 27(8):3257–3265. https://doi.org/10.1007/s00330-016-4713-8
101. Smith GT, Rahman AR, Li M et al (2015) Reproducibility of volumetric computed tomography of stable small pulmonary nodules with implications on estimated growth rate and optimal scan interval. PLoS One 10(9):e0138144. https://doi.org/10.1371/journal.pone.0138144
102. Bolte H, Riedel C, Müller-Hülsbeck S et al (2007) Precision of computer-aided volumetry of artificial small solid pulmonary nodules in ex vivo porcine lungs. Br J Radiol 80(954):414–421. https://doi.org/10.1259/bjr/23933268
103. Hwang EJ, Goo JM, Kim HY, Yi J, Kim Y (2021) Optimum diameter threshold for lung nodules at baseline lung cancer screening with low-dose chest CT: exploration of results from the Korean Lung Cancer Screening Project. Eur Radiol 31(9):7202–7212. https://doi.org/10.1007/s00330-021-07827-8
104. Petkovska I, Brown MS, Goldin JG et al (2007) The effect of lung volume on nodule size on CT. Acad Radiol 14(4):476–485. https://doi.org/10.1016/j.acra.2007.01.008
105. Guo XW, Wang Y, Li D et al (2014) The intra-observer variability of volumetric measurement of pulmonary nodules: Comparison of two-dimensional and three-dimensional method. Zhongguo Fei Ai Za Zhi 17(4):336–341. https://doi.org/10.3779/j.issn.1009-3419.2014.04.08
106. Han D, Heuvelmans MA, Vliegenthart R et al (2018) Influence of lung nodule margin on volume- and diameter-based reader variability in CT lung cancer screening. Br J Radiol 91(1090):20170405. https://doi.org/10.1259/bjr.20170405
107. Nair A, Devaraj A, Callister M, Bladwin D (2018) The Fleischner Society 2017 and British Thoracic Society 2015 guidelines for managing pulmonary nodules: keep calm and carry on. Thorax 73:806–812. https://doi.org/10.1136/thoraxjnl-2018-211764
108. Iwano S, Okada T, Koike W et al (2009) Semi-automatic volumetric measurement of lung cancer using multi-detector CT. Acad Radiol 16(10):1179–1186. https://doi.org/10.1016/j.acra.2009.04.007
109. Talwar A, Willaime JMY, Pickup LC et al (2018) Pulmonary nodules: assessing the imaging biomarkers of malignancy in a "coffee-break." Eur J Radiol 101:82–86. https://doi.org/10.1016/j.ejrad.2018.02.004
110. Volterrani L, Mazzei MA, Scialpi M et al (2006) Three–dimensional analysis of pulmonary nodules by MSCT with advanced lung analysis (ALA1) software. Radiol Med 111(3):343–354. https://doi.org/10.1007/s11547-006-0033-4
111. Zhao YR, van Ooijen PMA, Dorrius MD et al (2014) Comparison of three software systems for semi-automatic volumetry of pulmonary nodules on baseline and follow-up CT examinations. Acta Radiol 55(6):691–698. https://doi.org/10.1177/0284185113508177
112. Ko JP, Berman EJ, Kaur M et al (2012) Pulmonary nodules: growth rate assessment in patients by using serial CT and three-dimensional volumetry. Radiology 262(2):662–671. https://doi.org/10.1148/radiol.11100878
113. Pinto EG, Penha D, Hochhegger B et al (2022) The impact of cardio-pulmonary hemodynamic factors in volumetry for pulmonary nodule management. BMC Med Imaging 22(1):49. https://doi.org/10.1186/s12880-022-00774-w
114. Penha D, Pinto EG, Hochhegger B et al (2021) The impact of lung parenchyma attenuation on nodule volumetry in lung cancer screening. Insights Imaging 12(1):84. https://doi.org/10.1186/s13244-021-01027-0
115. Biederer J, Dinkel J, Bolte H et al (2007) Respiratory-gated helical computed tomography of lung: reproducibility of small volumes in an ex vivo model. Int J Radiat Oncol Biol Phys 69(5):1642–1649. https://doi.org/10.1016/j.ijrobp.2007.08.031
116. Goo JM, Kim KG, Gierada DS, Castro M, Bae KT (2006) Volumetric measurements of lung nodules with multi-detector row CT: effect of changes in lung volume. Korean J Radiol 7(4):243–248. https://doi.org/10.3348/kjr.2006.7.4.243
117. Picozzi G, Diciotti S, Falchini M et al (2006) Operator-dependent reproducibility of size measurements of small phantoms and lung nodules examined with low-dose thin-section computed tomography. Invest Radiol 41(11):831–839. https://doi.org/10.1097/01.rli.0000242837.11436.6e
118. Bolte H, Riedel C, Jahnke T et al (2006) Reproducibility of computer-aided volumetry of artificial small pulmonary nodules in ex vivo porcine lungs. Invest Radiol 41(1):28–35. https://doi.org/10.1097/01.rli.0000191366.05586.4d
119. Bolte H, Jahnke T, Schäfer FKW et al (2007) Interobserver-variability of lung nodule volumetry considering different segmentation algorithms and observer training levels. Eur J Radiol 64(2):285–295. https://doi.org/10.1016/j.ejrad.2007.02.031
120. Agnes SA, Anitha J (2022) Efficient multiscale fully convolutional UNet model for segmentation of 3D lung nodule from CT image. J Med Imaging (Bellingham). 9(5):052402. https://doi.org/10.1117/1.JMI.9.5.052402
121. Bhattacharyya D, Rao NT, Joshua ESN, Hu YC (2022) A bi-directional deep learning architecture for lung nodule semantic segmentation. Vis Comput 8:1–17. https://doi.org/10.1007/s00371-022-02657-1
122. Lu D, Chu J, Zhao R, Zhang Y, Tian G (2022) A novel deep learning network and its application for pulmonary nodule segmentation. Comput Intell Neurosci 17(2022):7124902. https://doi.org/10.1155/2022/7124902
123. Kido S, Kidera S, Hirano Y et al (2022) Segmentation of lung nodules on CT images using a nested three-dimensional fully connected convolutional network. Front Artif Intell 17(5):782225. https://doi.org/10.3389/frai.2022.782225
124. Song J, Huang SC, Kelly B et al (2022) Automatic lung nodule segmentation and intra-nodular heterogeneity image generation. IEEE J Biomed Health Inform 26(6):2570–2581. https://doi.org/10.1109/JBHI.2021.3135647
125. Lu Z, Long F, He X (2022) Classification and segmentation algorithm in benign and malignant pulmonary nodules under different CT reconstruction. Comput Math Methods Med 21(2022):3490463. https://doi.org/10.1155/2022/3490463

126. Bianconi F, Fravolini ML, Pizzoli S et al (2021) Comparative evaluation of conventional and deep learning methods for semi-automated segmentation of pulmonary nodules on CT. Quant Imaging Med Surg 11(7):3286–3305. https://doi.org/10.21037/qims-20-1356
127. Cui Y, Arimura H, Nakano R, Yoshitake T, Shioyama Y, Yabbuchi H (2021) Automated approach for segmenting gross tumor volumes for lung cancer stereotactic body radiation therapy using CT-based dense V-networks. J Radiat Res 62(2):346–355. https://doi.org/10.1093/jrr/rraa132
128. Dutande P, Baid U, Talbar S (2021) LNCDS: A 2D–3D cascaded CNN approach for lung nodule classification, detection and segmentation. Biomed Signal Process Control 67(6):102527. https://doi.org/10.1016/j.bspc.2021.102527
129. Yu H, Li J, Zhang L, Cao Y, Yu X, Sun J (2021) Design of lung nodules segmentation and recognition algorithm based on deep learning. BMC Bioinform 22(Suppl 5):314. https://doi.org/10.1186/s12859-021-04234-0
130. Jain S, Indora S, Atal DK (2021) Lung nodule segmentation using salp shuffled shepherd optimization algorithm-based generative adversarial network. Comput Biol Med 137:104811. https://doi.org/10.1016/j.compbiomed.2021.104811
131. Meng XL, Xing ZJ, Lu S (2021) A deep learning-based lung nodule density classification and segmentation method and its effectiveness under different CT reconstruction algorithms. Zhonghua Yi Xue Za Zhi 101(7):476–480. https://doi.org/10.3760/cma.j.cn112137-20201123-03171
132. Wang K, Zhang X, Zhang X, Huang S, Li J, HuangFu L (2021) Multi-granularity scale-aware networks for hard pixels segmentation of pulmonary nodules. Biomed Signal Process Control 69:102890. https://doi.org/10.1016/j.bspc.2021.102890
133. Wang Y, Zhou C, Chan H-P, Hadjiiski L, Chughtai A, Kazerooni E (2022) Hybrid U-Net-based deep learning model for volume segmentation of lung nodules in CT images. Med Phys 49(11):7287–7302. https://doi.org/10.1002/mp.15810
134. Zhang X, Liu X, Zhang B et al (2021) Accurate segmentation for different types of lung nodules on CT images using improved U-Net convolutional network. Medicine (Baltimore) 100(40):e27491. https://doi.org/10.1097/MD.0000000000027491
135. Dong X, Xu S, Liu Y et al (2020) Multi-view secondary input collaborative deep learning for lung nodule 3D segmentation. Cancer Imaging 20(1):53. https://doi.org/10.1186/s40644-020-00331-0
136. Sathish R, Sathish R, Sethuraman R, Sheet D (2020) Lung segmentation and nodule detection in computed tomography scan using a convolutional neural network trained adversarially using turing test loss. Annu Int Conf IEEE Eng Med Biol Soc 2020:1331–1334. https://doi.org/10.1109/EMBC44109.2020.9175649
137. Usman M, Lee B-D, Byon S-S, Kim S-H, Lee B-I, Shin Y-G (2020) Volumetric lung nodule segmentation using adaptive ROI with multi-view residual learning. Sci Rep 10(1):12839. https://doi.org/10.1038/s41598-020-69817-y
138. Wu W, Gao L, Duan H, Huang G, Ye X, Nie S (2020) Segmentation of pulmonary nodules in CT images based on 3D-UNET combined with three-dimensional conditional random field optimization. Med Phys 47(9):4054–4063. https://doi.org/10.1002/mp.14248
139. Aresta G, Jacobs C, Araújo T et al (2019) iW-Net: an automatic and minimalistic interactive lung nodule segmentation deep network. Sci Rep 9(1):11591. https://doi.org/10.1038/s41598-019-48004-8
140. Liu H, Cao H, Song E et al (2019) A cascaded dual-pathway residual network for lung nodule segmentation in CT images. Phys Med 63:112–121. https://doi.org/10.1016/j.ejmp.2019.06.003
141. Chung H, Ko H, Jeon SJ, Yoon K-H, Lee J (2018) Automatic lung segmentation with juxta-pleural nodule identification using active contour model and Bayesian approach. IEEE J Transl Eng Health Med 18(6):1800513. https://doi.org/10.1109/JTEHM.2018.2837901
142. Kidera S, Kido S, Hirano Y, Mabu S, Tanaka N (2018) (2018) Segmentation of lung nodules on MDCT images by using 3D Conv-DeconvNet. Int J CARS 13(Suppl 1):1–273. https://doi.org/10.1007/s11548-018-1766-y
143. Qin Y, Zheng H, Huang X, Yang J, Zhu Y-M (2019) Pulmonary nodule segmentation with CT sample synthesis using adversarial networks. Med Phys 46(3):1218–1229. https://doi.org/10.1002/mp.13349
144. Shakir H, Rasool Khan TM, Rasheed H (2018) 3-D segmentation of lung nodules using hybrid level sets. Comput Biol Med 1(96):214–226. https://doi.org/10.1016/j.compbiomed.2018.03.015
145. Feng X, Yang J, Laine AF, Angelini ED (2017) Discriminative localization in CNNs for weakly-supervised segmentation of pulmonary nodules. Med Image Comput Comput Assist Interv 10435:568–576. https://doi.org/10.1007/978-3-319-66179-7_65
146. Wang S, Zhou M, Gevaert O et al (2017) A multi-view deep convolutional neural networks for lung nodule segmentation. Annu Int Conf IEEE Eng Med Biol Soc 2017:1752–1755. https://doi.org/10.1109/EMBC.2017.8037182
147. Wang S, Zhou M, Liu Z et al (2017) Central focused convolutional neural networks: developing a data-driven model for lung nodule segmentation. Med Image Anal 40:172–183. https://doi.org/10.1016/j.media.2017.06.014
148. Li B, Chen Q, Peng G et al (2016) Segmentation of pulmonary nodules using adaptive local region energy with probability density function-based similarity distance and multi-features clustering. Biomed Eng Online 15(1):49. https://doi.org/10.1186/s12938-016-0164-3
149. Lassen BC, Jacobs C, Kuhnigk JM, van Ginneken B, van Rikxoort EM (2015) Robust semi-automatic segmentation of pulmonary subsolid nodules in chest computed tomography scans. Phys Med Biol 60(3):1307–1323. https://doi.org/10.1088/0031-9155/60/3/1307
150. Tan Y, Schwartz LH, Zhao B (2013) Segmentation of lung lesions on CT scans using watershed, active contours, and Markov random field. Med Phys 40(4):043502. https://doi.org/10.1118/1.4793409
151. Reeves AP, Chan AB, Yankelevitz DF, Henschke CI, Kressler B, Kostis WJ (2006) On measuring the change in size of pulmonary nodules. IEEE Trans Med Imaging 25(4):435–450. https://doi.org/10.1109/TMI.2006.871548
152. Yankelevitz DF, Reeves AP, Kostis WJ, Zhao B, Henschke CI (2000) Small pulmonary nodules: volumetrically determined growth rates based on CT evaluation. Radiology 217(1):251–256. https://doi.org/10.1148/radiology.217.1.r00oc33251
153. Hammer MM, Byrne SC (2022) Cancer risk in nodules detected at follow-up lung cancer screening CT. AJR Am J Roentgenol 218(4):634–641. https://doi.org/10.2214/AJR.21.26927
154. Silva M, Milanese G, Sestini S et al (2021) Lung cancer screening by nodule volume in Lung-RADS v1.1: negative baseline CT yields potential for increased screening interval. Eur Radiol 31(4):1956–1968. https://doi.org/10.1007/s00330-020-07275-w
155. Li K, Yip R, Avila R, Henschke CI, Yankelevitz DF (2017) Size and growth assessment of pulmonary nodules: consequences of the rounding. J Thorac Oncol 12(4):657–662. https://doi.org/10.1016/j.jtho.2016.12.010
156. Li M, Han R, Song W et al (2016) Three dimensional volumetric analysis of solid pulmonary nodules on chest CT: cancer risk assessment. Zhongguo Fei Ai Za Zhi 19(5):279–285. https://doi.org/10.3779/j.issn.1009-3419.2016.05.05
157. Horeweg N, Scholten ET, de Jong PA et al (2014) Detection of lung cancer through low-dose CT screening (NELSON): a prespecified analysis of screening test performance and interval cancers. Lancet Oncol 15(12):1342–1350. https://doi.org/10.1016/S1470-2045(14)70387-0
158. Shin KE, Lee KS, Yi CA, Chung MJ, Shin MH, Choi YH (2014) Subcentimeter lung nodules stable for 2 years at LDCT: Long-term follow-up using volumetry. Respirology 19(6):921–928. https://doi.org/10.1111/resp.12337
159. Horeweg N, van der Aalst CM, Vliegenthart R et al (2013) Volumetric computed tomography screening for lung cancer: three rounds of the NELSON trial. Eur Respir J 42(6):1659–1667. https://doi.org/10.1183/09031936.00197712
160. van Klaveren RJ, Oudkerk M, Prokop M et al (2009) Management of lung nodules detected by volume CT scanning. N Engl J Med 361(23):2221–2229. https://doi.org/10.1056/NEJMoa0906085
161. Revel MP, Merlin A, Peyrard S et al (2006) Software volumetric evaluation of doubling times for differentiating benign versus malignant pulmonary nodules. AJR Am J Roentgenol 187(1):135–142. https://doi.org/10.2214/AJR.05.1228
162. Ahn Y, Lee SM, Kim MS et al (2022) Volume doubling times of pulmonary metastases in patients with bone and soft-tissue sarcomas: associations with subsequent new metastases and survival after

metastasectomy. AJR Am J Roentgenol 218(4):624–632. https://doi.org/10.2214/AJR.21.26859
163. Setojima Y, Shimada Y, Tanaka T et al (2020) Prognostic impact of solid-part tumour volume doubling time in patients with radiological part-solid or solid lung cancer. Eur J Cardiothorac Surg 57(4):763–770. https://doi.org/10.1093/ejcts/ezz305
164. Kamiya S, Iwano S, Umakoshi H et al (2018) Computer-aided volumetry of part-solid lung cancers by using CT: solid component size predicts prognosis. Radiology 287(3):1030–1040. https://doi.org/10.1148/radiol.2018172319
165. Li Q, Gu Y-F, Fan L, Li Q-C, Xiao Y, Liu S-Y (2018) Effect of CT window settings on size measurements of the solid component in subsolid nodules: evaluation of prediction efficacy of the degree of pathological malignancy in lung adenocarcinoma. Br J Radiol 91(1088):20180251. https://doi.org/10.1259/bjr.20180251
166. Yanagawa M, Tanaka Y, Leung AN et al (2014) Prognostic importance of volumetric measurements in stage i lung adenocarcinoma. Radiology 272(2):557–567. https://doi.org/10.1148/radiol.14131903
167. Vogel MN, Schmücker S, Maksimovic O, Hartmann J, Claussen CD, Horger M (2012) Reduction in growth threshold for pulmonary metastases: an opportunity for volumetry and its impact on treatment decisions. Br J Radiol 85(1015):959–964. https://doi.org/10.1259/bjr/87835487
168. Solomon J, Ebner L, Christe A et al (2021) Minimum perceivable size difference: how well can radiologists visually detect a change in lung nodule size from CT images? Eur Radiol 31(4):1947–1955. https://doi.org/10.1007/s00330-020-07326-2
169. Mets OM, Chung K, Zanen P et al (2018) In vivo growth of 60 non-screening detected lung cancers: a computed tomography study. Eur Respir J 51(4):1702183. https://doi.org/10.1183/13993003.02183-2017
170. Sun Q, Huang Y, Zhao SJ et al (2018) The volume and mass growth of persisted pulmonary nodules detected in low-dose CT screening and its influence factors. Zhonghua Zhong Liu Za Zhi 40(4):274–279. https://doi.org/10.3760/cma.j.issn.0253-3766.2018.04.007
171. Heuvelmans MA, Vliegenthart R, de Koning HJ et al (2017) Quantification of growth patterns of screen-detected lung cancers: the NELSON study. Lung Cancer 108:48–54. https://doi.org/10.1016/j.lungcan.2017.02.021
172. Henschke CI, Yankelevitz DF, Yip R et al (2012) Lung cancers diagnosed at annual CT screening: volume doubling times. Radiology 263(2):578–583. https://doi.org/10.1148/radiol.12102489
173. Kim EY, Lee JI, Sung YM et al (2012) Pulmonary metastases from colorectal cancer: imaging findings and growth rates at follow-up CT. Clin Imaging 36(1):14–18. https://doi.org/10.1016/j.clinimag.2011.04.018
174. Tanimoto D, Ito K, Tamada T et al (2012) Serial 3-dimensional volumetric computed tomography evaluation of lung cancer growth rate in patients with chronic obstructive pulmonary disease findings. J Comput Assist Tomogr 36(2):181–186. https://doi.org/10.1097/RCT.0b013e3182483c32
175. Pauls S, Kürschner C, Dharaiya E et al (2008) Comparison of manual and automated size measurements of lung metastases on MDCT images: Potential influence on therapeutic decisions. Eur J Radiol 66(1):19–26. https://doi.org/10.1016/j.ejrad.2007.05.022
176. Shi J, Ye Y, Zhu D, Su L, Huang Y, Huang J (2021) Comparative analysis of pulmonary nodules segmentation using multiscale residual U-Net and fuzzy C-means clustering. Comput Methods Programs Biomed 209:106332. https://doi.org/10.1016/j.cmpb.2021.106332
177. Kakinuma R, Muramatsu Y, Yamamichi J, Gomi S, Oubel E, Moriyama N (2018) Evaluation of the 95% limits of agreement of the volumes of 5-year clinically stable solid nodules for the development of a follow-up system for indeterminate solid nodules in CT lung cancer screening. J Thorac Dis 10(1):175–189. https://doi.org/10.21037/jtd.2017.11.142
178. Christe A, Bronnimann A, Vock P, Bronnimann A, Vock P (2014) Volumetric analysis of lung nodules in computed tomography (CT): comparison of two different segmentation algorithm softwares and two different reconstruction filters on automated volume calculation. Acta Radiol 55(1):54–61. https://doi.org/10.1177/0284185113492454
179. Koike W, Iwano S, Matsuo K, Kitano M, Kawakami K, Naganawa S (2014) Doubling time calculations for lung cancer by three-dimensional computer-aided volumetry: effects of inter-observer differences and nodule characteristics. J Med Imaging Radiat Oncol 58(1):82–88. https://doi.org/10.1111/1754-9485.12128
180. Scholten ETh, de Hoop B, Jacobs C et al (2013) Semi-automatic quantification of subsolid pulmonary nodules: comparison with manual measurements. PLoS One 8(11):e80249. https://doi.org/10.1371/journal.pone.0080249
181. Dehmeshki J, Amin H, Valdivieso M, Ye X (2008) Segmentation of pulmonary nodules in thoracic CT scans: a region growing approach. IEEE Trans Med Imaging 27(4):467–480. https://doi.org/10.1109/TMI.2007.907555
182. Revel MP, Lefort C, Bissery A et al (2004) Pulmonary nodules: preliminary experience with three-dimensional evaluation. Radiology 231(2):459–466. https://doi.org/10.1148/radiol.2312030241
183. Heuvelmans MA, Walter JE, Vliegenthart R et al (2018) Disagreement of diameter and volume measurements for pulmonary nodule size estimation in CT lung cancer screening. Thorax 73(8):779–781. https://doi.org/10.1136/thoraxjnl-2017-210770
184. Shen S, Bui AAT, Cong J, Hsu W (2015) An automated lung segmentation approach using bidirectional chain codes to improve nodule detection accuracy. Comput Biol Med 57:139–149. https://doi.org/10.1016/j.compbiomed.2014.12.008

Publisher's Note

10. Full list of the summaries of all original research studies included in the systematic review and attempted meta-analysis

Authors (doi)	(n)	population	CT protocol	statistical methodology	outcome	Influencing factor understudy	Effect	statistical significance		interactions
2022										
Agnes et al. (10.1117/1.JMI.9.5.052402)	1010	CT data from open access *in vivo* databases (LIDC)	SDCT	Similarity analysis	Dice coefficient	segmentation algorithm (UNet vs GAP CNN)	↑			
Bartlett et al. (10.1007/s00330-021-08302-0)	100	Patients with small (30 - 150mm³) non-metastatic pulmonary nodules	128CT	Bland-Altman (mm3, %)	Interscan variability		[-14.2mm³, 12mm³] [-16.4%, 14.6%]			
Debnath et al. (10.1007/s00371-022-02657-1)	888	CT data from open access *in vivo* databases (LUNA-16)	SDCT	Similarity analysis	Dice coefficient	segmentation algorithm (MF-3D UNet vs custom UNets)	↑			
Lin et al. (10.1155/2022/7124902)	1018	CT data from open access *in vivo* databases (LIDC-IDRI)	SDCT	Similarity analysis	Dice coefficient, Precision, recall	segmentation algorithm (Dense-UNet vs FCN32s, SegNet, UNet, BN-UNet)	↑			
Kido et al. (10.3389/frai.2022.782225)	332	Local patient database	SDCT	Similarity analysis	Dice coefficient, Intersection-Over-Union	segmentation algorithm (3-D fully connected CNN vs 3D U-Net, 3D SegNet, watershed, graphcut)	↑			
Pinto et al. (10.1097/MD.0000000000030332)	195	Patients with pulmonary nodules detected on CCTA	CCTA	Bland-Altman (%)	Interscan variability	Cardiac phase (systole, diastole) Inter-software Inter-observer	[-47.0%, 52.3%] [-50.2%, 68.2%] [-14.5%, 27.8%]			
Pinto et al. (10.1186/s12880-022-00774-w)	195	Patients with pulmonary nodules detected on CCTA	CCTA	Multiple linear regression	volume	cardiac phase (systole, diastole) vascular distance from MPA to nodule MPA caliber change from systole to diastole location adequacy of segmentation (inadequate, adequate)	 ↓ ↑ ↑ (lower third, posterior third) ↓		N Y Y Y Y	
Song et al. (10.1109/JBHI.2021.3135647)	1018 91	CT data from open access *in vivo* databases (LIDC) Local patient dataset	SDCT	Similarity analysis	Dice coefficient	segmentation algorithm(LNHG vs UNet, nnUNet, L-MSE, L-VGG) (solid LNHG vs UNet) (juxta-pleural LNHG vs UNet) (juxta-vascular LNHG vs UNet) (solid LNHG vs others) (juxta-pleural LNHG vs others) (juxta-vascular LNHG vs others)	 ↓ ↓ ↓ ↑ ↑ ↑			
Werner et al. (10.1055/a-1656-9834)	54	Patients with part-solid pulmonary nodules	SDCT	Bland-Altman (%)	intraobserver variability interobserver variability interscan variability	kernel (smooth, hard)	solid component [-70%,49%] whole PSN [-111%,31%] solid component [-16%,16%] whole PSN [-102%,65%] solid component [-45.0%,39%] whole PSN [-21.0%,46%]			
Lin et al (10.1155/2022/3490463)	55	Local patient dataset	SDCT	Similarity analysis	Dice coefficient	kernel (lung, mediastinal, bone)			N	
2021										
Bianconi et al. (10.21037/qims-20-1356)	111 100	Local *in vivo* database PET/CT CT data from open access *in vivo* databases (LIDC-IDRI)	SDCT	Similarity analysis	Dice coefficient	segmentation algorithm (DL-based vs non-DL based)				
Cui et al. (10.1093/jrr/rraa132)	192	NSCLC patients	SDCT (DVN)	Similarity analysis	Dice coefficient	density (solid, part-solid, GGO)	↓			
Dutande et al. (10.1016/j.bspc.2021.102527)	1010 294 113	CT data from open access *in vivo* databases (LIDC, LNDb, ILCID)	SDCT	Similarity analysis	Dice coefficient	segmentation algorithm (SquExUNet vs 3D NodNet)	↑			
Yu et al. (10.1186/s12859-021-04234-0)	1010	CT data from open access *in vivo* databases (LIDC)	SDCT	Similarity analysis	Dice coefficient	segmentation algorithm (3D-ResNet, 3D-UNet)	↑			
Jain et al. (10.1016/j.compbiomed.2021.104811)	100	CT data from open access *in vivo* databases (LIDC-IDRI)	SDCT	Similarity analysis	Dice coefficient, Jaccard index	segmentation algorithm (SSSOA-based GAN vs kernel-based Bayesian clustering, SVM+K-nearest, FCM, region-based segmentation, DDRN, CoLe-CNN)	↑			
Meng et al. (10.3760/cma.j.cn112137-20201123-03171)	1018	CT data from open access *in vivo* databases (LIDC-IDRI)	SDCT	Similarity analysis	Dice coefficient	kernel (lung, mediastinal, bone)			N	
Kim et al. (10.1371/journal.pone.0270122)	4+3	solid and ground-glass artificial nodules	LD-CT vs ULD-CT	RM-ANOVA	Accuracy (APE)	reconstruction algorithm (DL-based: Truefidelity, ClariCT.AI, non-DL-based: ASiR) (for all density, size and radiation exposure)	↑(↓)		Y	
Shi et al. (10.1016/j.cmpb.2021.106332)	58	Local patient dataset	SDCT	Similarity analysis	Accuracy	segmentation algorithm (multiscale residual UNet vs fuzzy C-means clustering)	↑			
Wang et al. (10.1016/j.bspc.2021.102890)	1010	CT data from open access *in vivo* databases (LIDC)	SDCT	Similarity analysis	Dice coefficient	segmentation algorithm (MGSANet vs SegNet, FCN8s, UNet, UNet++)	↑			
Wang et al. (10.1002/mp.15810)	847	CT data from open access *in vivo* databases (LIDC-IDRI)	SDCT	Similarity analysis	Dice coefficient, Jaccard index	segmentation algorithm (H-DL vs deep Unet, shallow UNet)	↑			
Zhang et al. (10.1097/MD.0000000000027491)	1018	CT data from open access *in vivo* databases (LIDC-IDRI)	SDCT	Similarity analysis	Dice coefficient, Jaccard index	segmentation algorithm (UNet with BN + α-hull vs UNet with BN, UNet with α-hull	↑			
2020										
Dong et al. (10.1186/s40644-020-00331-0)	874	CT data from open access *in vivo* databases (LIDC-IDRI)	SDCT	Similarity analysis	DICE, ASD, HSD, accuracy, sensitivity	segmentation algorithm(MV-SIR vs MV-CNN, MV-I-CNN)	↑			
He et al. (10.1097/RCT.0000000000001102)	10	5 solid + 5 GGO synthetic nodules	dual-energy CT	Wilcoxon signed-rank	Accuracy (APE)	SECT vs DECT for same radiation dose exposure	↑(↓)		Y	
Lee et al. (10.1097/MD.0000000000020543)	8	spherical synthetic nodules (diameter 5, 8, 10, 12m; attenuation +100HU, -630HU)	256CT	Wilcoxon signed-rank Generalized estimating equations (GEE)	Accuracy (APE)	helical vs axial scan reconstruction algorithm - FBP vs ASIR (30%, 50%) tube current (10, 20, 30, 100mAs) density nodule size	 ↑(↓) ↑(↓)		N N N Y Y	
Penna et al. (10.1186/s13244-021-01027-0)	1265	LCS participants	LDCT	Binary logistic regression	Adequate segmentation	attenuation of adjacent lung parenchyma	↓		Y	
Rakshith et al (10.1109/EMBC44109.2020.9175649)	888	CT data from open access *in vivo* databases (LUNA-16)	SDCT	Similarity analysis	Dice coefficient	segmentation algorithm (segmentation network of 2D-CNNs vs UNet, R2UNet, SUMNet)	↑			
Usman et al. (10.1038/s41598-020-69817-y)	1010	CT data from open access *in vivo* databases (LIDC-IDRI)	SDCT	Similarity analysis	Dice coefficient, HD, sensitivity, PPV	segmentation algorithm (A-ROI with multi-view deep residual learning vs constant ROI with multi-view deep residual learning)	↑			
Wu et al. (10.1002/mp.14248)	936	CT data from open access *in vivo* databases (LIDC-IDRI)	SDCT	Similarity analysis	Dice coefficient	segmentation algorithm (3D-UNet + training 3D-CRF vs 2D-UNet, 2D-UNet-CRF, 3D-UNet, 3D-UNet-CRF)	↑			
2019										
Aresta et al. (10.1038/s41598-019-48004-8)	1012	CT data from open access *in vivo* databases (LIDC-IDRI)	SDCT	Similarity analysis	Intersection-Over-Union	Segmentation algorithm (1W-Net vs 3D-UNet)	↑			
Eberhard et al. (10.21037/jtd.2019.08.12)	66	synthetic nodules (diameter: 4 - 10mm; density: 20-80HU)	SDCT, LDCT, ULDCT, DECT	ANOVA	Accuracy (APE)	radiation dose exposure (1/8th, 1/20th, 1/70th of standard dose) reconstruction algorithm (FBP, ADMIRE) nodule diameter density	↓(↑) (at 1/70th) ↓(↑) (ADMIRE at strength level 5) ↑(↓) ≠		Y Y Y Y	
Kim et al. (10.3348/kjr.2018.0893)	8	synthetic nodules (diameter: 3, 5, 7, 9mm; density: 50HU); PSN (outer GGO diameter: 20mm; density: -650HU; inner solid portion similar to solid nodule)	128CT	Repeated-measures ANOVA	Accuracy (APE)	radiation dose exposure (120/100, 120/50, 120/20, 120/10, 80kVp/10mAs) reconstruction algorithm (FBP, HIR, MBIR) density	↓(↑) ↑(↓) (MBIR) ↑(↓)		Y Y Y	
Lin et al. (10.1016/j.ejmp.2019.06.003)	986	CT data from open access *in vivo* databases (LIDC-IDRI)	SDCT	Similarity analysis	Dice coefficient, ASD, sensitivity, PPV	segmentation algorithm (CDP-ResNet + IWS, CDP-ResNet + RS, CDP-ResNet + WS)	↑			
Liu et al. (10.1097/RCT.0000000000000908)	11	6 solid + 5 GGO synthetic nodules	256CT	mixed analysis of variance on aligned ranks	Accuracy (APE)	tube voltage (80, 100, 120kV) tube current (10 to 30 mAs) density	↑(↓) ↑(↓)		Y N Y	density * tube voltage
2018										
Balagurunathan et al. (10.1002/mp.12766)	100	LCS participants	LDCT	Concordance correlation coefficient	volume volume variability	tube current (10, 20, 30, 100mAs) density	 ↑(↓)		N Y	
Chung et al. (10.1109/JTEHM.2018.2837901)	84	Local patient dataset	SDCT	Similarity analysis	Dice coefficient, MHD, sensitivity, specificity and accuracy	segmentation algorithm (active contour model and baysian approach vs Chan-vese, normalized and modified Chan-Vese, snake algorithm)	↑			
Gavrielides et al. (10.1016/j.acra.2018.09.006)	8	synthetic nodules (diameter: 5 - 5.75, 8 - 8.75mm) phantom (background difference: 1000, 50-100HU)	16CT	AUROC	percent error, CV	nodule to background contrast (low, high)	↓		Y	
Jin et al. (10.21037/qims.2018.06.05)	82	Patients with cancer	LDCT, SDCT, 256CT	paired sample t-test	volume	nodule size	↑(↓) (part solid, calcified)		Y N	
Kakinuma et al. (10.21037/jtd.2017.11.142)	226	Patients with stable nodules	16CT	Bland-Altman (%)	intraobserver variability interobserver variability		[-33.5%,26.5%] [-17.1%,67.9%]			
Kidera et al. (10.1007/s11548-018-1766-y)	330	Local patient dataset	SDCT	Similarity analysis	Dice coefficient, Jaccard index	segmentation algorithm (Conv-DeconvNet vs watershed)	↑			
Kim et al.	15120			RC	Repeatability	single energy vs monoenergetic images	↓		Y	

(10.21037/qims.2018.10.06)		simulated virtual sub-solid nodules (diameter: 8, 10, 12mm; contrast to background: +100HU) + (diameter: 6, 8, 10mm; contrast to background: 270HU)	dual-layer CT 64CT			tube current (30, 15, 10mAs) reconstruction algorithm (FBP, IR)	↑ (less significant with IR) ↓	Y Y	
Milanese et al. (10.1016/j.ejrad.2018.02.020)	65	Patients	LDCT	Bland-Altman (mm3)	volume	post-processing (normal, vessel-suppression)		N	
Paks et al. (10.1097/MD.0000000000012019)	176 97 68 102	Patients under LDCT surveillance for solid pulmonary nodules >2mm subset of indeterminate nodules BMI <25 BMI ≥25	LDCT vs ULDCT 128CT	Bland-Altman (%)	interscan variability	radiation dose exposure (LDCT vs ULDCT)	[-18.0%,22.7%] [-12.7%,21.9%] [-17.5%,23.6%] [-18.3%,20.8%]		
Qin et al. (10.1002/mp.13349)	1018	CT data from open access *in vivo* databases (LIDC-IDRI)	SDCT	Similarity analysis	Dice coefficient, PPV, Accuracy	segmentation algorithm (3D-CNN vs SegNMaps, SegNEdgem Seg-NLBP, Seg-Nsynthetic)	↑		
Shakir et al. (10.1016/j.compbiomed.2018.03.015)	72	CT data from open access *in vivo* databases (LIDC) and phantom databases (CUMC, FDA)	CT	Bland-Altman (mm3)	volume	segmentation method	hybrid method [-0.1,0.3] Gao et al. method [-0.8,1.1] Chan Vese method [-0.1,0.7]		
2017									
Cohen et al. (10.1007/s00330-016-4716-5)	73	Patients with part-solid pulmonary nodules	SDCT	Bland-Altman	intraobserver variability	reconstruction algorithm (FBP, MBIR)	FBP; solid component [-81.3%,90.8%] FBP, whole SSN [-40.1%,42.6%] MBIR, solid component [-85.8%,74%] MBIR, whole SSN [-35.6%,36.2%]	N	
					interobserver variability	reconstruction algorithm (FBP, MBIR)	FBP; solid component [-126.2%,129.4%] FBP, whole SSN [-32.6%,51.7%] MBIR, solid component [-142.2%,116.8%] MBIR, whole SSN [-36.3%,47.3%]	N	
					interscan variability	reconstruction algorithm (FBP, MBIR)	solid component [-51.9%,64.6%] whole SSN [-20.9%,27.3%]	Y	
Feng et al. (10.1007/978-3-319-66179-7_65)	1010	CT data from open access *in vivo* databases (LIDC)	SDCT	Similarity analysis	Dice coefficient	segmentation algorithm (UNet vs GAP CNN)	↑		
Gavrielides et al. (10.21037/qims.2017.12.07)	12	synthetic nodules (diameter: 5, 10mm; density: -800, -630, -10HU; shape: spherical, spiculated)	LDCT	ANOVA	Accuracy (APE)	density (-800, -630, -10HU) shape (spherical, spiculated) reconstruction algorithm (FBP, AIDR 3D, FIRST)	↑(↓) ↓(↑) ≠	Y Y Y	nodule size * density, nodule size * shape
					Repeatability coefficient (RC%)	radiation dose exposure	↓ (5mm)	Y	
den Harder et al. (10.1007/s00330-017-4938-1)	63	Consecutive series of patients with non-calcified solid nodules	dual-layer CT	Bland-Altman (mm3, %)	volume	VNC (40, 70, 100, 130, 160, 200 kev) nodule size (≤200mm3, >200mm3)	↓ (except at 70kev)	Y N	
Han et al. (10.1259/bjr.20170405)	100	LCS participants	LDCT	Bland-Altman (%)	interobserver variability		all [-23.7%,23.7%] smooth [-21.4%,21.4%] lobulated [-18.1%,18.1%] spiculated [-28.2%,28.2%] irregular [-27.0%,27.0%]		
Liang et al. (10.2214/AJR.16.17159)	171	117 LCS participants with stable nodules >2 years	64CT	Levene test	volume variance	software nodule size (<4, 4-5, 6-9, >10mm)	≠ ↓	Y Y	
Moser et al. (10.1016/j.crad.2017.06.117)	88	Patients with emphysema	128CT	Bland-Altman (%) Multiple linear regression	Volume Volume variability	Inspiration vs expiration % reduction in lung volume at expiration local emphysema extent nodule size	↑ [-24.1,39.1%]	Y N N N	
Su et al. (10.3779/j.issn.1009-3419.2017.08.11)	9	synthetic nodules (diameter: 2.5, 5, 10mm; density: -100HU, 60HU, 100HU)	64CT	repeated-measures ANOVA	Accuracy (APE)	tube current (10, 20, 50, 80, 100, 150, 350mAs) reconstruction algorithms (FBP, ASIR 30%, ASIR 50%, ASIR 80%) nodule diameter	↑(↓)	N N Y	
Talwar et al. (10.1016/j.ejrad.2018.02.004)	40	Patients with indeterminate pulmonary nodules (20) + lung metastases (20)	LDCT	Bland-Altman (%) Mann-Whitney U test	interscan variability volume volume variability	level of inspiration Nodule size location	[-22.6%; 35.6%] slightly smaller for nodules <500mm3	N N	
Wang et al. (10.1109/EMBC.2017.8037182)	847	CT data from open access *in vivo* databases (LIDC-IDRI)	SDCT	Similarity analysis	Dice coefficient, ASD	segmentation algorithm (MV-CNN vs level set, graph cut)	↑		
Wang et al. (10.1016/j.media.2017.06.014)	1018 74	CT data from open access *in vivo* databases (LIDC-IDRI) Local *in vivo* patient dataset	SDCT	Similarity analysis	Dice coefficient, ASD, sensitivity, PPV	segmentation algorithm (CF-CNN vs CF-CNN-MP, level set, graphcut, UNet)	↑		
2016									
Kalpathy-Cramer et al. (10.1007/s10278-016-9859-z)	52 12	*In vivo* clinical databases (CIA) phantom database (CUMC)	SDCT	two-way ANOVA Concordance correlation coefficient	bias volume repeatability volume reproducibility	segmentation algorithms	≠ ≠ ≠	Y Y Y	
Li et al. (10.1186/s12938-016-0164-3)	157	*In vivo* clinical database from several hospitals + open access database (LIDC)	SDCT	Jaccard index	Adequacy of segmentation (error rate)		juxtavascular 0.17 ground-glass opacities 0.2 juxtavascular GGO 0.24		
Ohno et al. (10.1016/j.ejrad.2016.05.001)	30	simulated nodules (diameter: 3, 5, 8, 10, 12mm, density: -800, -630, +100HU)	LDCT	ANOVA	Accuracy (APE)	reconstruction algorithm (FBP, AIDR 3D, FIRST) tube current (10, 20, 40, 80, 120, 200, 270mAs)	↑(↓) (at 10 and 20mAs) ↑(↓)		
Sui et al. (10.1016/j.ejrad.2015.12.013)	105	Patients resembling NLCST	LDCT, ULDCT	Bland-Altman (%)	interobserver variability interscan variability	reconstruction algorithm (FBP, SAFIRE) radiation dose exposure (LDCT vs ULDCT)	FBP [-12.9%,12.1%] SAFIRE [-12%,13.1%] FBP [-20%,20.4%] SAFIRE [-9.7%,10.4%]		
den Harder et al. (10.1097/RCT.0000000000004408)	37	Patients under pulmonary nodule follow-up	256CT	Wilcoxon signed-rank test	volume	tube current (60, 33, 24, 15 mAs) reconstruction algorithm (FBP vs hybrid vs MBIR)	↓ ↓ (MBIR)	Y Y	
2015									
Gavrielides et al. (10.1117/1.JMI.3.1.013504)	8	synthetic nodules (outer and inner diameters: 20/10, 10mm/5mm; densities: 100/-630, 10/-630, -630/100, -630HU/-10HU)	16CT	ANOVA	Accuracy (APE)	collimation (0.75,1.5) slice thickness (0.8,1.5,2.3,5mm) kernel (medium, hard) tube current (20, 100, 200mAs)		Y Y N N	nodule size * collimation x slice thickness, collimation x slice thickness * radiation dose exposure
Hwang et al. (10.3348/kjr.2015.16.3.641)	45	synthetic nodules (diameter: 4, 6, 8mm; density: 90HU)	dual-energy 128CT	paired t-test Tuckey's test	Accuracy (RPE) IVV	pitch (conventional = 1, high-pitch = 3) nodule size	↓(↑) ↓	Y Y	
Lassen et al. (10.1088/0031-9155/60/3/1307)	59	*In vivo* open access database of SSN	CT	Jaccard index Wilcoxon signed-rank test	agreement with manual reference segmentation	segmentation algorithm			
Li et al. (10.1118/1.4921734)	48	synthetic nodules (diameter: 5, 8, 10, 20mm; shape: spherical, elliptical, lobulated, spiculated); density: -630, -10, +100 HU)	16CT	Linear regression, analysis of variance and restricted maximum likelihood	volume variability	nodule size (5, 8, 10, 20mm) slice thickness x collimation (0.8x0.75, 1.5x0.75, 3x0.75, 2x1.5, 3x1.5, 5x1.5mm) radiation dose exposure kernel (detail, medium) attachment to vessels or chest wall pitch (0.9, 1.2)	↓ ↑ ↑ ↑ ↑	Y Y N Y Y Y	nodule size * slice thickness, nodule size * shape, nodule size * density, shape * density
Young et al. (10.1118/1.4918919)	33	Patients with clinical indication to follow a pulmonary nodule	SDCT	paired t-test	intraobserver variability repeatability reproducibility	simulated dose reduction (25%, 10, 3%) reconstruction algorithm (FBP, SAFIRE)		N N	
2014									
Christie et al. (10.1177/0284185113492454)	113 13	Patients with pulmonary nodules >3mm, not attached to vessels or pleura	64CT	Bland-Altman	interscan variability	software (LMS Lung, LungCare) kernel (b30, b70) nodule size	[-53.9%,138.4%] [-7.9%,49%]	Y Y N	
Doo et al. (10.1259/bjr.20130644)	8	synthetic nodules (diameter: 5, 8, 10, 12mm); density: +100HU, -630HU	LDCT	Linear mixed model regression	Accuracy (APE)	tube current (10, 20, 30, 50 mAs) reconstruction algorithm (FBP vs IR) scan type (helical vs volumetric) nodule size density	↑(↓) ↑(↓) ↑(↓) ↑(↓) ↑(↓)	Y Y Y Y Y	nodule size*tube current, density*tube current, density*scan type, nodule size*density, nodule size* scan type
Guo et al. (10.3779/j.issn.1009-3419.2014.04.08)	86	Patients with non-calcified pulmonary nodules 3-30mm	64CT	Logistic regression Bland-Altman	Segmentation adequacy interscan variability	shape (smooth, lobulated, irregular) location (intra-parenchymal, attached to vessel, attached to pleura)	↓ ↓ (attached to vessel or pleural) [-14%,-11.6%]	Y Y	
Kim et al. (10.1016/j.ejrad.2014.01.025)	6	synthetic nodules (diameter: 10, 12mm); density: +100, -630, -800HU)	256CT	Generalizes estimating equations	Accuracy (APE)	radiation dose exposure reconstruction algorithm (FBP, IR) density	↑(↓)	N N Y	
Koike et al. (10.1111/1754-9485.12128)	71	Patients with peripheral lung cancer ≤30mm	16CT, 64CT	Bland-Altman (%)	interobserver variability		[-18.6%; 15.4%]		
Petrick et al. (10.1016/j.acra.2013.09.020)	10	synthetic nodules (diameter: 10, 20mm; shape: spherical, elliptical, lobulated, spiculated; density: -10, +100HU)	16CT	ANOVA	volume bias volume variability	slice thickness (0.8, 5mm) slice thickness (0.8, 5mm)	↓ ↓	Y Y	
Zhao et al. (10.1177/0284185113508177)	147	LCS participants	16CT	Wilcoxon signed-rank test	volume	software (LungCare, OncoTreat, Vitrea) location (peripheral, non-peripheral) attachment (intra-parenchymal, fissure attached, vessel attached, pleural attached) shape (spherical, non-spherical) margin (smooth, nonsmooth)	≠	Y Y Y Y Y	
2013									
Chen et al. (10.1118/1.4823463)	35	synthetic nodules (diameter: 4.76, 9.53mm; density: 80HU	dual-energy CT	Generalized estimating equations	Accuracy (APE) volume variability	reconstruction algorithm (FBP, ASIR, MBIR) slice thickness (0.625,1.25,2.5) software (Lung VCAR, iNtuitioin) reconstruction algorithm (FBP, ASIR, MBIR) slice thickness (0.625,1.25,2.5) software (Lung VCAR, iNtuitioin)	≠ (larger nodules) ↑(↓) ≠	Y Y Y N N N	

Christe et al. (10.1371/journal.pone.0082919)	579	synthetic nodules (density: -630, +100HU; diameter: 5, 8, 10, 12mm)	64CT	Confidence intervals	Accuracy (APE)	radiation dose exposure	↑(↓) (at the lowest dose level 25mAs/100kVp)	N	
						nodule size at highest dose level (100mAs)	↓(↑) (10, 12mm)	Y	
					volume variability		↑ (at lowest dose level)	Y	
Coenen et al. (10.1007/s11604-013-0235-3)	4	synthetic nodules (diameter: 5, 8, 10, 12mm); density: +100HU	64CT	one-way ANOVA	Accuracy (APE, RPE)	radiation dose exposure	↑(↓)	Y	
						nodule size (5, 8, 10, 12mm)	↑(↓) (5mm)	Y	
						scan mode (conventional, high-resolution)	↑(↓)	Y	
						iterative reconstruction level (0%, 50%, 100%)	↑(↓)	N	
Gavrielides et al. (10.1016/j.acra.2012.08.014)	2880	synthetic nodules (diameter: 5, 8, 10, 20mm; shape: spherical; density: -630, +100HU)	64CT	n-way ANOVA	volume	overlapping (0%, 50%)	↓(smaller nodules)	Y	overlap * nodule size, overlap * slice thickness, overlap * radiation dose exposure, nodule size * density, nodule size * slice thickness, nodule size * kernel, density * slice thickness
						slice thickness	↓ (even more in thicker slices)	Y	
						density	↓	Y	
					volume variability	overlapping (0%, 50%)	↓(smaller nodules)	Y	
						slice thickness	↓ (even more in thicker slices)	Y	
						density	↓	Y	
					volume or volume variability	radiation dose exposure		N	
						pitch		N	
						kernel (B40f, B60f)		N	
Kim et al. (10.1148/radiology.13121849)	94	Patients with PSN and GGO	16CT	Bland-Altman (%)	intraobserver variability	R1	[-7.6%,8.5%]		
						R2	[-7.4%,8.5%]		
					interobserver variability		[-11.7%,18.1%]		
					interscan variability	R1	[-17.3%,16.5%]		
						R2	[-14.8%,18.5%]		
Scholten et al. (10.1371/journal.pone.0080249)	33	LCS participants with SSN >5mm	LDCT 16CT	Bland-Altman (mm3,%)	semi-automatic volume vs manual volume	intra-observer variability	R1 [-72.8%,24.1%] R2 [-89.0%,36.0%]		
Tan et al. (10.1118/1.4793409)	55	*In vivo* open-access database (CIA)	64CT	Descriptive statistics	Volume overlap ratio		All 76% <20mm 69%		
				ICC			0.998		
	22	synthetic nodules (diameter: 10, 20mm; density: -630, +100HU)		95% Confidence interval	Accuracy (APE)	nodule size	↑(↓) (smaller nodules) [-21%,15%]	Y	
Wielputz et al. (10.1016/j.ejrad.2013.04.035)	162	synthetic nodules (density 20HU)	MDCT	Repeated measures ANOVA on ranks	Accuracy (APE)	radiation dose exposure	↑(↓)		
				Wilcoxon signed-rank	Accuracy (APE)	reconstruction algorithm (FBP vs IR) all dose exposure		N	
					volume	reconstruction algorithm (FBP vs IR) dose exposure < 1mGy	↓	Y	
Willemink et al. (10.1371/journal.pone.0058053)	78	Patients with solid pulmonary nodules and known or suspected malignancy	64CT	Bland-Altman (mm3)	volume	reconstruction algorithm (FBP vs IR)		N	
Xie et al. (10.1007/s00330-012-2570-7)	15	synthetic nodules (diameter: 3, 5, 8, 10, 12mm; density: -800, -630, +100HU)	16CT, 64CT, LDCT	Bland-Altman (%)	interobserver variability		14mm3 [-54.3%,34.4%] 65mm3 [-40.7%,49.4%] 268mm3 [-26.2%,22.1%] 524mm3 [-26.2%,22.1%] 905mm3 [-20.3%,19.2%]		
					interscan variability		14mm3 [-55.6%,49.0%] 65mm3 [-35.8%,42.2%] 268mm3 [-24.2%,27.1%] 524mm3 [-23.7%,24.9%] 905mm3 [-18.7%,19.4%]		
				t-test	volume	nodule size	↓	Y	
Xie et al. (10.1259/bjr.20130160)	5	synthetic nodules (diameter: 3, 5, 8, 10, 12mm; density: +100HU)	LDCT (64CT)	Bland-Altman	volume	CT vendor (all sizes)		N	
						CT vendor (3mm nodules)		Y	
					interscanner and intrascanner variability	nodule size	↓		
Xie et al. (10.2214/AJR.13.10830)	40	synthetic nodules (shape: irregular, lobulated; density: -51, 2, 57, 125, 157HU)	64CT	Bland-Altman (%)	interobserver interscan		[-33.9%, 40.4%] [-33.3%, 34.5%]		
				Univariate analysis	volume	CT scanner (Sensation 64 Siemens, Brilliance 64 Philips)	↓	Y	
						density (-51, 2, 57, 125, 157HU)		N	
						shape (spiculated, lobulated)	↓	Y	
2012									
de Jong et al. (10.2214/AJR.11.7577)	101	Patients with lung metastases	SDCT enhanced, LDCT	Bland-Altman (%) Wilcoxon signed-rank test	volume	protocol (SDCT enhanced, LDCT)	↓ (<200mm3) (>200mm3)	Y N	
Willemink et al. (10.2214/AJR.12.8727)	5	synthetic nodules (diameter: 3, 5, 8, 10, 12mm; density: +100HU)	256CT	Visual assessment	Accuracy (APE)	nodule size	↑(↓)	N	
						reconstruction algorithm (FBP vs IR)		N	
						tube current (25, 50, 100 mAs)	↑(↓) (size 3mm)	N	
						tube voltage (80, 100, 120kV)	smallest at 100kVp	N	
Yang et al. (10.3779/j.issn.1009-3419.2012.02.02)	52	Patients under follow-up for indeterminate pulmonary nodules <15mm	64CT, SDCT	repeated-measures ANOVA	volume	kernel (standard, bone, lung)	↑	Y	
						slice thickness (0.625, 1.25, 2.5mm)	↑ (2.5mm)	Y	
2010									
Ashraf et al. (10.1007/s00330-010-1749-z)	188	LCS participants with nodules > 5mm	16CT	Bland-Altman	interobserver variation	segmentation algorithm (small size, all size, subsolid)	↓	Y	
					volume	segmentation algorithm (small size, all size, subsolid)	↑	Y	
Hein et al. (10.1007/s10278-008-9157-5)	202	Patients with primary lung carcinoma, lung metastases or suspicious nodules	16CT	Bland-Altman	interobserver variability	radiation dose exposure (LDCT vs ULDCT)	[-12.6%;12.4%]		
					Interscan variability		[-25.1%;-23.4%]		
Rampinelli et al. (10.2214/AJR.09.3212)	35	Patients with pulmonary nodules	16CT, SDCT	Wilcoxon signed-rank test	volume	contrast enhancement (pre-, post-contrast)	↑	Y	
						contrast delay (30, 60, 120, 180, 300s)		N	
						software	≠	Y	
Rinaldi (10.1007/s11547-010-0511-6)	100	Patients with solid intra-parenchymal pulmonary nodules	16CT, SDCT	case count	volume variability	segmentation software version (LungCare 2006G, 2007G)			
Wang et al. (10.1007/s00330-009-1634-9)	200	LCS participants	64CT, LDCT	Bland-Altman	volume repeatability	slice thickness (1, 2mm)	↓	Y	shape * location * slice thickness * kernel
						kernel (soft, sharp)	↓	Y	
2009									
Iwano et al. (10.1016/j.acra.2009.04.007)	60	Patients with peripheral lung cancer	64CT, SDCT	ANOVA	interobserver variability			N	
						margins (clear, obscure)	↓	Y	
						nodule size (≤20, >20mm)		N	
						density (solid, part solid, nonsolid)		N	
						spiculation (present, absent)		N	
						attachment to vessels or chest wall (present, absent)		N	
Marchiano et al. (10.1148/radiol.2513081313)	233	LCS participants	16CT	Bland-Altman	volume	interscan variability ±27%			
Marten et al. (10.1259/bjr/40733553)	31	synthetic nodules (diameter:2.94 - 10.1mm, shape: spherical, density: 35HU)	fpCT, 64CT	ANOVA	intraobserver variation	scanner type (fpCT, 64CT)	↑	Y	
					interobserver variation	scanner type (fpCT, 64CT)	↑	Y	
				Wilcoxon signed-rank test	volume	scanner type (fpCT, 64CT)	↓	Y	
					volume variability	nodule size	↓	Y	
						slice thickness (0.625, 1.25mm)	↑	Y	
						location		N	
Nietert et al. (10.1378/chest.08-2040)	29	synthetic nodule (diameter: 3 - 15.9mm)	16CT	Nonlinear regression model	volume variability	slice thickness (0.625, 1.25, 2.5, 5mm)	↑	Y	
2008									
Dehmeshki et al. (10.1109/TMI.2007.907555)	815	*In vivo* clinical database	SDCT	case count	Subjectively adequate segmentation result	location	83 - 85% ↓ (juxtavascular)		
de Hoop et al. (10.1007/s00330-008-1229-x)	214	Patients with lung metastases	LDCT	Bland-Altman (upper LOA %)	interscan variability	software	highest with software D and satisfactory segmentation 27.6%		
				F-test		software	≠	Y	
				F-test		adequacy of segmentation (excellent, satisfactory)	↑	Y	
				one-way ANOVA		nodule size	↓	Y	
				Pearson correlation coefficient		level of inspiration		N	
Hein et al. (10.1055/s-2008-1027874)	229	33 patients: 25 for staging or follow-up; 8 with suspected pulmonary nodules	16CT	Bland-Altman (%)	intrascan SDCT intrascan ULDCT interscan (SDCT vs ULDCT)	radiation dose exposure (SDCT vs ULDCT)	[-8%,9.4%] [-12.9%,13.1%] R1 vs R2 [-26.5%,29.1%] R2 vs R1 [-25.2%,29.6%] R1 vs R1 [-25.1%,28.1%] R2 vs R2 [-26.4%,30.4%]		
Larici et al. (10.1007/s11547-008-0231-3)	3	synthetic nodules (location: juxtavascular, intraparenchymal, juxtapleural; density: +100HU)	16CT	Student t-test	Accuracy (difference cm3)	tube current (40, 100mAs)		N	
						tube current (40, 100mAs) with lung kernel	↑(↓)	Y	
						slice thickness (1.25, 2.5mm)		N	
						slice thickness (1.25, 2.5mm) with 40mAs and high-spatial kernel	↓(↑)	Y	
						kernel (lung, detail, bone, bone+)	lung kernel most accurate for 100mAs and 2.5mm slice thickness bone+ kernel most accurate for 40mAs and 1.25mm slice thickness		
					successful segmentation	location (juxtavascular, intraparenchymal, juxtapleural)	juxtapleural nodule, 2.5mm slice thickness and 40mAs failed to segment		
						kernel (lung, detail, bone, bone+)	only lung kernel segmented the juxtapleural nodule		
Tateishi et al. (10.1007/s00330-008-1002-1)	44	3 patients with lung metastases	4D 256CT	one-way ANOVA	volume	level of inspiration	↑ (end-expiratory)	Y	

Kampmeijer et al. (10.2214/AJR.08.1825)	83	Patients with lung nodules between 5-10mm	LDCT, SDCT	Bland-Altman (%)	interscan SDCT		[-19.7%,53.7%]		
					interscan LDCR		[-9.7%,35.3%]		
				Spearman correlation coefficient		% emphysema		N	
						nodule size		N	
				Kruskal-Wallis test		shape (smooth, lobulated, irregular)		N	
						location		N	
Ravenel et al. (10.1148/radiol.2472070868)	56	synthetic nodules (diameter: 3 - 16mm; shape: spherical, lobulated)	16CT	General linear regression	Accuracy (APE)	kernel (standard, lung, bone, bone+, edge, detail, soft)		N	
						slice thickness (0.625, 1.25, 2.5, 5mm)	↓(↑)	Y	
						nodule size	↑(↓)	Y	
						FOV (9.6, 15, 26, 36cm)		N	
Vogel et al. (10.1055/s-2008-1027562)	80	Patients undergoing staging CT for malignancy	64CT	Bland-Altman (%)	volume	slice thickness (1, 3, 5mm)	smallest at 3mm	N	
Wang et al. (10.1148/radiol.2482070957)	4225	LCS participants	16CT, LDCT	Bland-Altman (mm3, %)	interobserver variability		[-13.4%,14.0%]		
				Multivariate logistic regression	measurement discrepancy	location (pleural based, attached to fissure, intra-parenchymal, juxtavascular)	↑	Y	
						shape (polylobulated, spiculated, smooth, irregular)	↑	Y	
						nodule size (≤50mm3, >50mm3)	↓	Y	
Way et al. (10.1088/0031-9155/53/5/009)	41	synthetic nodules (diameter: 4.8, 9.5, 16mm)	64CT	Student t-test	Accuracy (APE)	slice thickness (0.625, 2.5mm)	↓(↑)	Y	
				ANOVA		pitch (0.531:1 - 1.375:1)		N	
						FOV (25 - 36cm)		N	
						tube current (80 - 400mAs)		N	
2007									
Biederer et al. (10.1016/j.ijrobp.2007.08.031)	55	synthetic nodules (mean diameter: 8.4mm ± 1.8)	4DCT 40CT	Wilcoxon matched-pairs test	volume	level of inspiration	↑ (end-respiratory)	Y	
						scan (static, dynamic)		N	
					variation coefficient	scan (static, dynamic)	↑	Y	
						nodule size		N	
						nodule displacement during breathing		N	
						caudal location	↑	Y	
Bolte et al. (10.1016/j.ejrad.2007.02.031)	46	synthetic nodule (fat-wax-Lipiodol, density: 50-150HU)	16CT, SDCT	Wilcoxon signed-rank test	variation coefficient	training effect (untrained, trained)	↓	Y	
						observer (unexperienced, experienced)		N	
Bolte et al. (10.1055/s-2007-962929)	20	synthetic nodules (fat-wax-Lipiodol mixture)	16CT	Ansari-Bradley test	intrascan	CT protocol (routine thoracic RTP, special volumetric protocol SVP)	RTP [-3.1%,4.3%] SVP [0,1.5%]	Y	
					interscan		RTP [-7.0%,3.5%] SVP [-10.8%,2.9%]	N	
					interobserver		RTP [-0.4%,6.8%] SVP [-4.3%,3.3%]	Y	
Bolte et al. (10.1259/bjr/29933268)	202	synthetic nodule (fat-wax-Lipiodol, density: 50-150HU)	16CT	ANOVA	volume error (%)	semi-automatic	size: all [-29.9%,11.6%] size: 5-10mm [-30.1%,12.7%] size: ≥10mm [-28.2%,-2.4%]		
						manually corrected	size: all [-13.0%,12.4%] size: 5-10mm [-13.8%,13.2%] size: ≥10mm [-7.9%,7.3%]		
						semi-automatic vs manually corrected	≠ (5-10mm)	Y	
Das et al. (10.1007/s00330-006-0562-1)	40	synthetic nodules (location: intraparenchymal, juxtavascular, attached to vessel, juxtapleural, attached to pleura; diameter: 3-10mm)	16CT	Three-way ANOVA	Accuracy (APE)	CT scanner vendors (Siemens, GE, Philips, Toshiba)		Y	
						radiation dose exposure (SDCT, LDCT)		N	
						tube current (20, 100mAs)		N	
						collimation (thin, thick)		Y	
						slice thickness		Y	
						nodule size	↑(↓) (5-10mm)		
Gietema et al. (10.1148/radiol.2452061054)	218	Patients with lung metastases	16CT, LDCT	Bland-Altman (%)	interscan variability		[-21.2%,23.8%]		
				ANOVA		segmentation (complete, incomplete)	complete [-11.9%,12.4%] incomplete [-26.8%,30.0%]	Y	
				Univariate linear regression	volume	level of inspiration		N	
Honda et al. (10.1148/radiol.2453062116)	60	Patients with lung nodules <3cm	64CT	Wilcoxon signed-rank test	volume	kernel (standard, bone)	↑	Y	
						contrast enhancement (pre-, post-contrast)	↑	Y	
Obenauer et al. (10.1097/01.rli.0000258663.13199.bf)	4	synthetic nodules (diameter: 3, 3.18, 3.97, shape: spherical; material: nylon, teflon, polypropylene); (shape: irregular)	fpVCT, 64CT	repeated-measures ANOVA	volume error (mm3)	segmentation algorithm (region growing, threshold, planimetry, ellipsoid, single advanced lung analysis [ALA])	≠	Y	
						scanner (fpVCT, 64CT)	↓	Y	
Petkovska et al. (10.1016/j.acra.2007.01.008)	75	Emphysema related trial participants	6CT, 16CT, 64CT	Linear regression	absolute volume change	level of inspiration	↓	Y	
2006									
Bolte et al. (10.1097/01.rli.0000191366.05586.4d)	70	synthetic nodules (density: 50 - 150HU)	16CT	Variation coefficient	intrascan reproducibility	volumetry tool / human	6.2% / 6.7%		
					interscan reproducibility		9.2% / 3.7%		
				Kruskal-Wallis test	intrascan variation coefficient	nodule size		Y	
Das et al. (10.1097/01.rli.0000258683.20123.c4)	40	synthetic nodules (diameter: 3-10mm; location: intraparenchymal, around vessel, attached to vessel, around pleura, attached to pleura)	SSCT, 4CT, 16CT, 64CT	ANOVA	Accuracy (APE)	radiation dose exposure (SDCT, LDCT)		N	
						collimation (thin, thick)		Y	
						location		Y	
						nodule size	↑(↓)	Y	
						scanner detectors	(4CT vs 64CT and 16CT vs 64CT)	Y	
Gietema et al. (10.1148/radiol.2411050860)	430	LCS participants with solid intraparenchymal, non-calcified nodules	16CT, LDCT	Spearman correlation coefficient	interobserver correlation	nodule size	↓	Y	
						shape (smooth, polylobulated, irregular, spiculated)	↓ (irregular)	Y	
						form (round, oval, elliptic)		N	
				Bland-Altman (mm3, %)	interobserver variability		all [-8.2%,9%] discrepancies [-21.9%,28.5%]		
Goo et al. (10.3348/kjr.2006.7.4.243)	33	Patients with severe asthma	16CT, SDCT	paired t-test	volume	level of inspiration (inspiration, expiration)	↑	Y	
				Linear correlation analysis	Accuracy (APE)	density		N	
						total lung volume	(diameter ≥3mm)	Y	
						whole lung attenuation		N	
						attenuation of adjacent lung parenchyma	↑(↓)	Y	
Honda et al. (10.1016/j.ejrad.2006.11.017)	39	50 nonconsecutive patients with solid peripheral non-calcified and non-cavitating pulmonary nodules	8CT	Kruskal-Wallis test Wilcoxon signed-rank test	volume	slice thickness (1.25, 2.5, 3.75, 5mm)	↑ (5mm)	N	
						FOV (10, 20, 30cm)	↑ (20cm)	N	
						kernel (high-spatial, low-spatial frequency)	↓	Y	
						overlap (0%, 50%)	↓	Y	
Kuhnigk et al. (10.1109/TMI.2006.871547)	42	3 software nodules (diameter: 3, 6, 9mm; shape: spherical; density: 50HU) + 39 synthetic nodules (shape: spherical, nonspherical, location: intra-parenchymal, juxtavascular, juxtapleural, diameter: 3 - 10mm)	64CT	plot	% volume change	threshold	≠ (conventional segmentation algorithm)	Y	
				Bland-Altman (%)	inter-algorithm variability	tube current (120, 120mAs)	CONV algorithm [-1.5%,11.1%] SPVA algorithm [-1.9%,9.6%]		
						slice thickness (0.6, 1, 2mm)	CONV algorithm [-31.9%,1.6%] SPVA algorithm [-19.7%,3.1%]		
						kernel (B46f, B50f, B60f)	CONV algorithm [-30.5%,-1.8%] SPVA algorithm [-8.4%,4.6%]		
	8	Patients with lung metastases	4CT	Bland-Altman (mm3, %)	interobserver variability		[-7.1%,7.1%]		
					interscan variability		[-27%,27%]		
Petrou et al. (10.2214/AJR.05.1063)	75	Patients with pulmonary nodules between 3-20mm, solid, intra-parenchymal	16CT LDCT	Student t-test	Accuracy (APE)	slice thickness / interval (1.25/0.625, 2.5/2, 5/2.5mm)	↑(↓) (small nodules)	Y	
	69			Multiple linear regression	volume variability	slice thickness (1.25, 2.5mm)		Y	
						shape (smooth, spiculated)	↑	Y	
						software	≠ (2.5mm slice thickness)	Y	
Picozza et al. (10.1097/01.rli.0000242837.11436.6e)	20	synthetic nodules (diameter: 8mm, density: 115HU, shape: irregular) + (diameter: 8mm, location: adjacent to pulmonary structures) + (diameter: 8.3mm; density: 50HU, deformable)	SSCT, 4CT	Wilcoxon matched-pairs test Kendal τ test	observer-dependent reproducibility	scanner (SSCT, 4CT)		N	
						observer-dependent repeatability		N	
	37	LCS participants with solid nodules ≥5mm		Kendal τ test		observer-dependent repeatability		Y	
				Bland-Altman	intraobserver variability		phantom [-3%,3%] in vivo [-3.1%,2.8%]		
Reeves et al. (10.1109/TMI.2006.871548)	50	*in vivo* screening database	SDCT		percent volume change	segmentation algorithm	≠	Y	
Votterrani et al. (10.1007/s11547-006-0033-4)	103	Patients with solid, noncalcified nodules, with peripheral ground-glass attenuation and central cavitation	16CT	ANOVA	volume reproducibility	location (intra-parenchymal, juxtavascular, juxtapleural)	↓	Y	
						nodule size		N	
2005									
Goo et al. (10.1148/radiol.2353040737)	720	synthetic nodules (diameter: 3.2, 4.8, 6.4, 12.7mm)	16CT, LSDCT	MANOVA	Accuracy (APE)	slice thickness (0.75, 1, 2, 3, 5mm)		Y	threshold * slice thickness
						threshold (-600, -500, -400, -300HU)		Y	
						FOV (10, 20, 30cm)		N	
						reconstruction internal (0.5, 1, 2mm)		N	
				Regression		nodule size	↑(↓)	Y	
Ko et al. (10.1148/radiol.2371041079)	51	LCS participants	LDCT	mixed-model ANOVA	volume	image compression (10:1, 20:1, 30:1, 40:1)	↓ (images compressed to ≥20:1) (more significant in subsolid nodules)	Y	compression * nodule size, compression * location, compression * density
					Accuracy (APE)	nodule size (≤5, >5mm)	↑(↓)	Y	
						location (central, peripheral, juxtapleura, juxtavascular)		Y	
						density	↑(↓)	Y	
2004									
Boll et al. (10.2214/ajr.183.5.1831217)	30	synthetic nodules (shape: spherical)		one-way ANOVA		cardiac phase		N	
	73		16CT		volume variation	cardiac phase		Y	

		Patients who underwent ECG-gated CT		Pillai-Bartlett trace Wilks lambda test		location (pulmonary lobe segments)	↑ (segments close to the heart and aorta)	Y
						density		N
				logistic regression		nodule size	↓	Y
Goodman et al. (10.2214/AJR.04.1821)	43	Patients with pulmonary nodules <20mm	8CT, 16CT, SDCT	Bland-Altman (%)	interobserver variability		[-0.018%,0.018%]	
					interscan variability		[-25.6%,25.6%]	
						diameter	<6mm [-27.6%,27.6%] 6 - <9mm [-31.4%,31.4%] ≥9mm [-17.9%,17.9%]	
						density	solid [-24.4%,24.4%] partly calcified [-23.6%,23.6%] totally calcified [-22.7%,22.7%]	
						contrast	enhanced [-32.7%,32.7%] unenhanced [-24.8%,24.8%]	
						margins	smooth/lobulated [-26.4%,26.4%] irregular/spiculated [-25.2%,25.2%]	
						adjacent parenchyma	normal [-25.6%,25.6%] abnormal [-27.1%,27.1%]	
						calcified or enhanced	yes [-28.4%,24.8%] no [-24.8%,24.8%]	
Kostis et al. (10.1148/radiol.2312030553)	115	LCS participants with stable nodules	SSCT, MDCT, SDCT	mean, SD	percent volume change	nodule size	↓	
						motion artifacts (absent, present)	↑	
Marten et al. (10.1097/01.rti.0000131591.12777.a8)	70	synthetic nodules (diameter: 10, 12mm); density: +100, -630, -800HU)	fpVC1, 4CT	Wilcoxon signed-rank test	Accuracy (APE)	scanner (fpVC1, 4C1)	↓(↑)	Y
						collimation (0.63, 1.25)	↓(↑)	Y
						nodule size	↑(↓)	Y
Marten et al. (10.1055/s-2004-813020)	50	synthetic nodules (diameter: 1.36-5.34mm)	fpVC1	Wilcoxon signed-rank test	Accuracy (APE)	deformation	↓(↑)	Y
						nodule size	↑(↓)	Y
Mullally et al. (10.1118/1.1656593)	40	synthetic nodules (diameter: 2.4, 3.2, 4, 4.9mm) shape: spherical, density: -360HU, 50HU	4C1	Sum of squared errors	Accuracy (APE)	nodule size	↑(↓)	Y
						density (ground-glass, solid)	↑(↓)	Y
						segmentation algorithm		N
						kernel		N
	29	Patients with chest CT for clinical indications		Sum of squared errors	Accuracy (APE)	segmentation algoritgm	≠	Y
Revel et al. (10.1148/radiol.2312030241)	52	Patients with solid, noncalcified pulmonary nodules between 5 - 18mm	4CT	Bland-Altman (%)	intraobserver variability		R1 [-8.9%,8.9%] R3 [-7.6%,7.6%]	
				pooling of measurements	global repeatability of volume		[-6.38%,6.38%]	
Wormanns et al. (10.1007/s00330-003-2132-0)	151	Patients with lung metastases	LDCT 4CT	Bland-Altman (%)	intraobserver		[-3.9%,5.7%]	
					interobserver		[-5.5%,6.6%]	
					intrascan		[-20.4%,21.9%]	
					intrascan	nodule size <10mm	[-19.3%,20.4%]	
2003								
Ko et al. (10.1148/radiol.2283020059)	40	synthetic nodules (diameter: 2 - 5mm, density: -360, 50HU; shape: spherical)	4C1, LDCT, SDCT	ANOVA	Accuracy (APE)	tube current (20, 120 mAs)	↑(↓)	Y
						density (ground-glass, solid)	↑(↓)	Y
						nodule size	↑(↓)	Y
						segmentation algorithm (partial volume, threshold method)	↓(↑) (small nodules)	Y
						location		N
2000								
Yankelevitz et al. (10.1148/radiology.217.1.r00oct33251)	21 + 20 + 35	synthetic nodules (diameter: 3.2, 3.96mm, shape: spherical) + (nodules before and after deformation) + (nodules of various shapes and sizes)	SSCT, SDCT	Coefficient of variation	Accuracy (APE)	nodule size	↓(↑) (small nodules) < 3%	
	13	Patients with pulmonary nodules <10mm	SSCT, SDCT	Coefficient of variation	Accuracy (APE)	nodule size	↓(↑) (small nodules) < 3%	

segmentation algorithm * nodule size, segmentation algorithm * tube current, segmentation algorithm * density